

Whole Powder Pattern Modelling (analysis of nanocrystalline materials)

Matteo Leoni, Paolo Scardi

Department of Materials Engineering and
Industrial Technologies, University of Trento

Matteo.Leoni@unitn.it



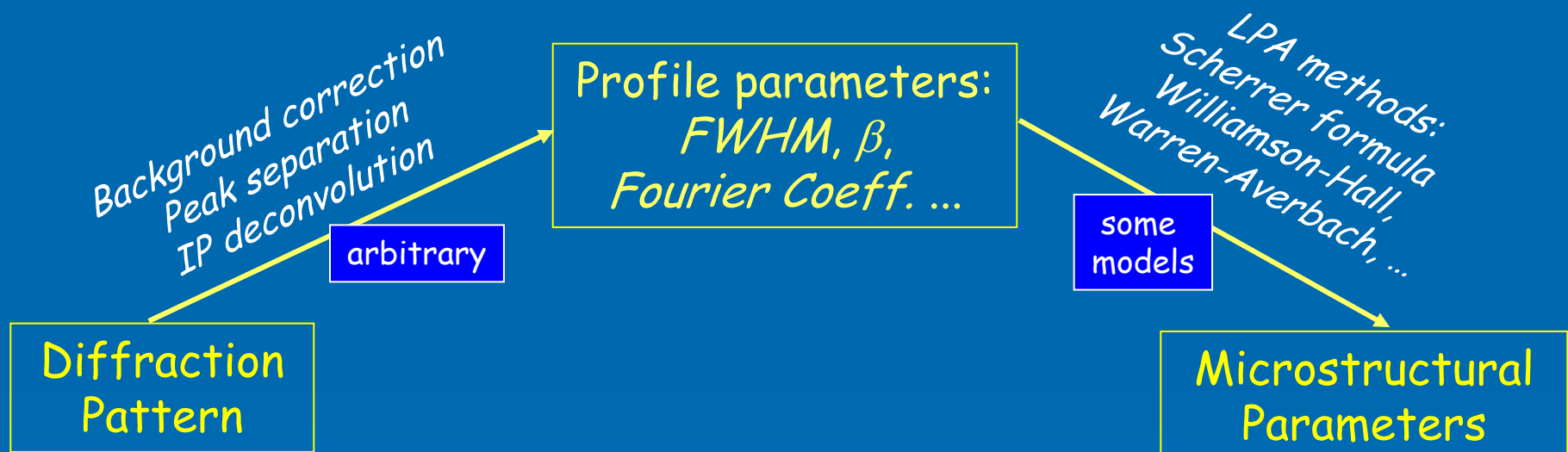
WPPM : basics





Towards a whole pattern approach

In traditional methods of analysis we loose the direct contact with the experimental data

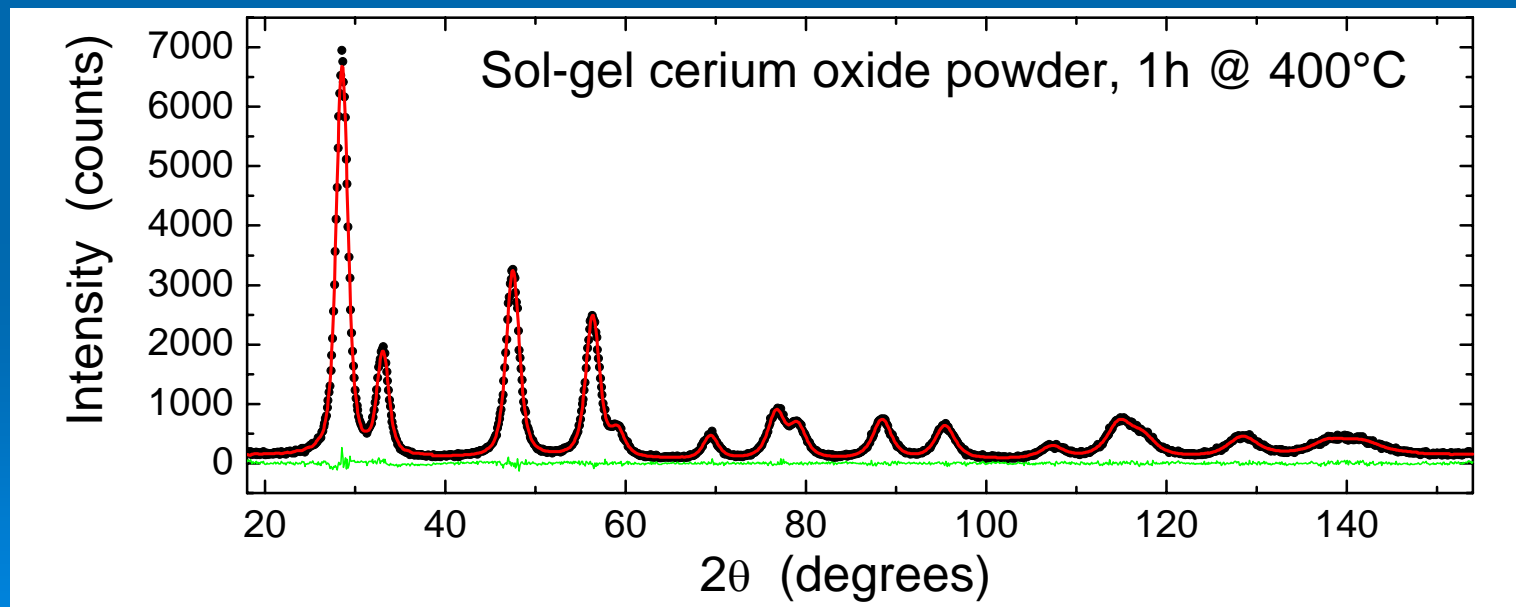


This has been the main driving force towards the introduction of Whole Powder Pattern Modelling, aimed at directly extract the information from the experimental pattern



Whole Powder Pattern Modelling: WPPM

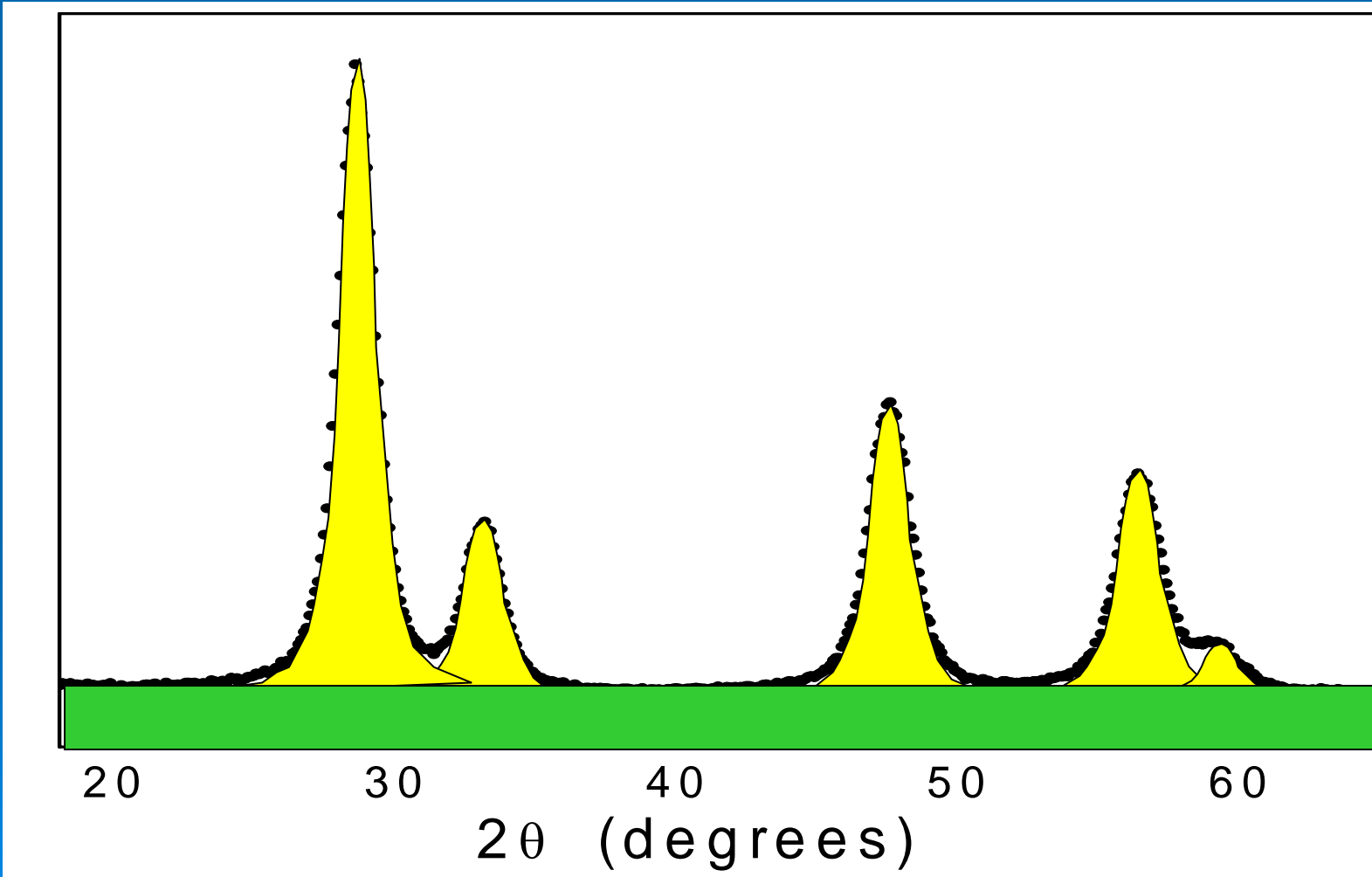
WPPM is based on a direct modelling of the experimental pattern, based on physical models of the microstructure and lattice defects:





WPPM: basics

Pattern built as sum of broadened peaks plus a background





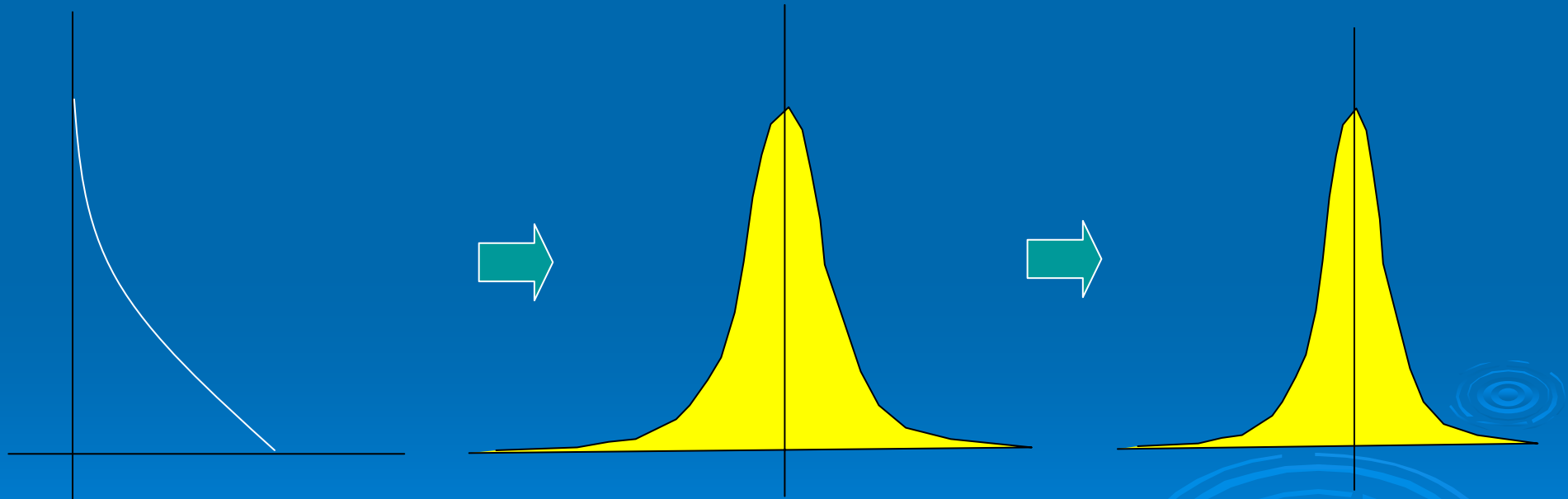
WPPM: basics

Each peak is synthesised in reciprocal space from its Fourier transform and then remapped into 2θ space through the use of a suitable interpolation algorithm

Fourier space

reciprocal space

2θ space



For any broadening source, the corresponding Fourier transform can be calculated

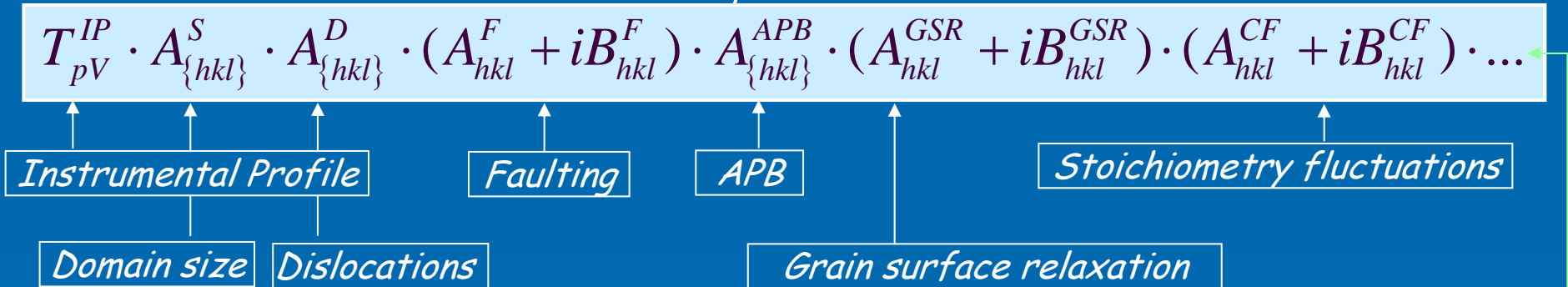


WPPM: basics

$$I_{\{hkl\}}(d^*, d_{\{hkl\}}^*) = k(d^*) \cdot \sum_{hkl} w_{hkl} \int_{-\infty}^{\infty} C_{hkl}(L) \exp(2\pi i L \cdot s_{hkl}) dL$$

Diffraction profiles result from a convolution of effects.

Therefore, Fourier Transforms of the various effects are multiplied:



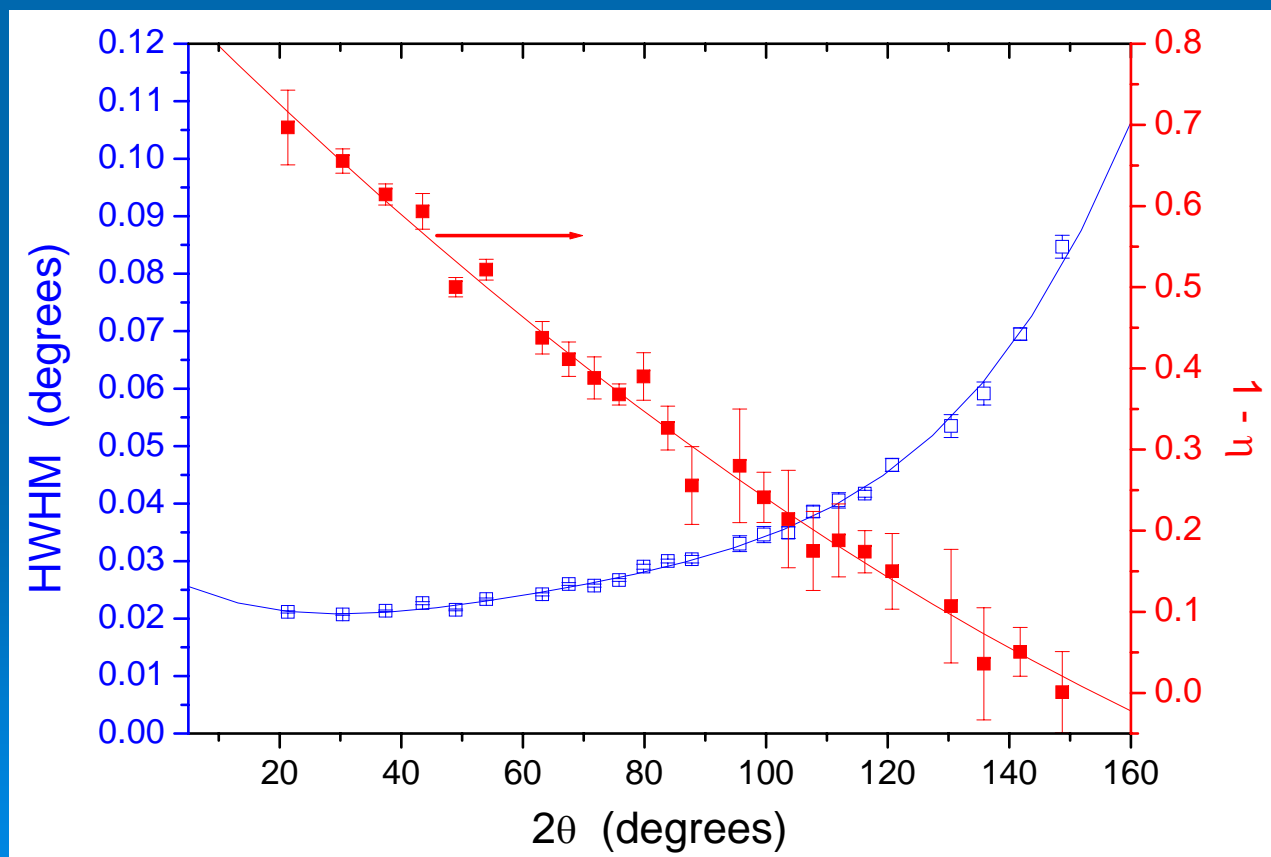
Instrumental Profile, Domain Size, Dislocations, Anti-Phase Domain terms are real functions of L (Fourier length), whereas Faulting, Grain Surface Relaxation and fluctuations in the composition give complex ($A+iB$) contributions

Additional line broadening sources can be included by adding (multiplying) corresponding FTs



WPPM: instrumental profile

The following curves, e.g. can be obtained by plotting the half width at half maximum and the gaussian content of the pseudo-Voigt profile for the fit of the LaB₆ SRM 660A standard peaks measured on a Rigaku diffractometer:





WPPM: instrumental profile

When a pseudo-Voigt curve is used for the modelling, the following expression can be used for the corresponding Fourier cosine coefficients:

$$T_{pV}^{IP}(L) = (1 - k) \cdot \exp\left(-\pi^2 \cdot \sigma_s^2 L^2 / \ln 2\right) + k \exp\left(-2\pi \cdot \sigma_s L\right)$$

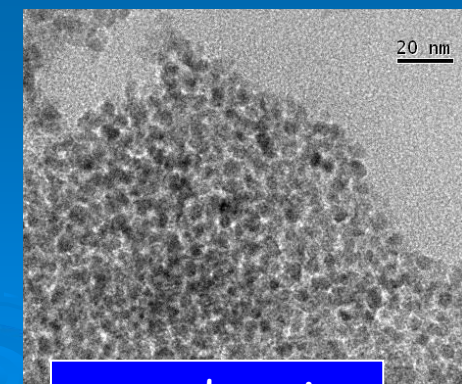
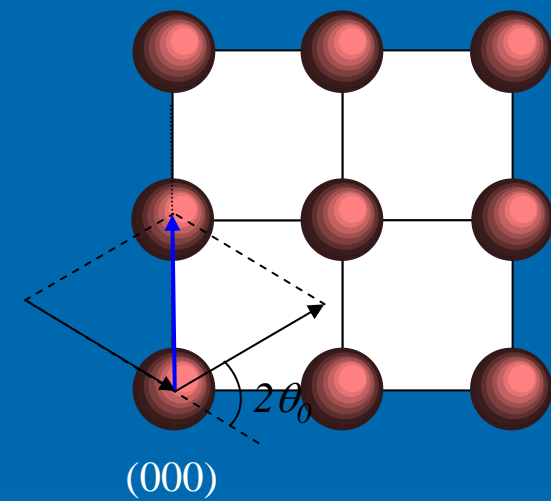
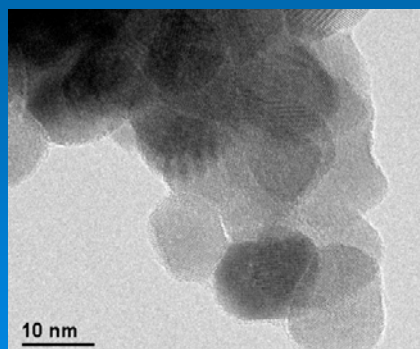
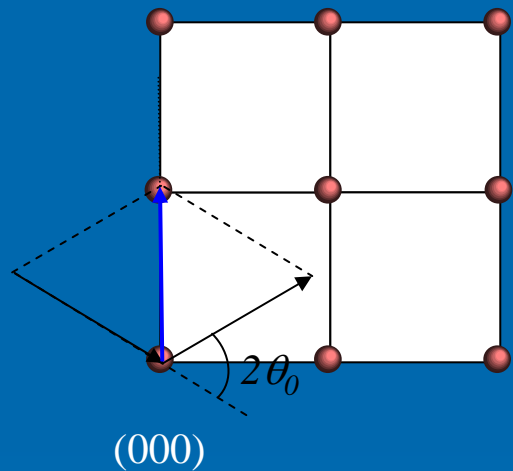
Sine coefficients are zero if the curve is considered as symmetric.

Width (σ_s) and shape (related to k) parameters for the given reflection (e.g. given Bragg angle) are determined from the parametric description of the instrumental profile.



WPPM: domain size effects

In a nanocrystalline material, the most important broadening source is perhaps the small size of coherently diffracting domains





WPPM: general size distribution

Size coefficients can be written as:

$$A^S(L) = \frac{L \zeta^c(hkl)}{\int_0^\infty w(D) dD}$$

constant related to the shape under consideration

Fourier transform for the particular grain shape considered

weight function, related to the domain size distribution $g(D)$ through the relationship

$$w(D) = g(D)V_c(D)$$

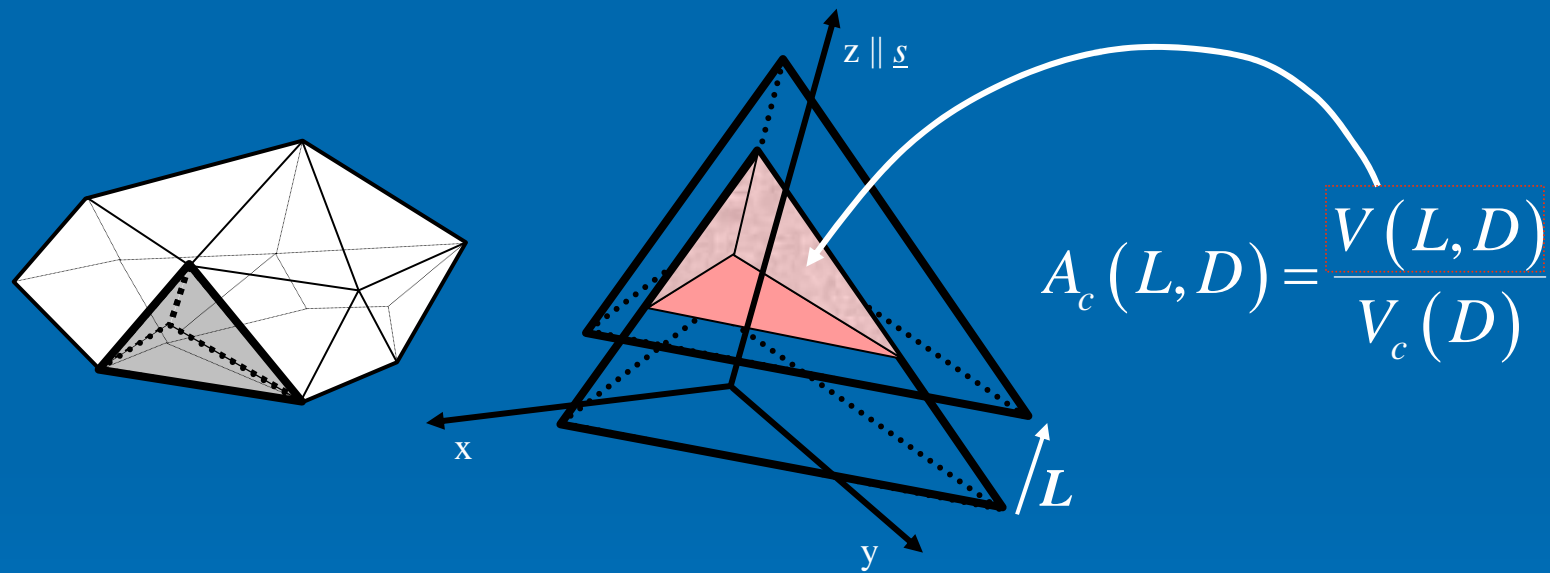
where $V_c(D)$ is the volume of the domain

If the domain size distribution is represented by an histogram and the length of the columns in the histogram are refined together with the other parameters, the optimal "least squares" size distribution is obtained



WPPM: domain size effects

Expressions for $A_c(L,D)$ can be calculated for different crystal shapes by means of the 'ghost' concept of Wilson:



It can be demonstrated that for any polyhedron $A_c(L,D)$ is a cubic in L :

$$A_c(L,D) = \sum_{n=0}^3 H_n^c (L/D)^n$$



WPPM: domain size effects

Fourier Coefficients:

$$A_i(L) = \left[M_{i,3} \right]^{-1} \int_{LK}^{\infty} A_c(L,D) D^3 g_i(D) dD$$

$$A_l(L) = \sum_{n=0}^3 \operatorname{Erfc} \left[\frac{\ln(L \cdot K^c) - \mu - (3-n)\sigma^2}{\sigma\sqrt{2}} \right] \frac{M_{l,3-n}}{2M_{l,3}} \cdot H_n^c L^n \quad \text{LOGNORMAL}$$

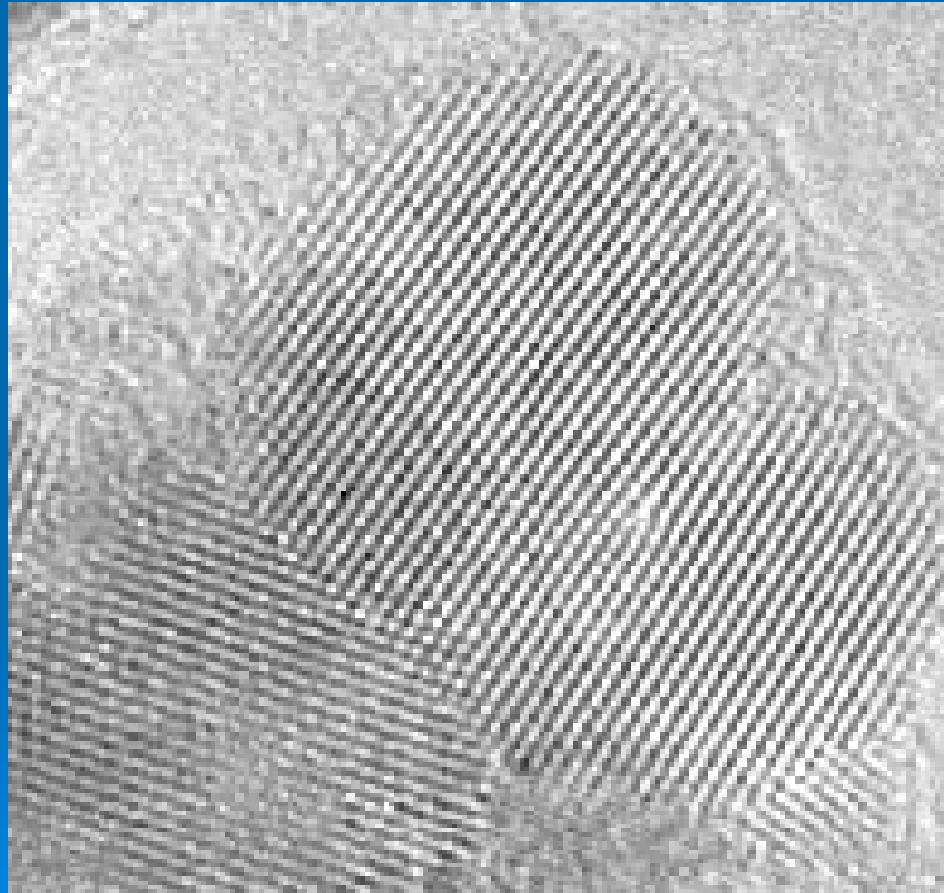
$$A_p(L) = \sum_{n=0}^3 \left(\frac{\sigma}{\mu} \right)^n \frac{\Gamma(\sigma + (3-n), \frac{K^c L \sigma}{\mu})}{\Gamma(\sigma + 3)} \cdot H_n^c L^n \quad \text{GAMMA}$$

$$A_Y(L) = \sum_{n=0}^3 \left(\frac{\sigma}{\mu} \right)^n \frac{\Gamma(\sigma + (4-n), \frac{K^c L \sigma}{\mu})}{\Gamma(\sigma + 4)} \cdot H_n^c L^n \quad \text{YORK}$$



WPPM: dislocations

Dislocations are quite often the main kind of lattice defect present in a nanocrystalline material



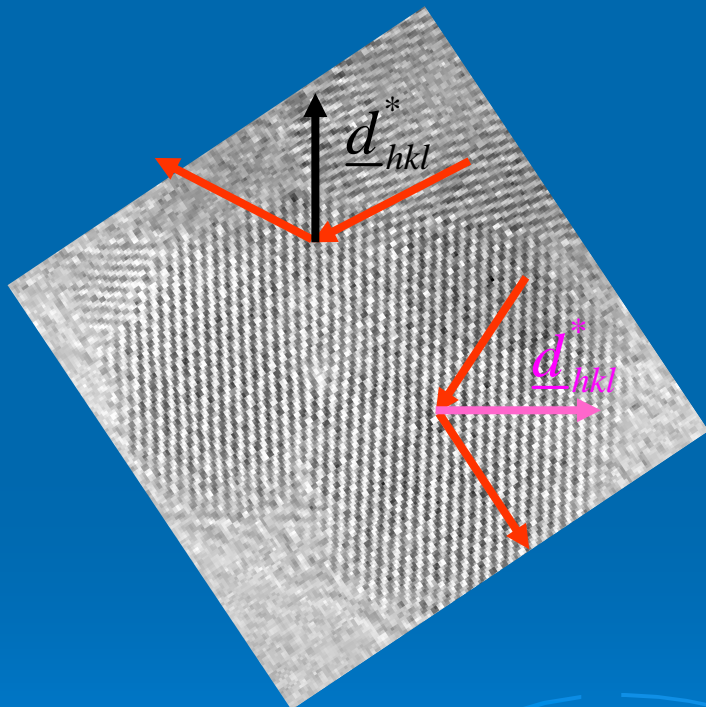
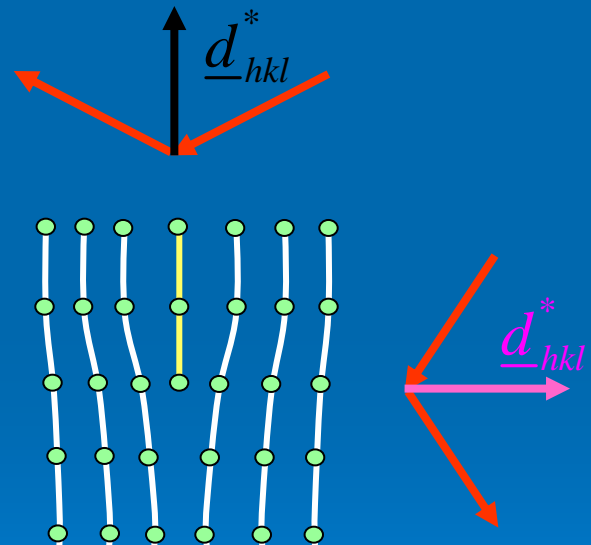
edge dislocation in ceria



WPPM: dislocation contrast

Line broadening due to dislocation is markedly anisotropic (it introduces specific hkl /dependence)

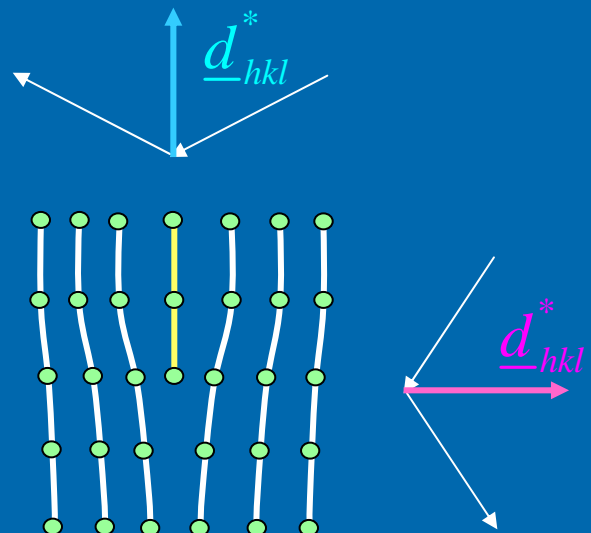
Dislocation contrast



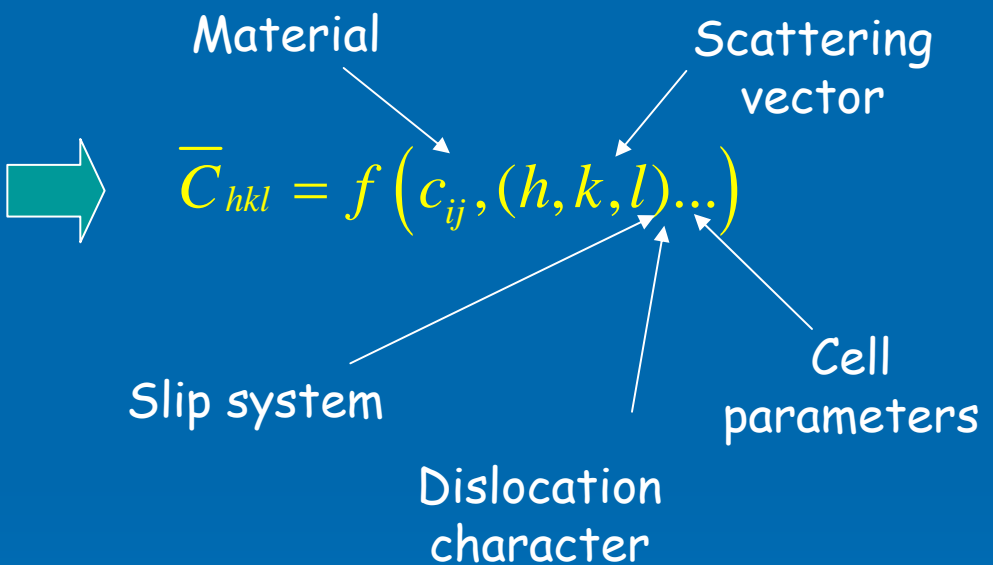
The visibility of a dislocation depends on the viewing direction: it is invisible if we're perpendicular to the slip plane



WPPM: dislocation contrast



Expressed in terms of contrast factor
(KNOWN function for **ANY** symmetry)



Contrast Factor in cubic materials
is linear in H

$$\bar{C}_{hkl} = A + B \cdot \frac{h^2 k^2 + k^2 l^2 + l^2 h^2}{(h^2 + k^2 + l^2)^2} = A + B \cdot H$$



WPPM: dislocation contrast

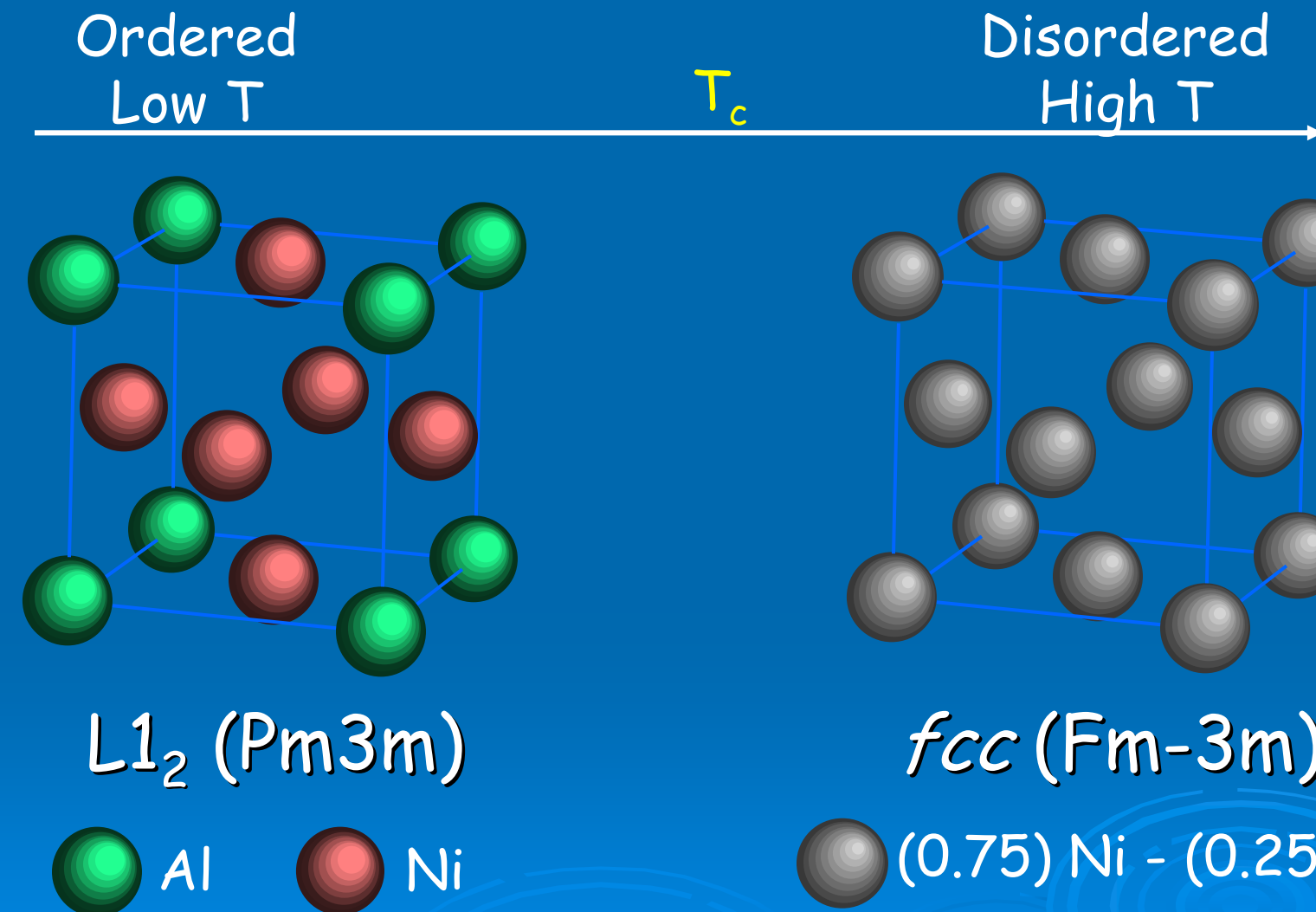
The Fourier coefficients relative to **dislocations** (average density ρ , effective outer cut-off radius R_e , Burgers vector b and average contrasts factor \bar{C}_{hkl}) read:

$$A_{\{hkl\}}^D(L) = \exp \left[-\frac{1}{2} \pi |b|^2 \bar{C}_{hkl} \rho d_{\{hkl\}}^{*2} \cdot L^2 f^*(L/R_e) \right]$$

where $f^*(L/R_e)$ is Wilkens' function.



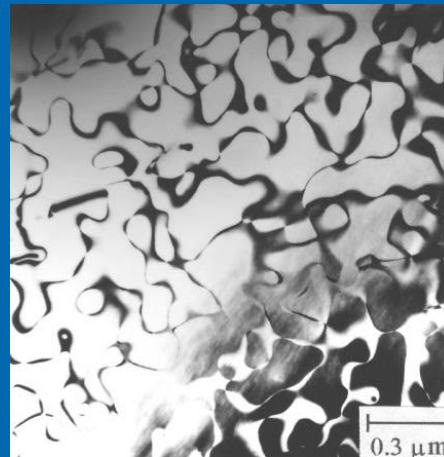
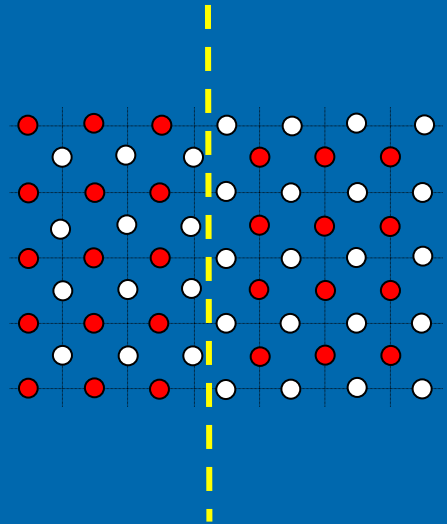
WPPM: ordered/disordered phase



Symmetry of the structure changes: different peaks present in the pattern!



WPPM: antiphase boundaries



For the presence of anti-phase domain boundaries (where the probability of finding a fault along the chosen direction is γ) :

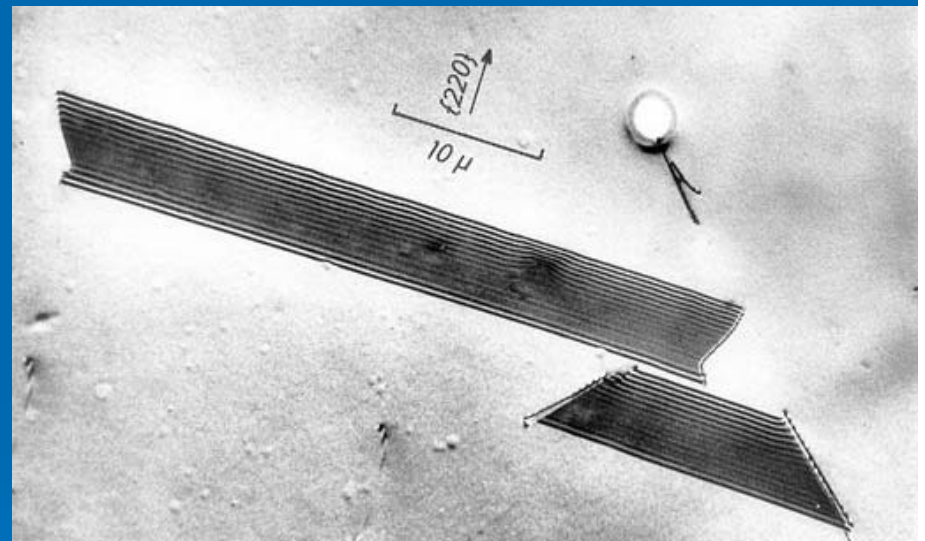
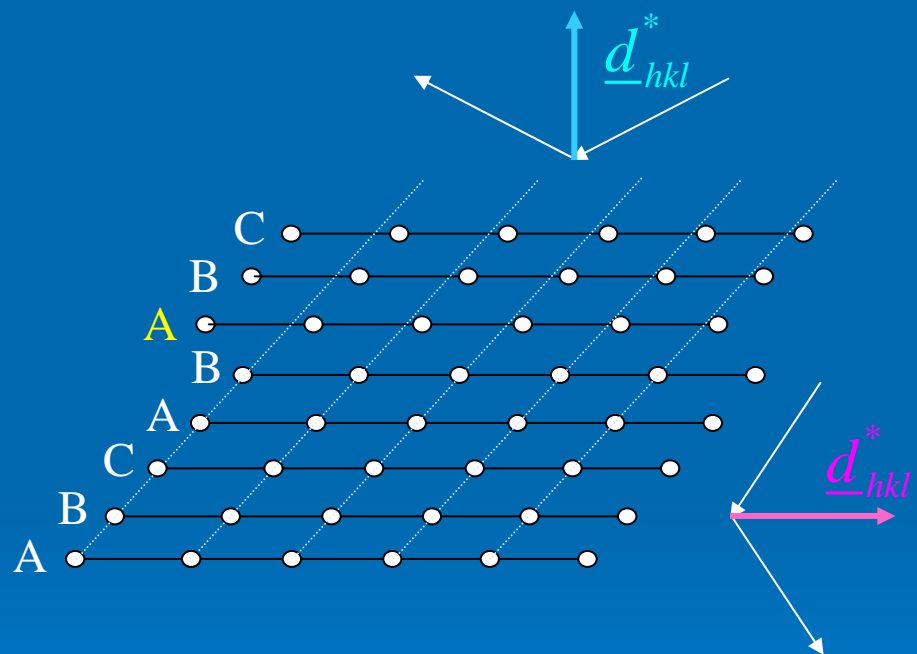
$$A_{\{hkl\}}^{APB}(L) = \exp \left[-\frac{-2\gamma(|h|+|k|) \cdot L}{d_{hkl} (h^2 + k^2 + l^2)} \right]$$

Only superstructure peak profiles are affected



WPPM: planar defects

Line broadening due to faulting is markedly anisotropic (it introduces specific hkl /dependence)



hkl dependence is different than that seen for dislocations



WPPM: faulting

For twin and deformation faults in fcc (probability β and α , respectively):

$$A_{hkl}^F(L) = \left(1 - 3\alpha - 2\beta + 3\alpha^2\right) \left| \frac{1}{2} L d_{\{hkl\}}^* \cdot \frac{L_o}{h_o^2} \sigma_{L_o} \right|$$

$$B_{hkl}^F(L) = -\sigma_{L_o} \cdot \frac{L}{|L|} \cdot \frac{L_o}{|L_o|} \cdot \beta / \left(3 - 6\beta - 12\alpha - \beta^2 + 12\alpha^2\right)^{1/2}$$

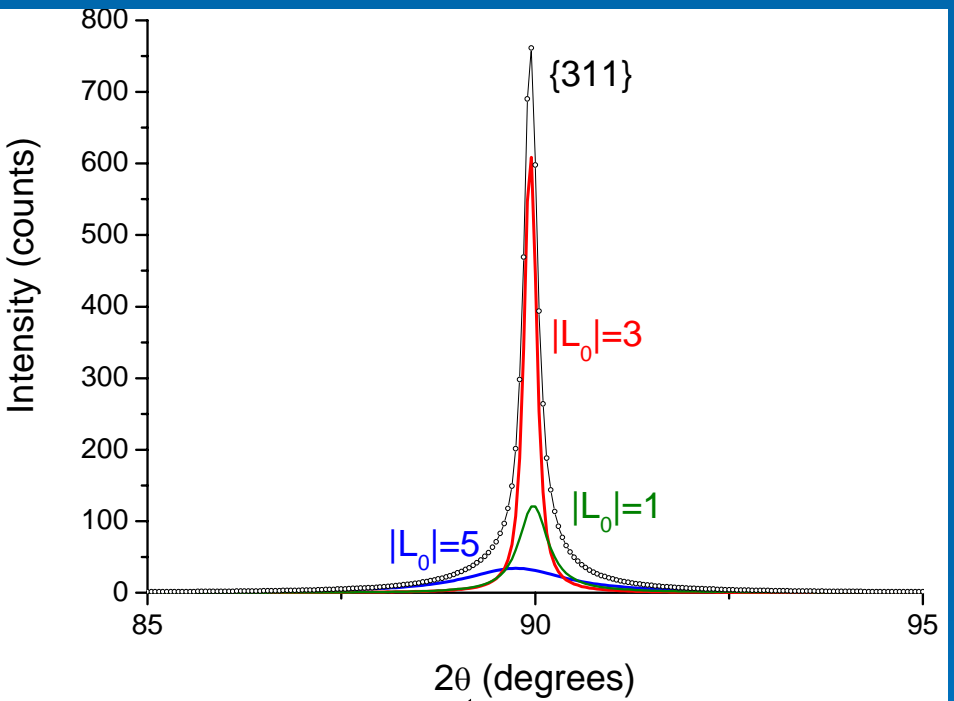
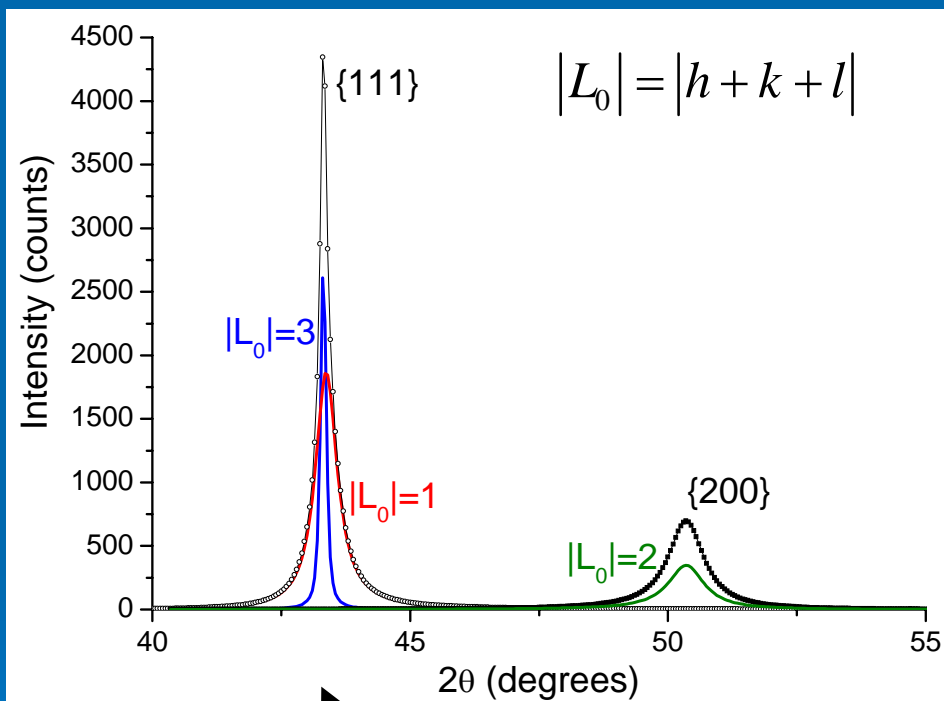
The modelling is highly simplified (rough description of the phenomena), but it can be seen that the profile is not symmetrical (a sine term is present).

Each member of the $\{hkl\}$ family can possibly be broadened, asymmetric and shifted from its Bragg position:



WPPM simulation: effect of faulting

(111) faulting in *fcc* metal structures
 $\alpha=2\%$, $\beta=5\%$, $\langle D \rangle=59$ nm, $\rho=10^{13}$ m $^{-2}$



Members of the same family show different broadening characteristics



WPPM: fingerprint of the effects

$$I_{\{hkl\}}(d^*, d_{\{hkl\}}^*) = k(d^*) \cdot \sum_{hkl} w_{hkl} \int_{-\infty}^{\infty} C_{hkl}(L) \exp(2\pi i L \cdot s_{hkl}) dL$$

$$T_{pV}^{IP} A_{\{hkl\}}^S A_{\{hkl\}}^{APB} (A_{hkl}^F + iB_{hkl}^F) A_{\{hkl\}}^D$$

T_{pV}^{IP} Sample independent (fixed parameters from a profile standard powder)

$A_{\{hkl\}}^S$ Depends on grain shape and size distribution (may depend on $\{hkl\}$)

$A_{\{hkl\}}^{APB}$ Only superstructure $\{hkl\}$ profile are affected (with a specific law)

A_{hkl}^F, B_{hkl}^F Complex hkl dependence on the diffraction profile sub-components

$A_{\{hkl\}}^D$ Depends on $\{hkl\}$ through \bar{C}_{hkl} according to the Laue group invariant.

WPPM : software





WPPM: PM2K software

PM2K is a general problem-independent fit program.

- based on a multiple client/server architecture
- server implements a problem-independent multi-purpose fit routine, driven through a TCP-IP interface
- plugins are used to extend the functionality of the routine:
 - the WPPM algorithm is built as plug-in for the server
 - broadening models used in WPPM are designed as plugins
 - input/output file type managers are plugins
 - a plugin development kit allows an easy implementation of new models
- the program uses a versatile input file format



WPPM: PM2K software

Possible broadening plugins for WPPM (most of them already implemented):

➤ **Instrumental broadening**

- Caglioti pV
- FPA

➤ **Size broadening**

- HISTOGRAM MODEL
(sphere, cube, tetrahedron, octahedron, ellipsoid, hexagonal prism, cylinder, harmonics)
- ANALYTICAL MODEL
delta, lognormal, gamma, generalised gamma, York distributions
(sphere, cube, tetrahedron, octahedron, ellipsoid, hexagonal prism, cylinder, harmonics)
- Column Length Distribution (a la Bertaut)



WPPM: PM2K software

➤ Strain broadening

- dislocations (all symmetries)
(simplified Wilkens, full Wilkens models)
- dislocations (all symmetries)
(harmonics invariant, Green function model)
- dislocation configurations (arrays, pile-ups, walls)
- van Berkum model
- Houska-like (Houska, Adler-Houska, modified Houska)

➤ Effective models (size/strain mix)

- Stephens/Popa

➤ Faulting

- recursion equations (Warren) for fcc, bcc and hcp
- correlation probability
- correlation matrices
- recursive approach (convergence towards DIFFaX⁺)



WPPM: PM2K software

➤ Antiphase Boundaries

- Wilson-Zsoldos finite differences
- Wilson-Zsoldos differential equations

➤ Grain Surface Relaxation

- original model (size-independent relaxation-zone width)
- modified model (size-dependent relaxation)

➤ Additional broadening models

- full micromechanical model
- grain-dependent lattice parameter
- stoichiometry fluctuation

A plugin development kit is available (example written in C++) for those willing to implement their models into PM2K. Just throw the plugin in plugins directory and the new function will be automatically available to PM2K.



WPPM: PM2K software

PM2K interface

File Edit Min Help

New Open Save As... Copy Connect... Iter... Stop DATH INIT OUT Update Plot Get Init files Get Result

```
1 // Cerium oxide, test
2 // instrumental parameters (Caglioti)
3 par !W 1.790000E-02, !V 9.270000E-03, !U 3.060000E-03
4 par !a 1.287000E-01, !b 1.510000E-02, !c -4.900000E-05
5
6 loadData("a60433.raw", WPPM())
7 enableFileFit()
8
9 // Emission profile is made of 5 components (wavelength in nm and relative intensity)
10 // wavelengths from Berger et al.
11 addWavelength(!w11 0.1534753, !iRel11 0.0159)
12 addWavelength(!w12 0.1540596, !iRel12 0.57 )
13 addWavelength(!w13 0.1541058, !iRel13 0.0762)
14 addWavelength(!w14 0.1544441, !iRel14 0.2417)
15 addWavelength(!w15 0.1544721, !iRel15 0.0871)
16
```

Kernel address

Address: localhost Port: 5432

Remember kernel

OK Cancel

Input file Output file Plots Parameters



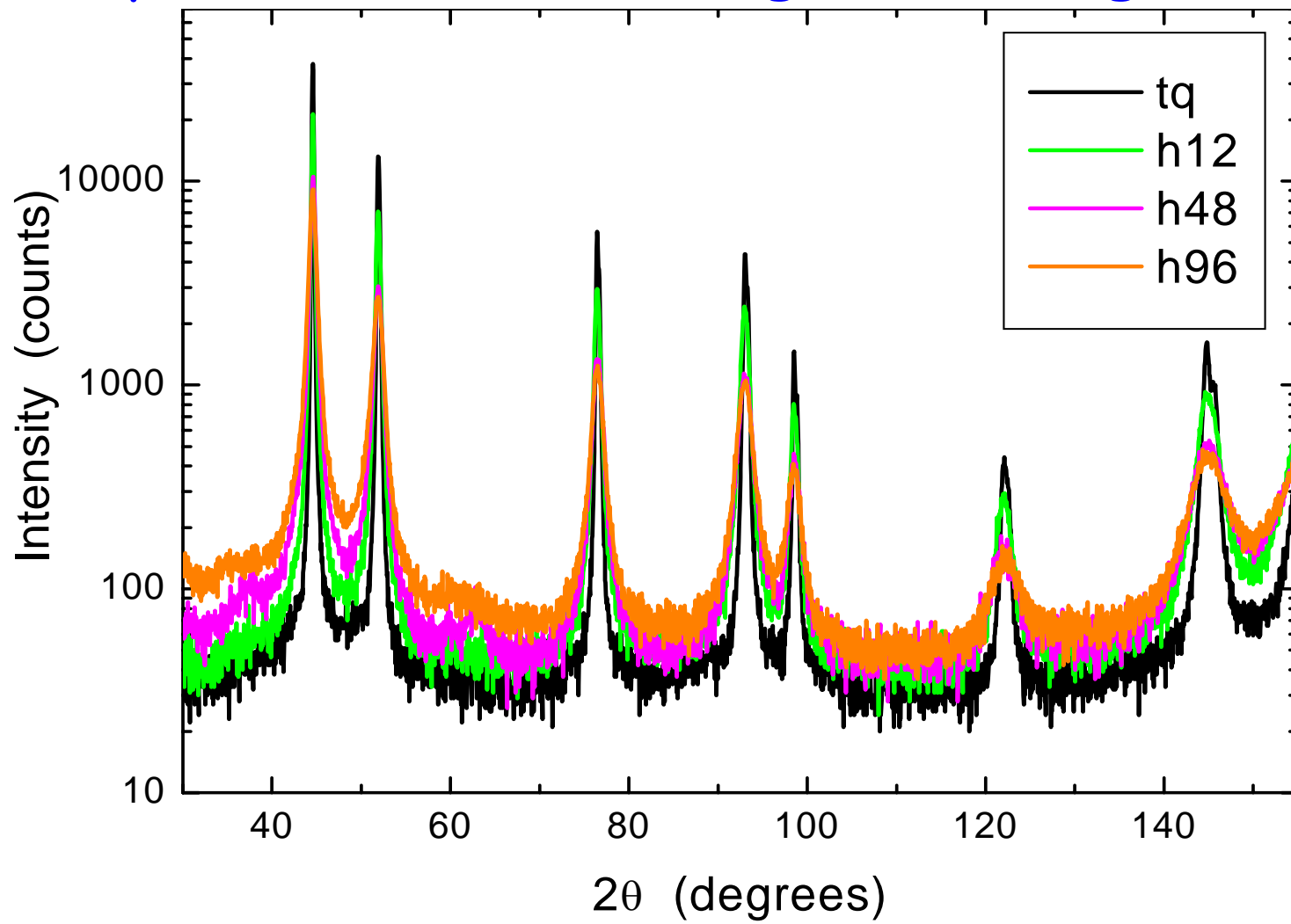
WPPM: applications

- Ball milled nickel powder
- Antiphase domains in Cu_3Au
- Nanocrystalline cerium oxide
- Ball milled Fe-1.5Mo
- Ball milled fluorite



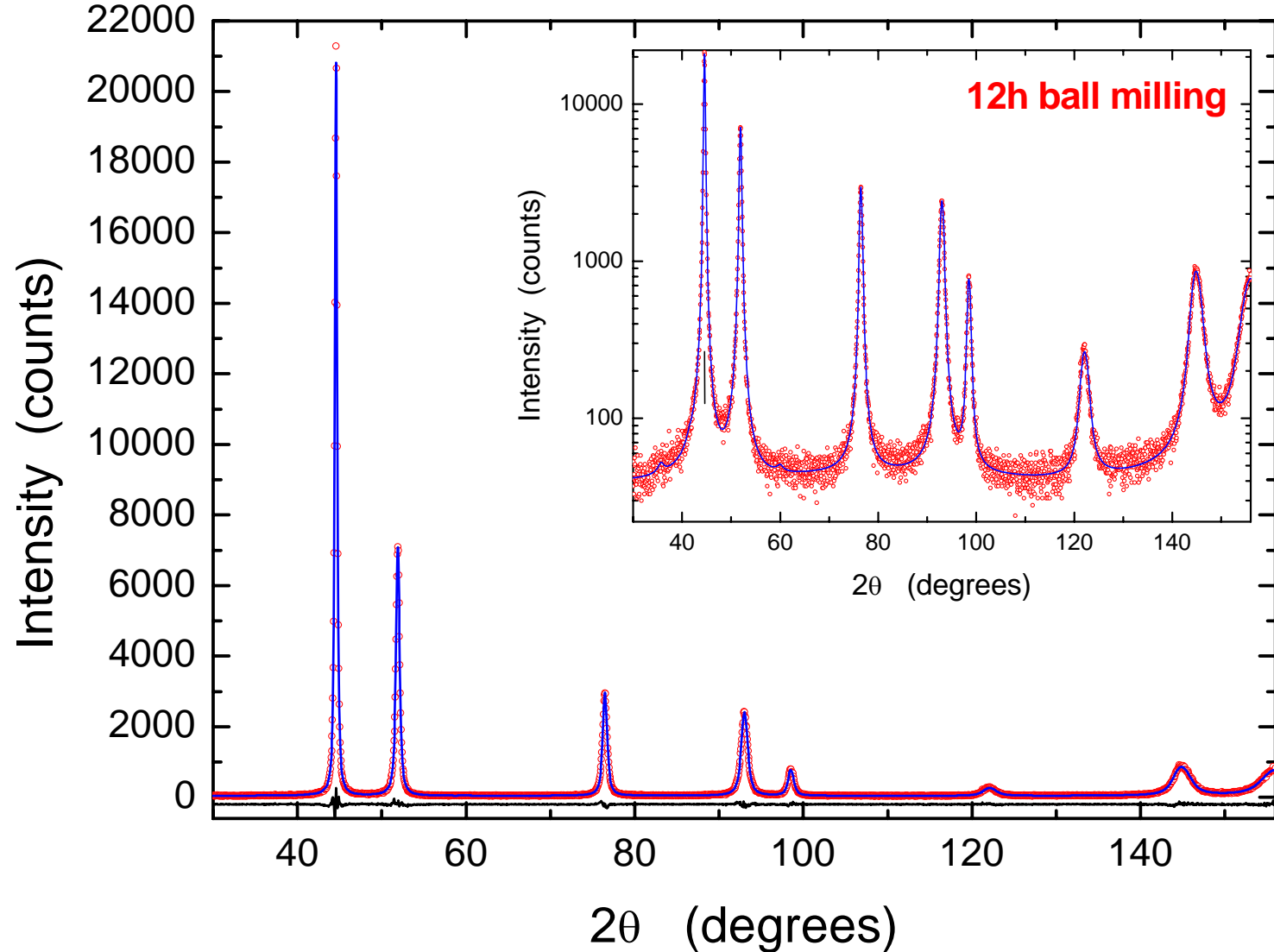
ball milled Ni, WPPM

Ni patterns at increasing ball milling time



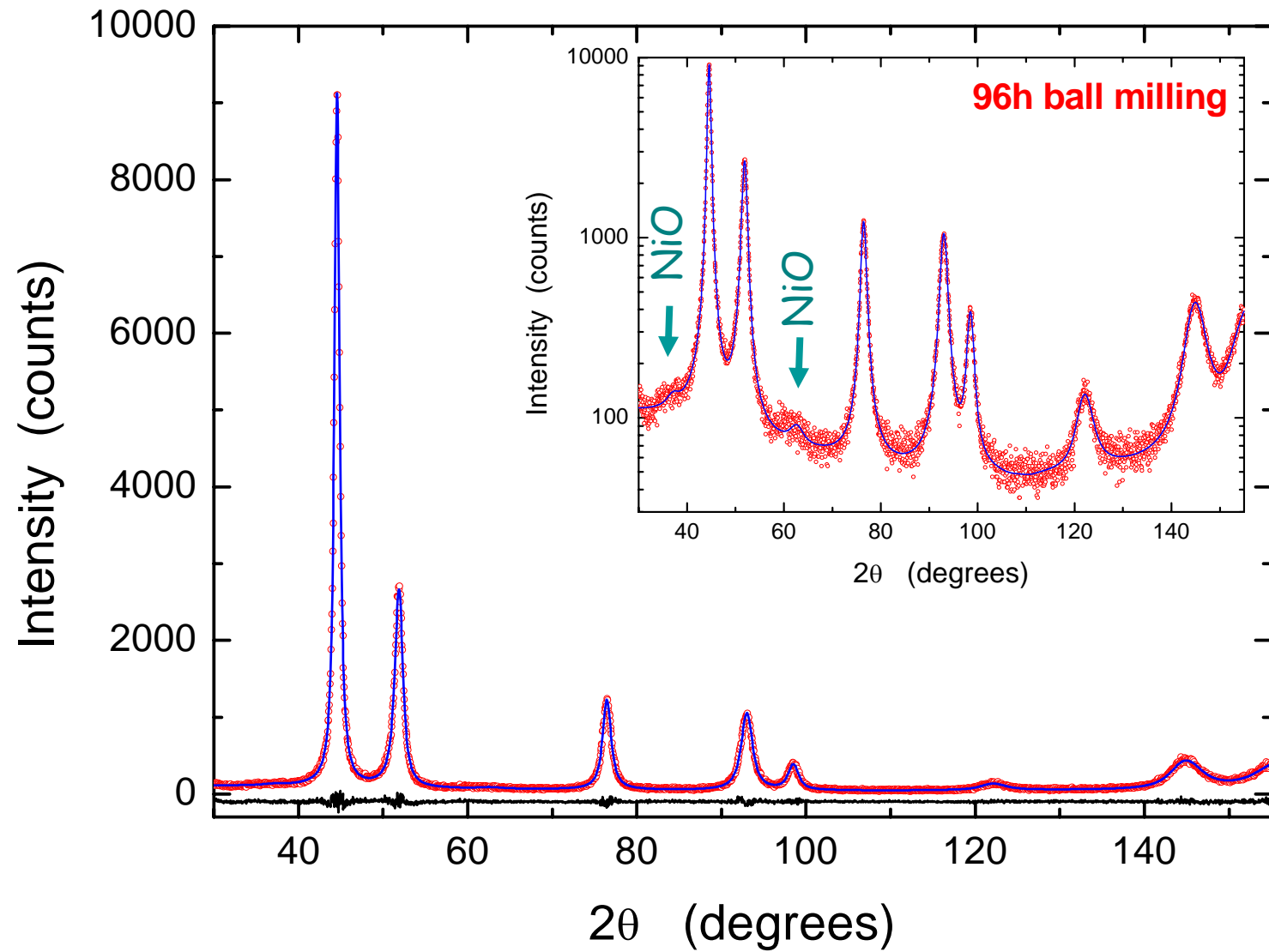


ball milled Ni, WPPM



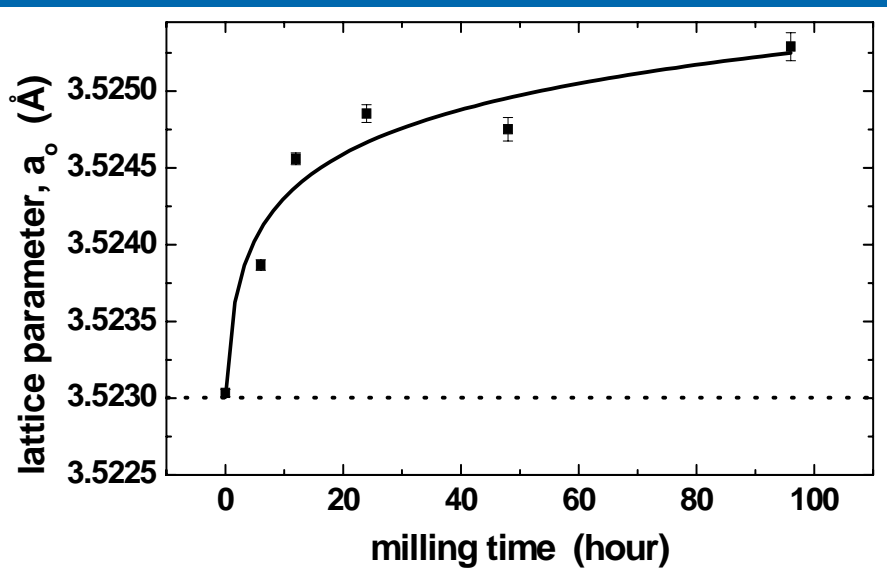
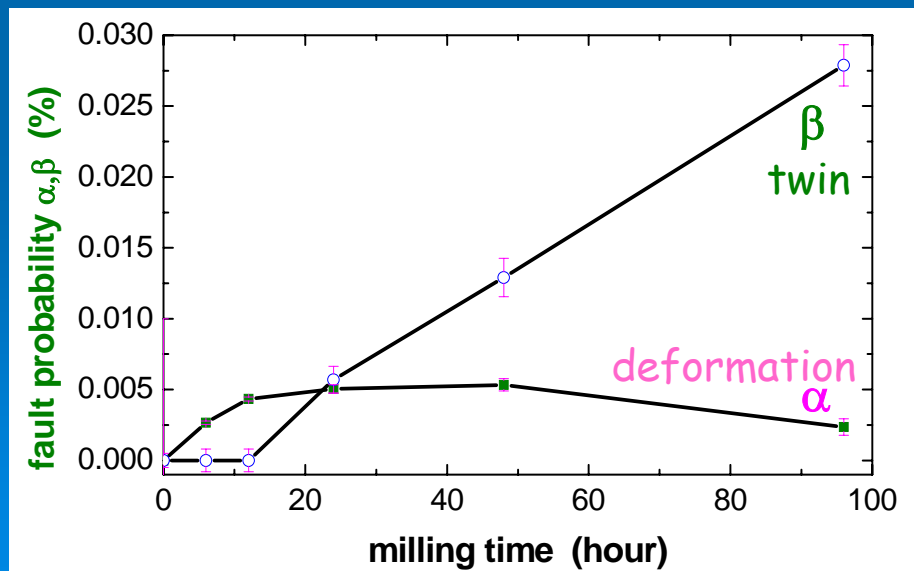
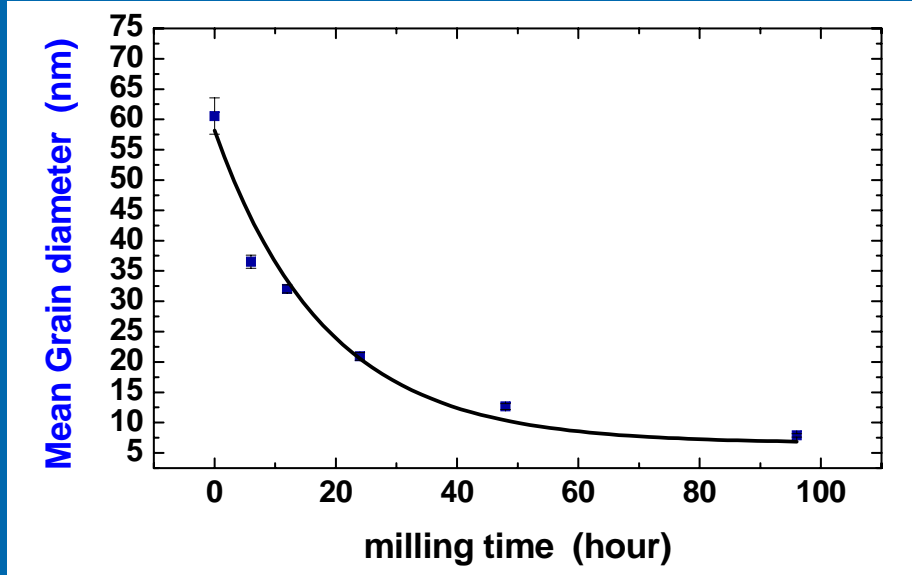
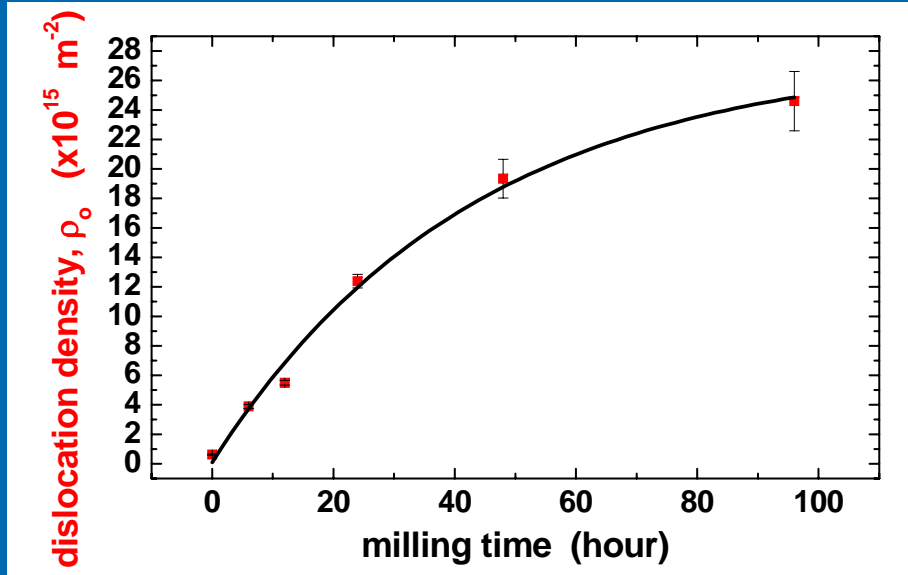


ball milled Ni, WPPM





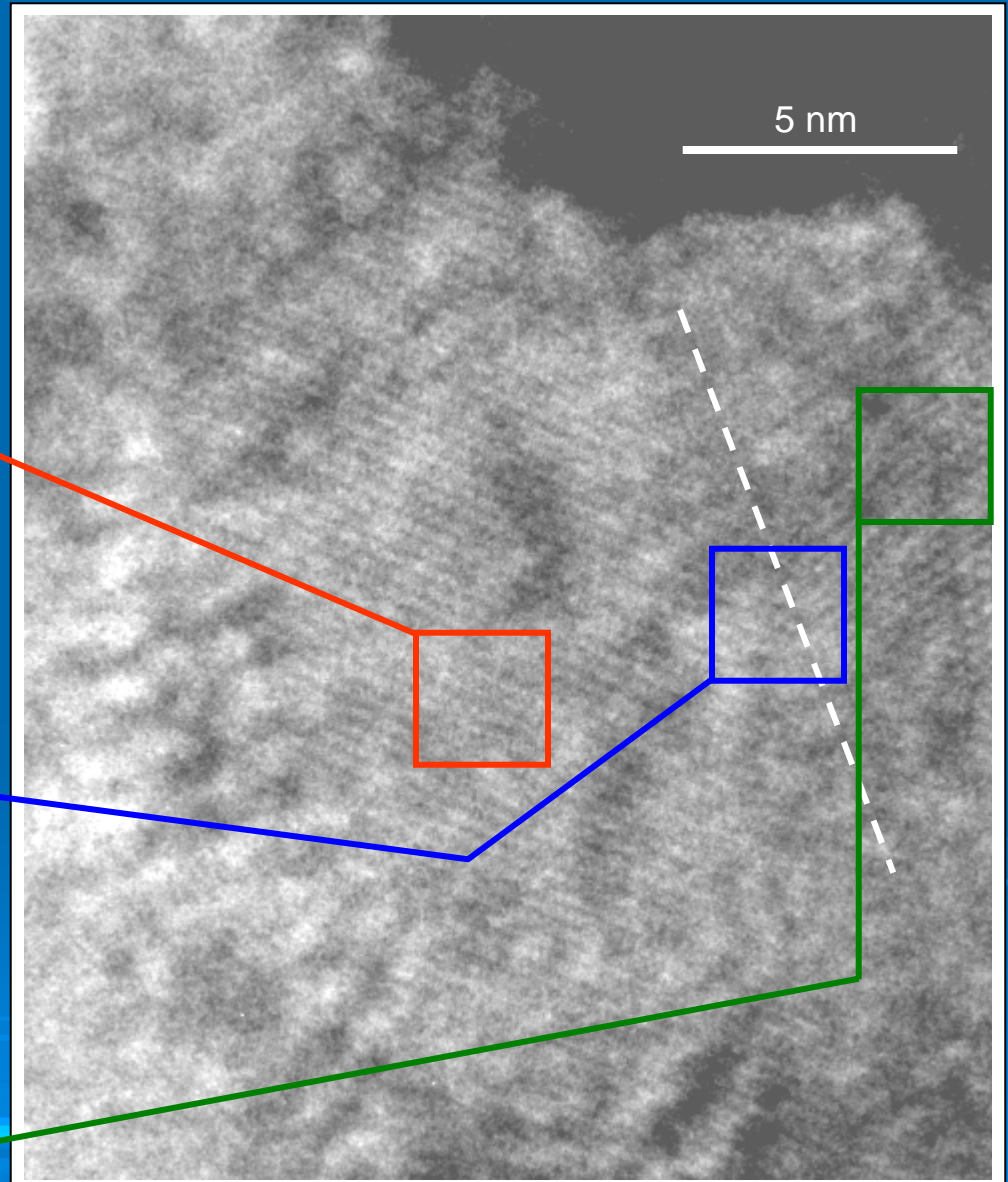
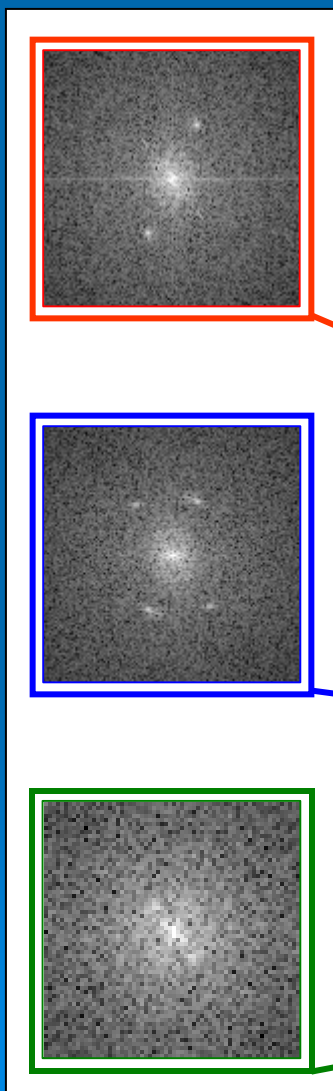
ball milled Ni, WPPM results





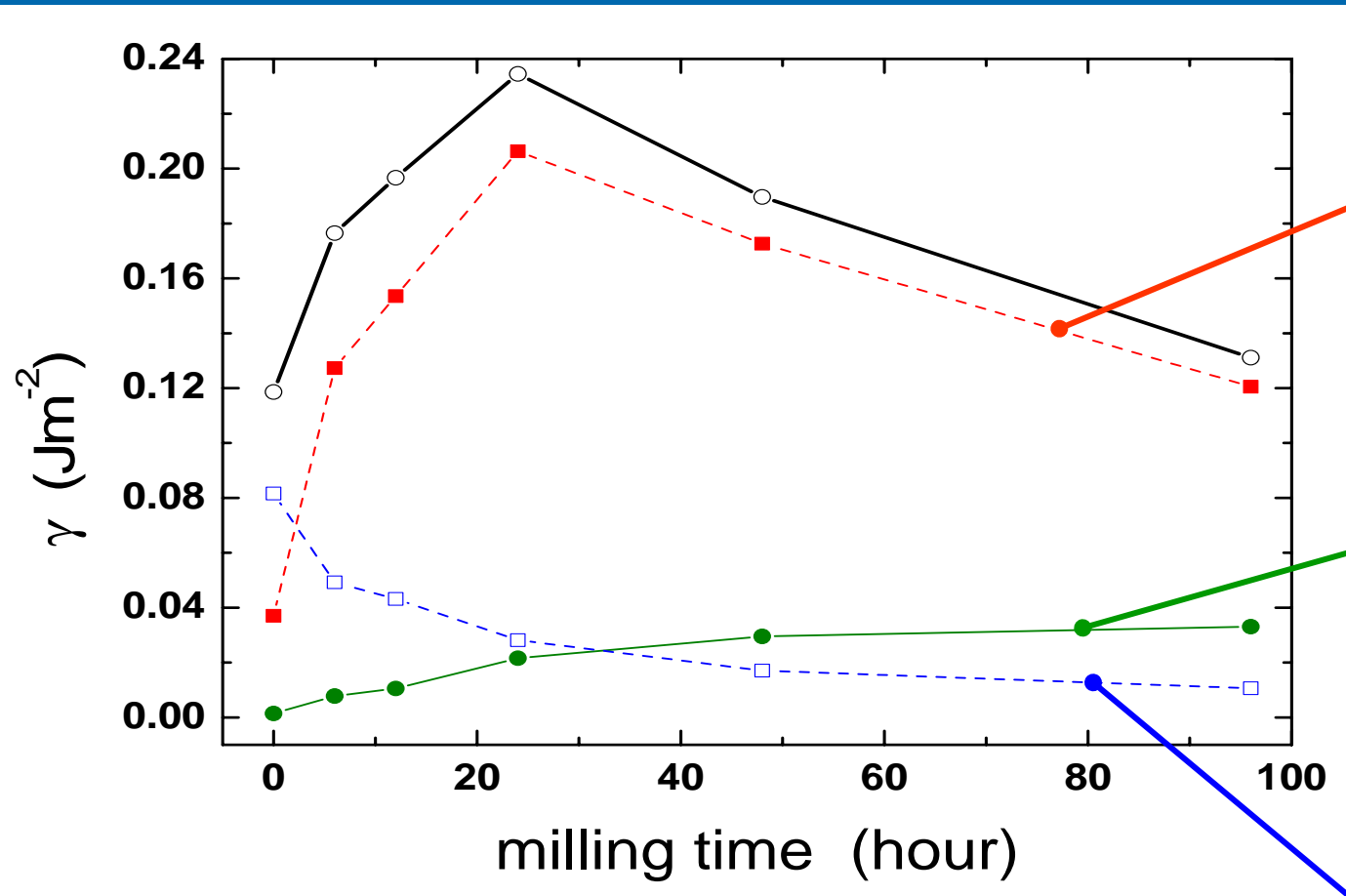
ball milled Ni, TEM evidence

96h ball milling





ball milled Ni, stored energy



GB Dislocations

$$\gamma_{Disl} = \frac{Gb^2 \rho D}{12\pi(1-\nu)} \ln\left(\frac{D}{b}\right)$$

RD Dislocations

$$\gamma_{RD} = AGb^2 \rho \ln\left(\frac{R_e}{b}\right)$$

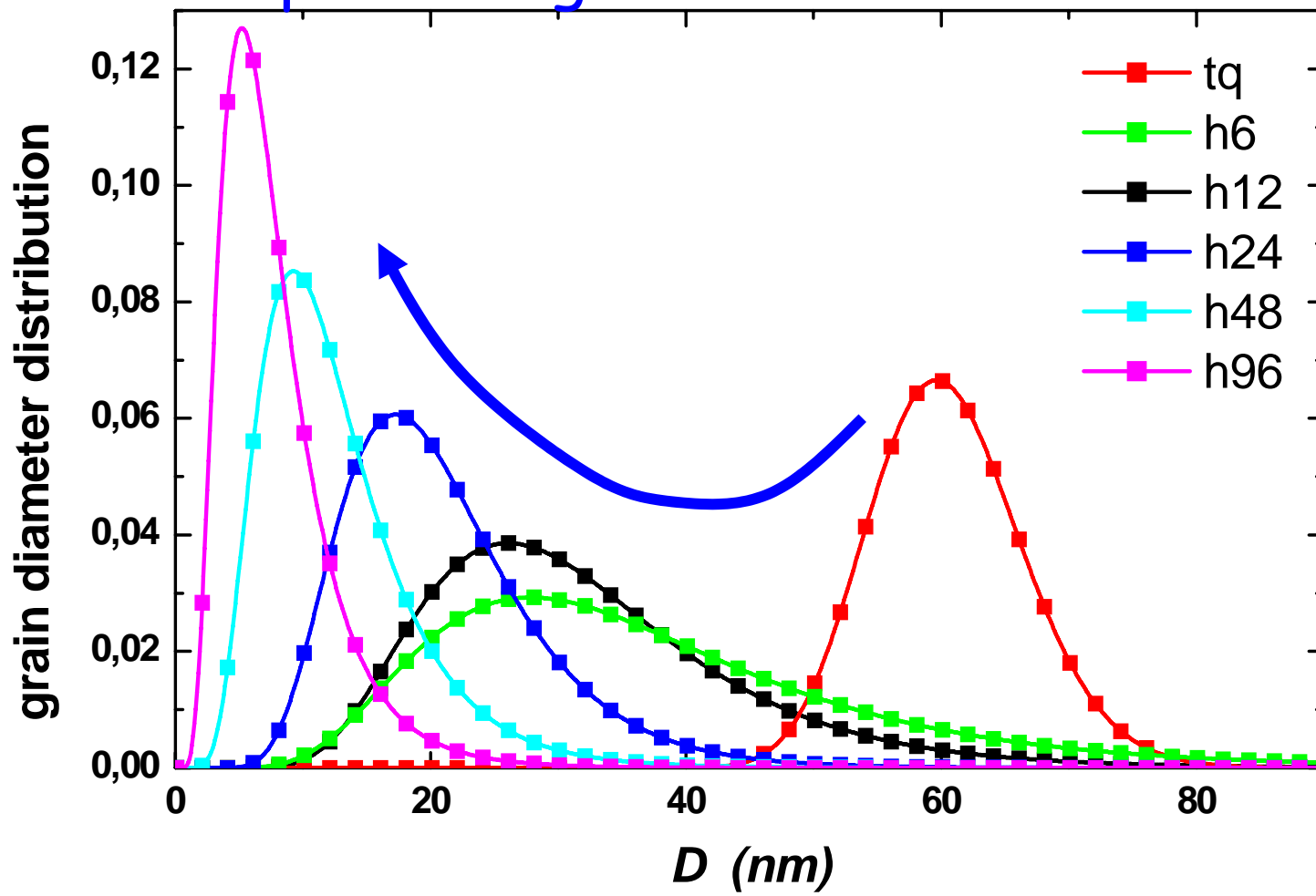
$$\gamma_{Disc} = \frac{G\langle\Omega^2\rangle D \ln 2}{16\pi(1-\nu)}$$

Disclinations



ball milled Ni, WPPM domain size distribution

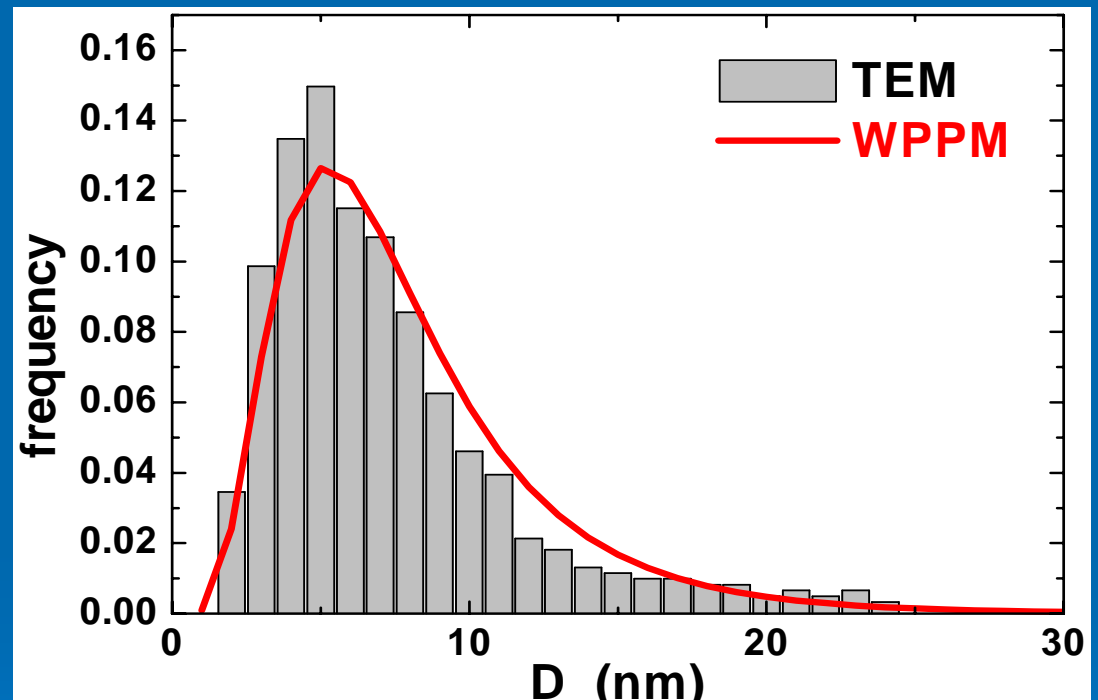
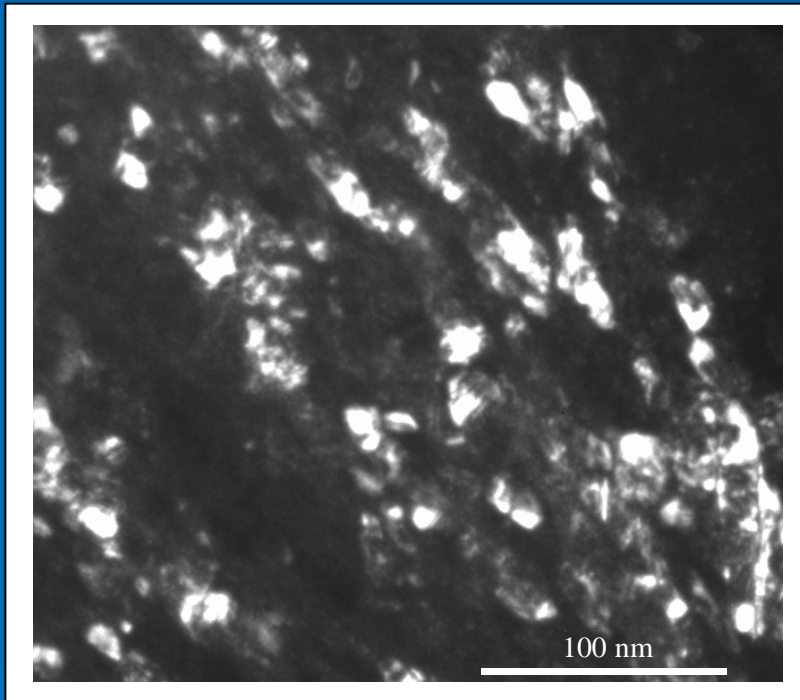
Spherical grain size distributions





ball milled Ni, comparison WPPM-TEM

Nickel powder ball milled for 96 h





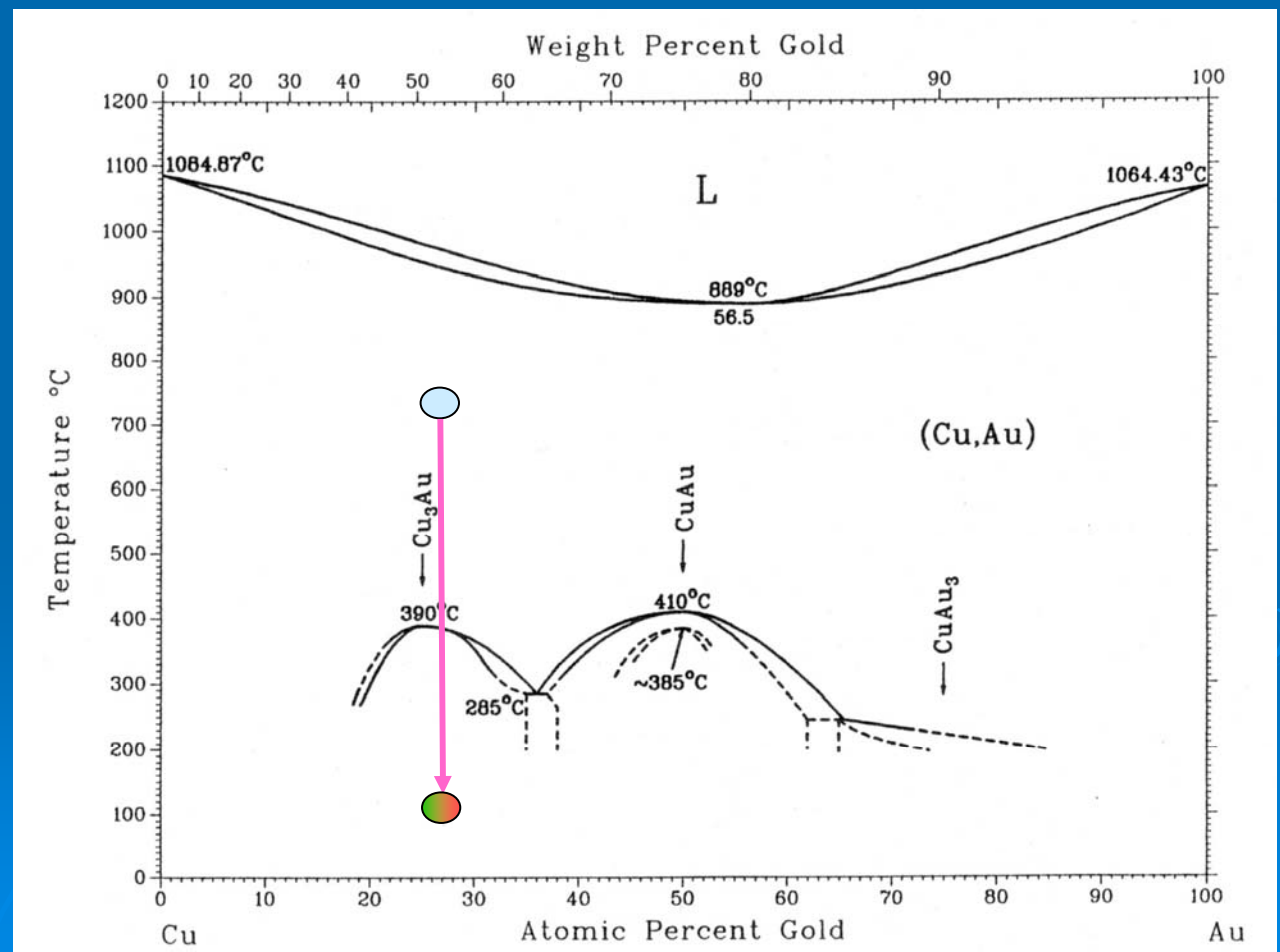
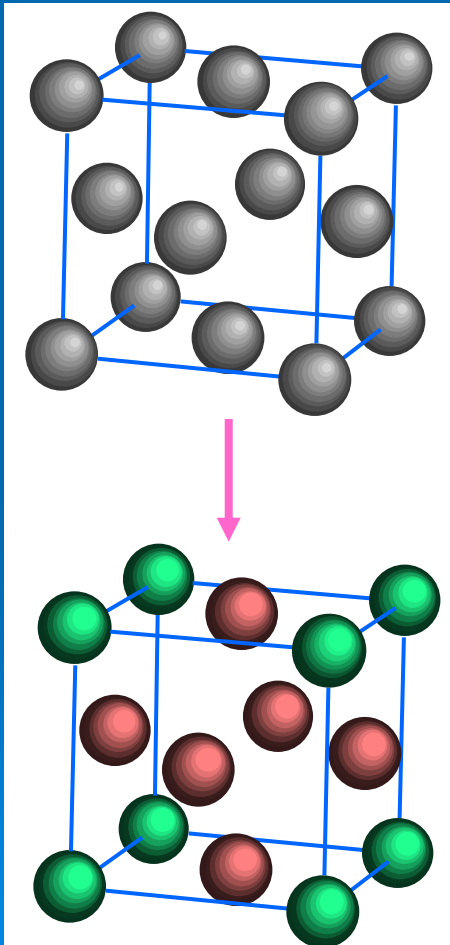
WPPM: applications

- Ball milled nickel powder
- Antiphase domains in Cu_3Au
- Nanocrystalline cerium oxide
- Ball milled Fe-1.5Mo
- Ball milled fluorite



WPPM application: APBs in Cu₃Au

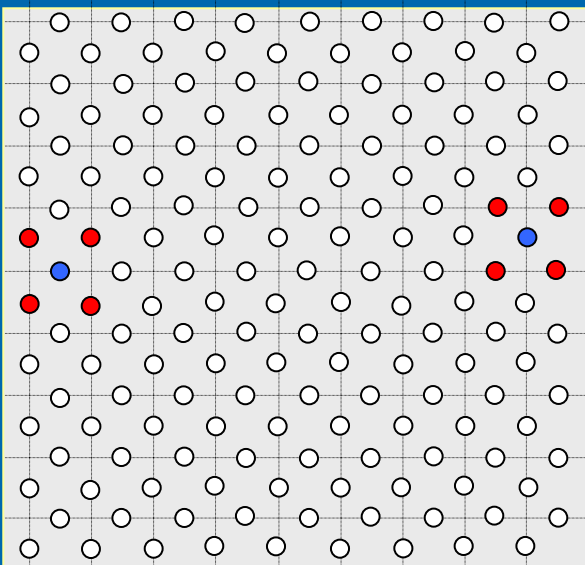
Anti Phase Domains form during the ordering process in Cu₃Au. The o/d process can be thermally activated





Antiphase boundaries

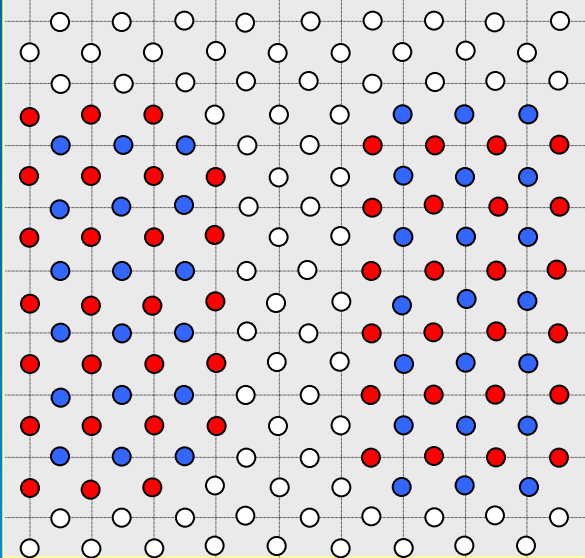
(1)



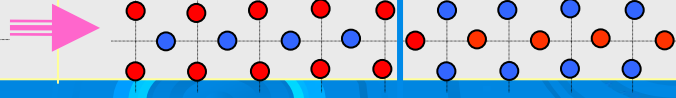
(2)

- 'Statistical' Cu(3/4) Au(1/4)
- Cu
- Au

(3)



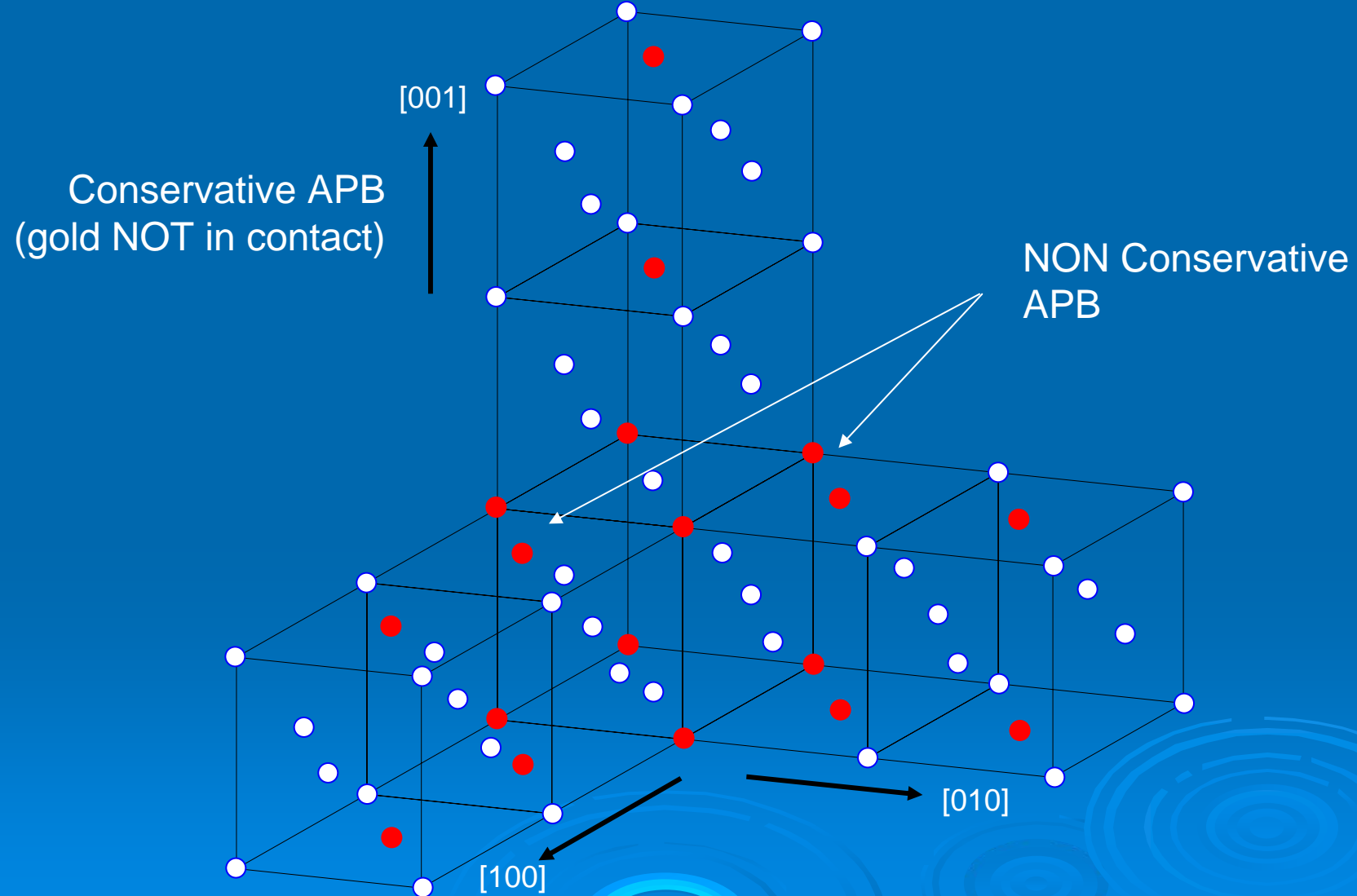
(4)



APB

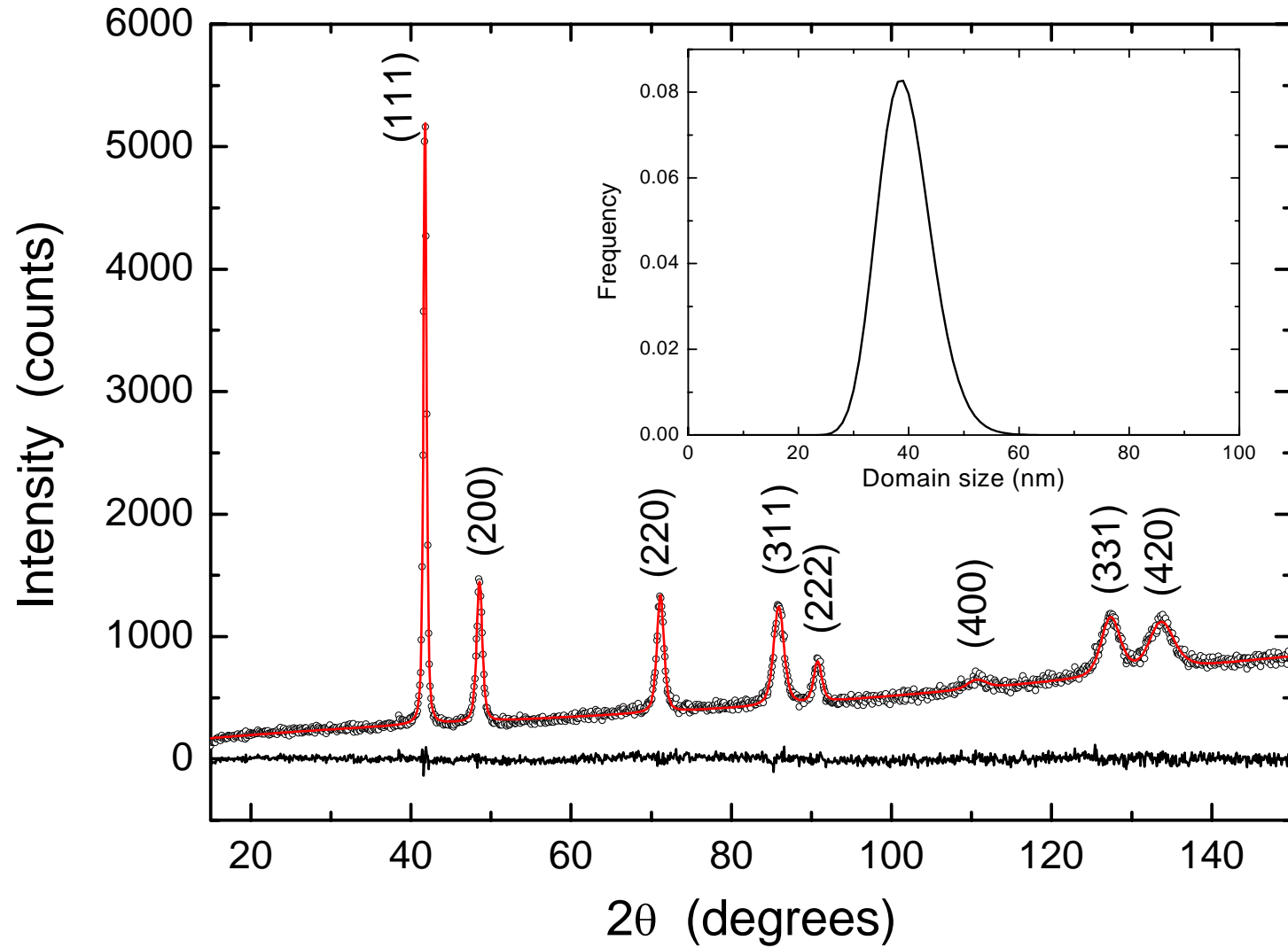


Conservative/non conservative APBs



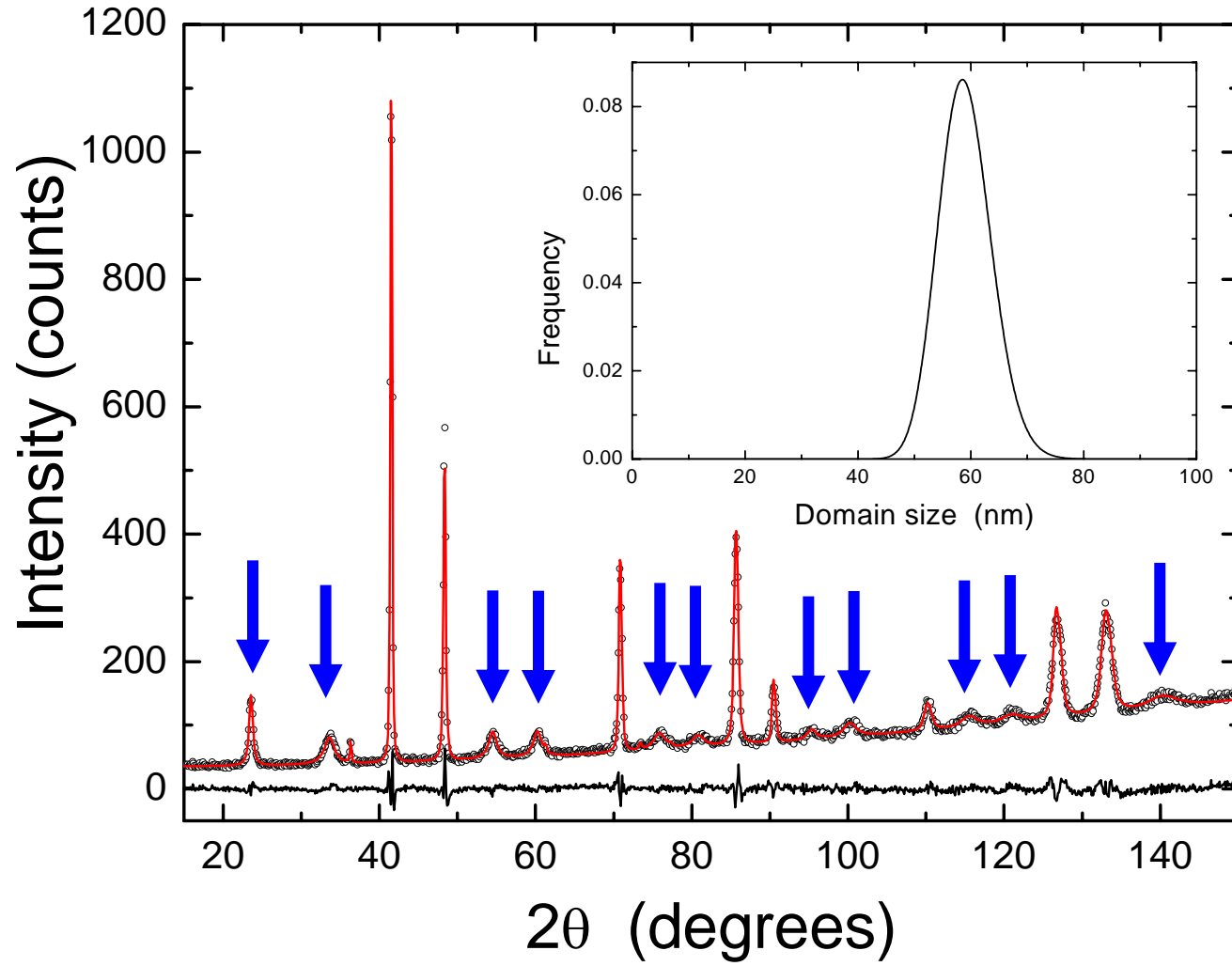


Disordered phase



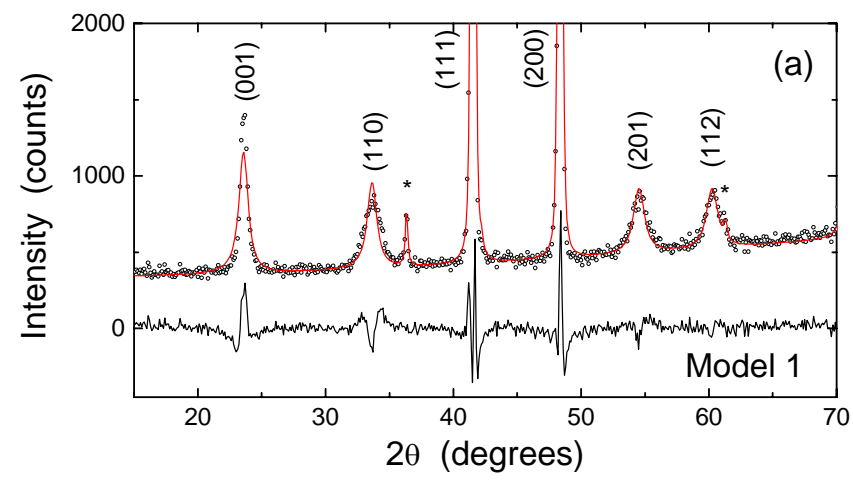
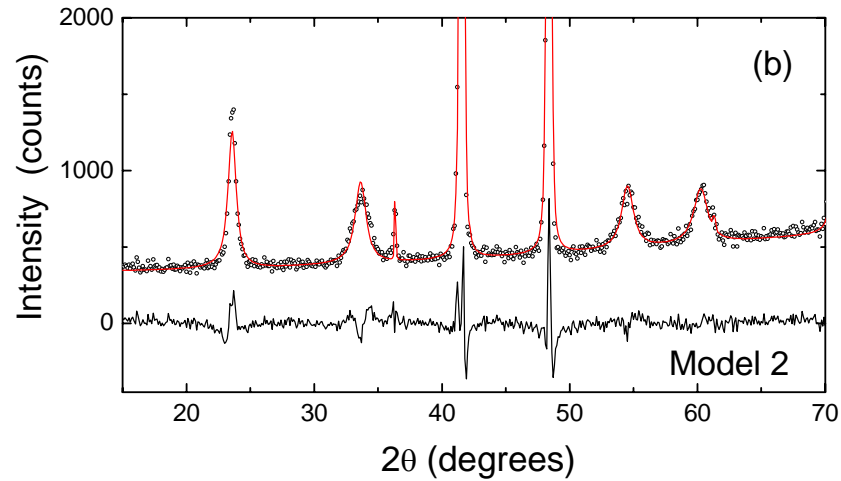
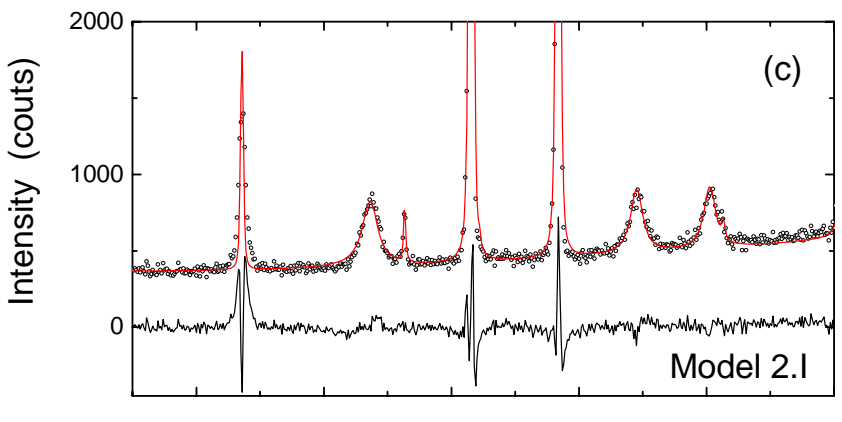
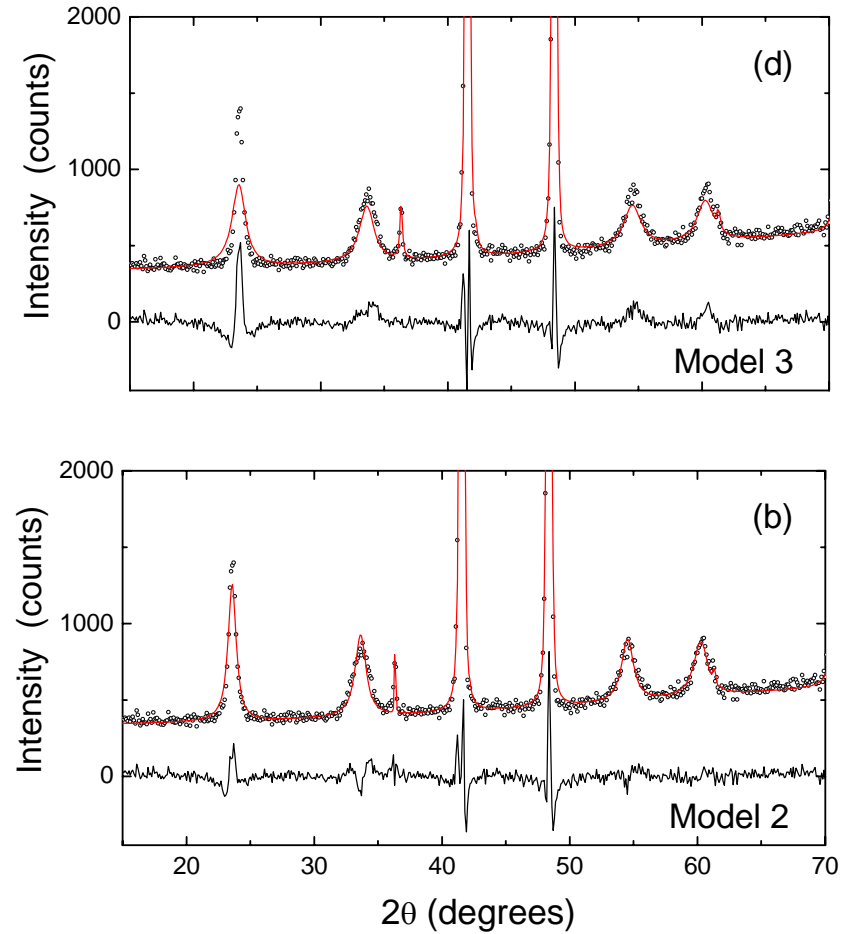


Ordered phase





Various models used in WPPM





WPPM results

	As received (disordered phase)	Thermally treated (ordered phase)
Average dislocation density, ρ [m ⁻²]	9.2(6) x10 ¹⁵	4.7(10) x10 ¹⁴
Effective outer cut-off radius, R_e [nm]	26(4)	1150(50)
Wilkins arrangement parameter	2.5(3)	25(1)
Effective edge fraction, f_E	0.66(7)	0.99(10)
Deformation fault probability, α [%]	0.7(1)	-
Average domain size [nm]	39.5(5)	59.0(5)
APDB model 2.I, δ' [%]	-	2.7(17)
APDB model 2.II, δ'' [%]	-	4.3(15)
Cu ₂ O phase content [wt%]	-	1.4(5)
Unit cell parameter, a_0 [nm]	0.3750(2)	0.3755(1)
R _{wp} [%]	5.09	6.25
R _{exp} [%]	4.25	5.07
GoF	1.20	1.23

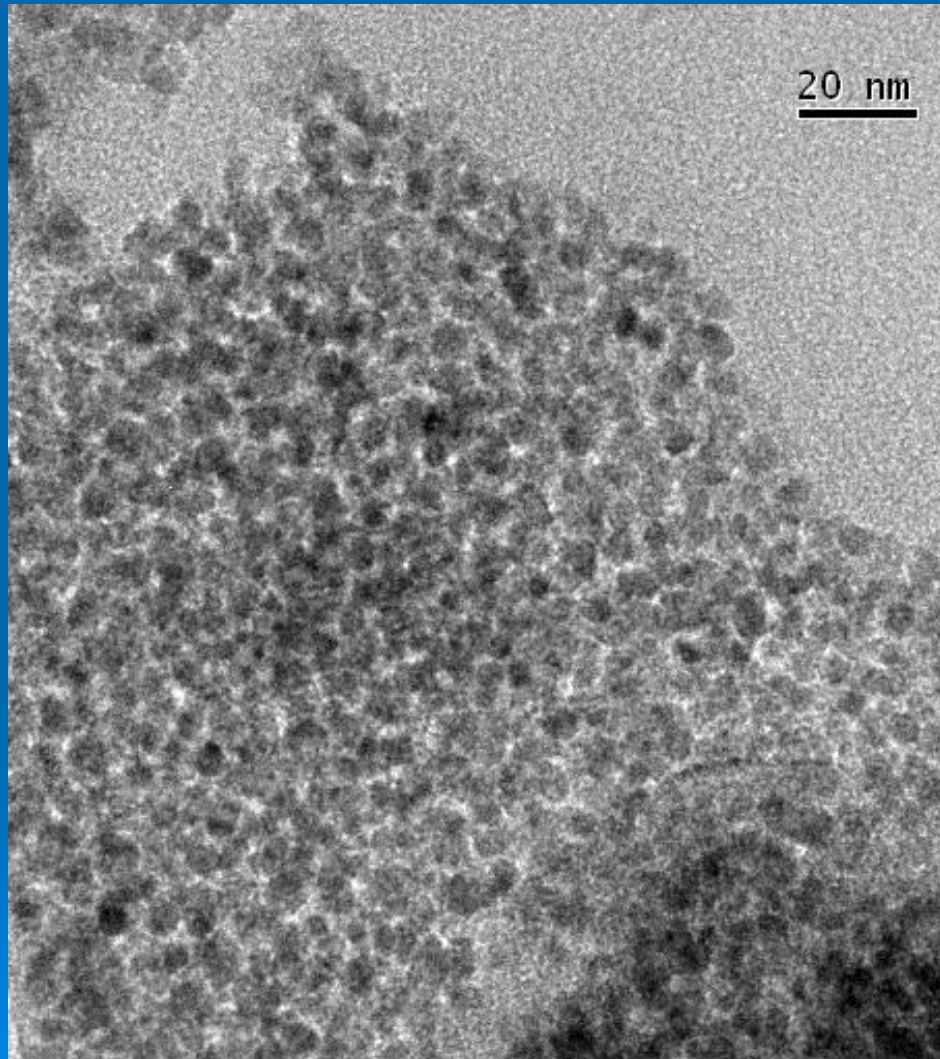


WPPM: applications

- Ball milled nickel powder
- Antiphase domains in Cu_3Au
- Nanocrystalline cerium oxide
- Ball milled Fe-1.5Mo
- Ball milled fluorite

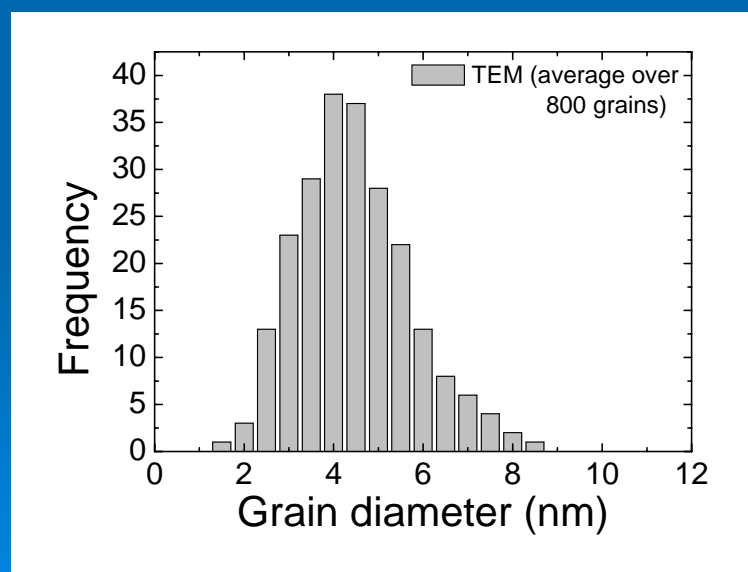


nanocrystalline CeO_2 , TEM



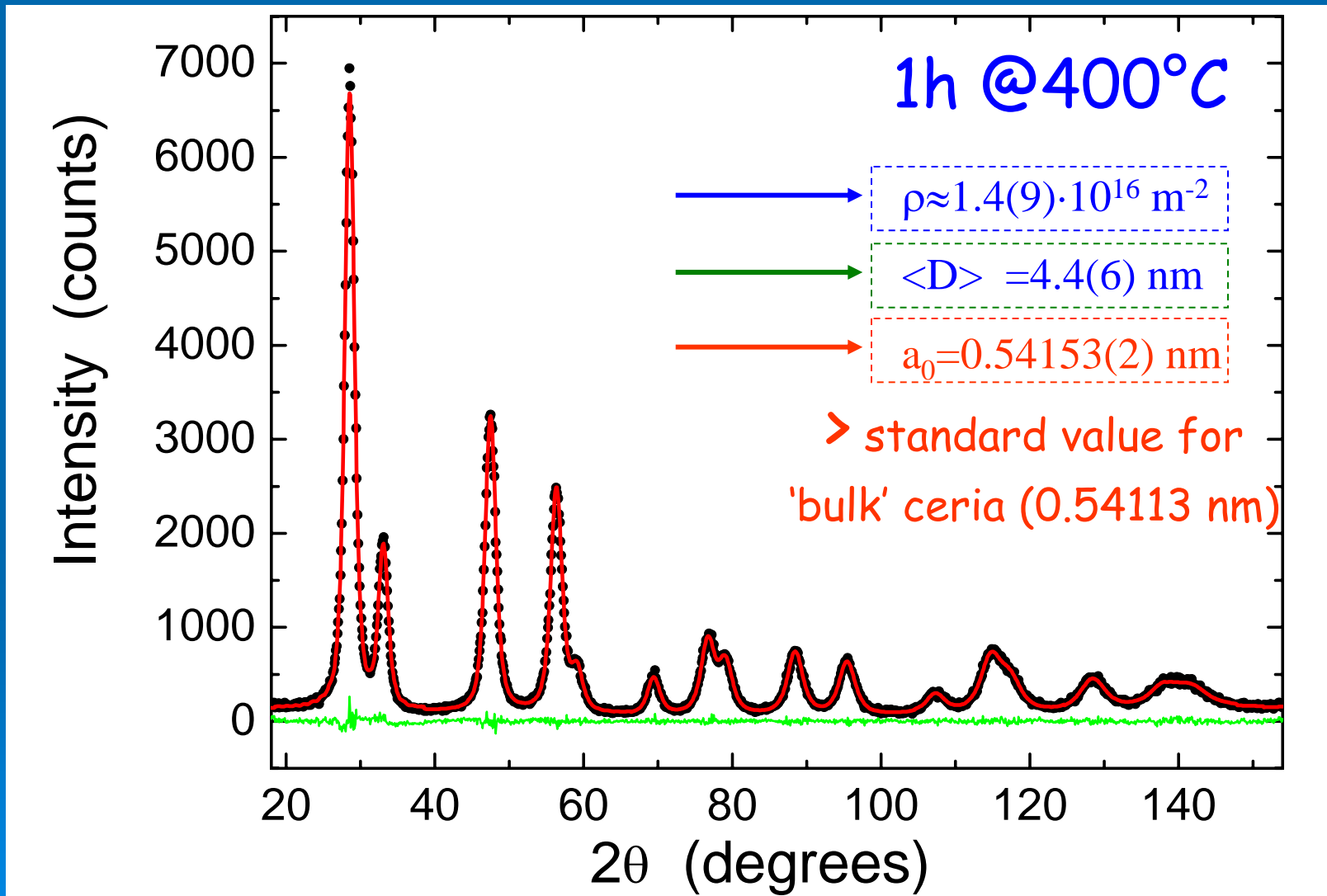
CeO_2 calcinated at
400°C for 1h

Grains are almost
spherical and well
separated



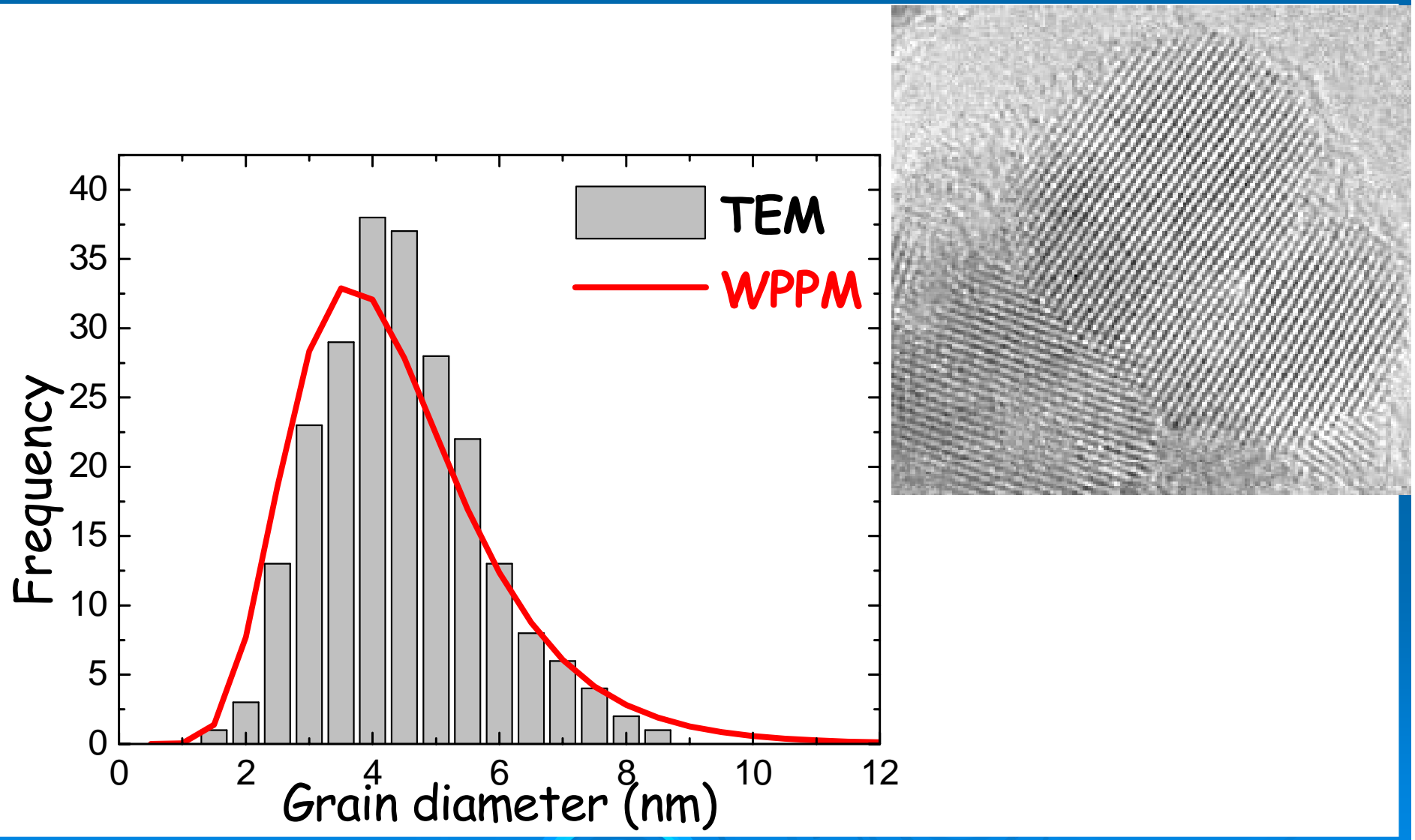


nanocrystalline CeO_2 , WPPM



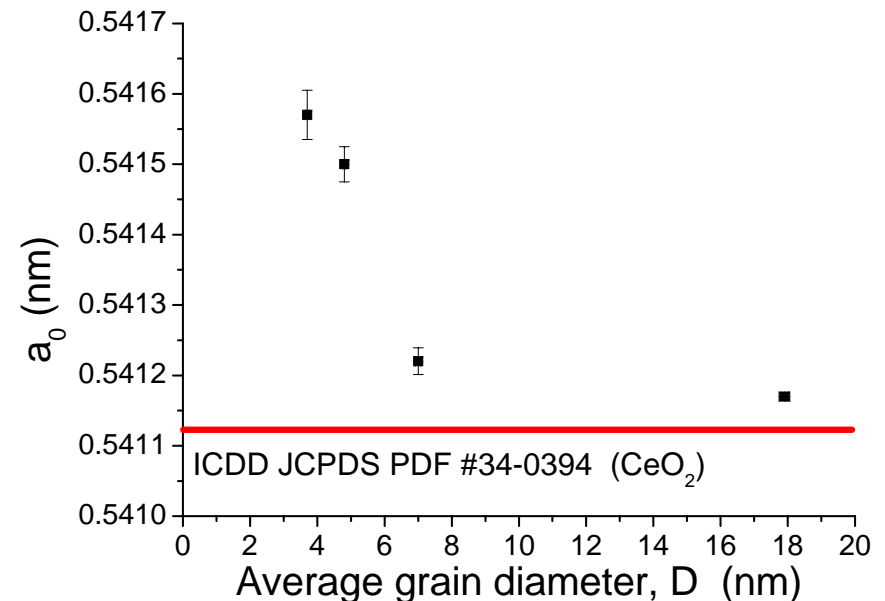
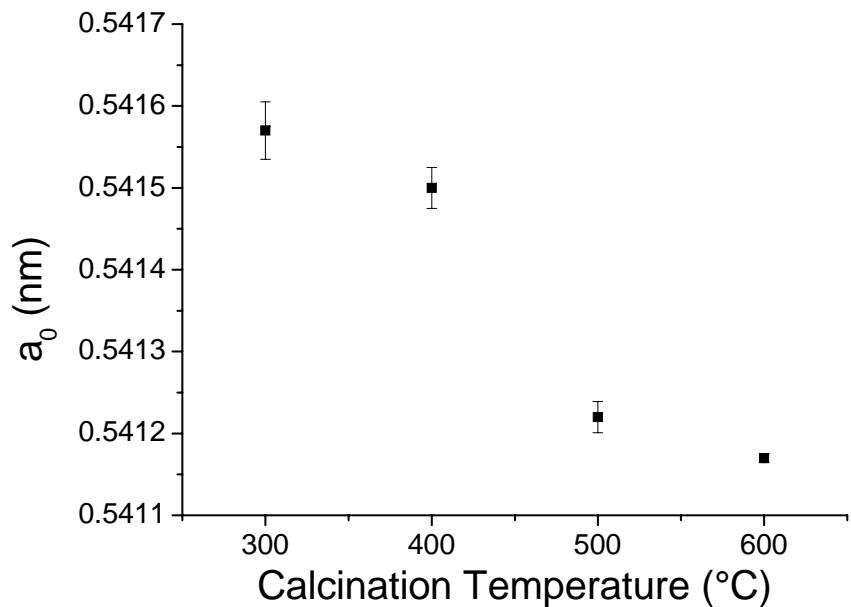


nanocrystalline CeO_2 , WPPM vs. TEM





nanocrystalline CeO_2 , WPPM result



Refined cell parameters increase with decreasing average grain diameter



nanocrystalline CeO_2 , surface effects

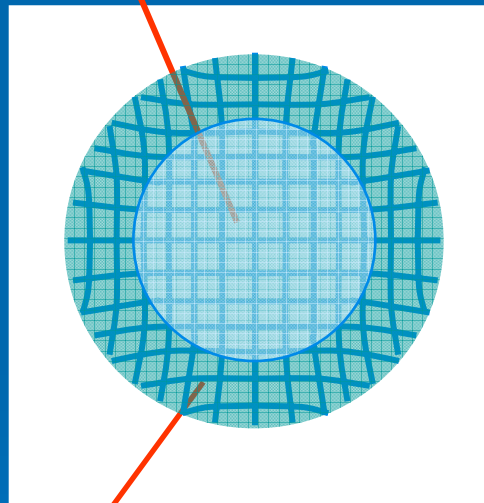
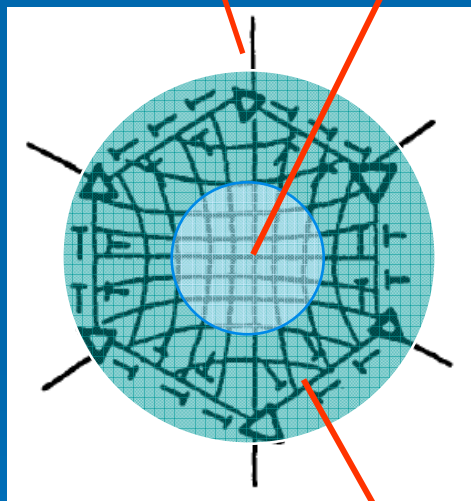
grain in polycrystalline sample

grain of powder

Disclinations

Unaltered core

Altered corona

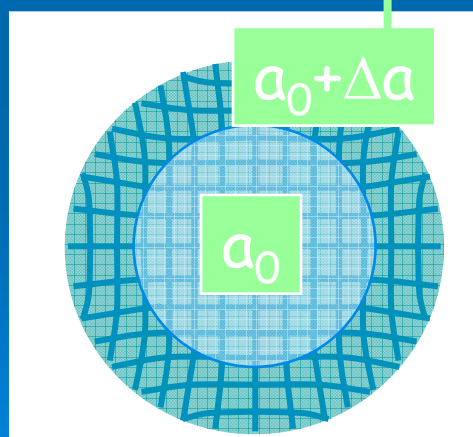




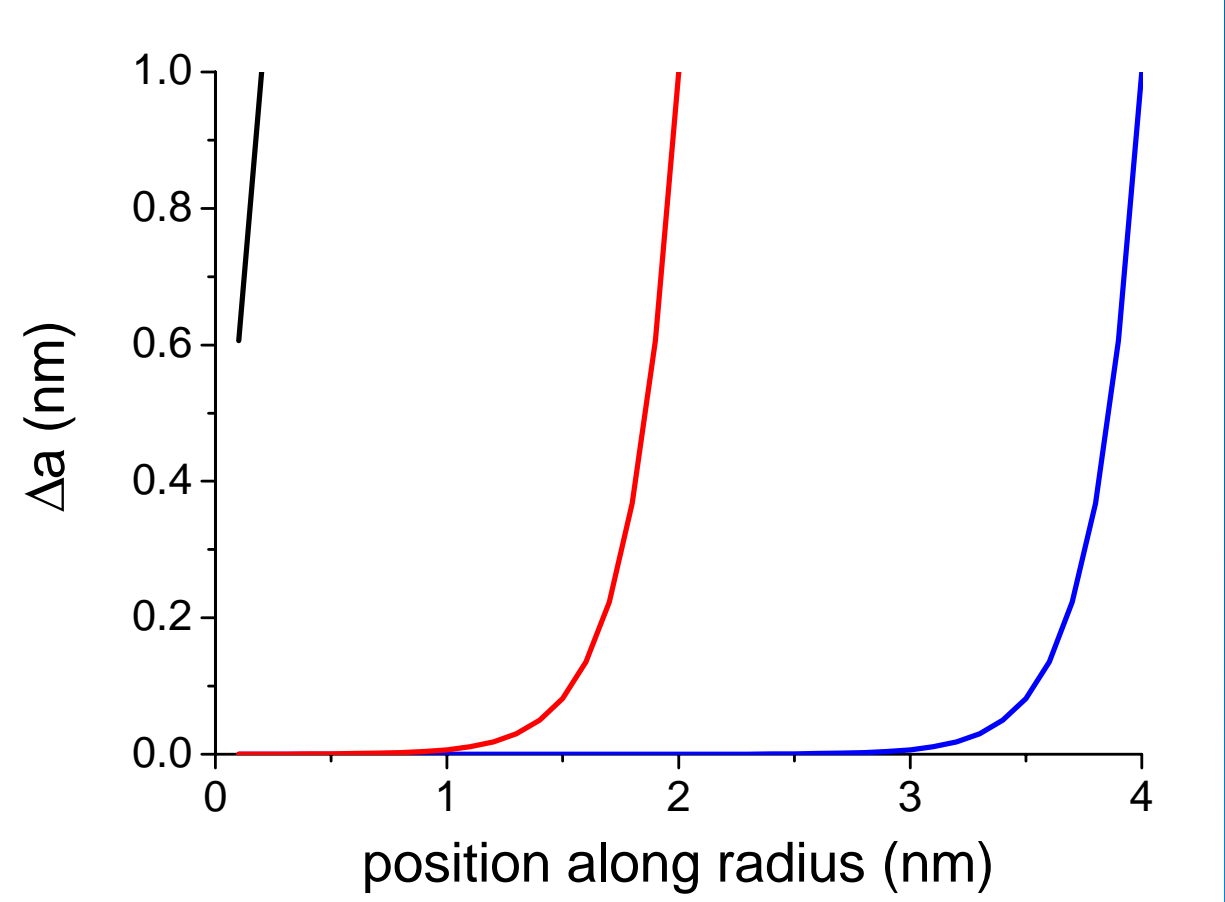
nanocrystalline CeO_2 , surface relaxation

$$\Delta d = \frac{\Delta a}{\sqrt{h^2 + k^2 + l^2}}$$

$$\Delta a = \xi \frac{x}{|x|} e^{-\frac{R-|x|}{\kappa}}$$



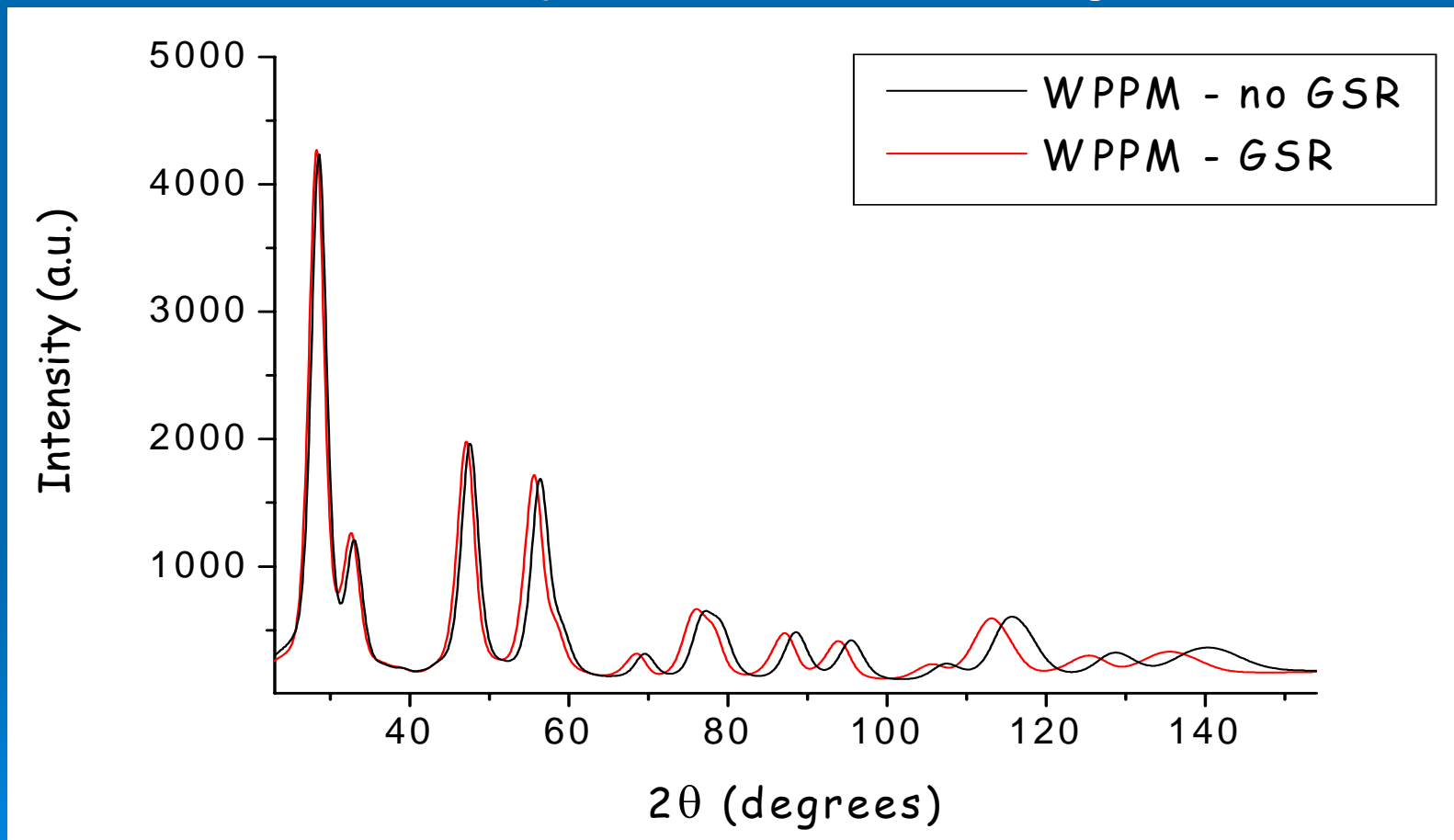
Shift of atomic layers in the outer corona





WPPM: surface relaxation effect

Simulation for CeO_2 , lognormal distribution of spheres (average 3nm, lognormal variance 0.3), surface relaxation ($A=0.05\text{nm}$, affected zone $B=0.3\text{ nm}$), dislocations (10^{16} m^{-2} , $R_e=3\text{nm}$), twins (1%) and stacking faults (2%)



Main effect of GSR is peak shift (a_0 changes)



nanocrystalline CeO_2 , WPPM result

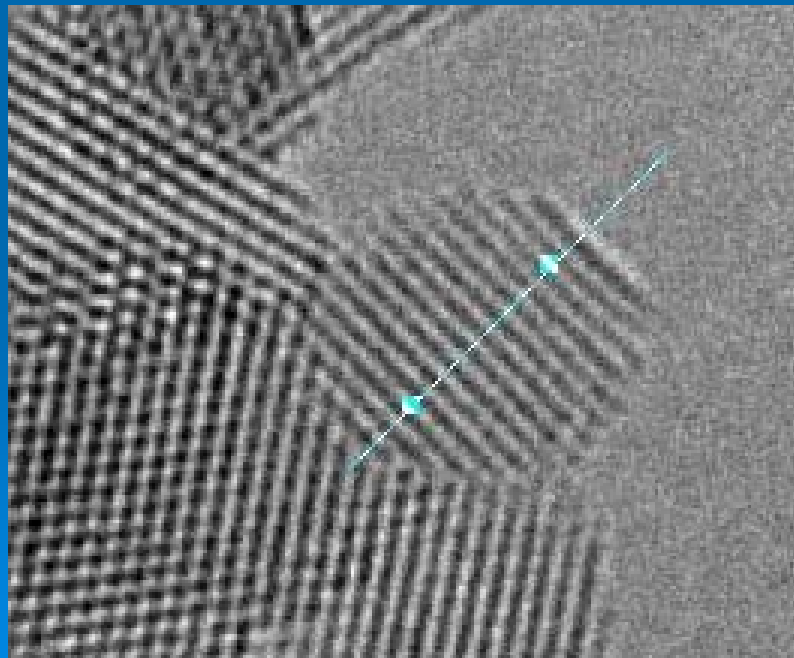
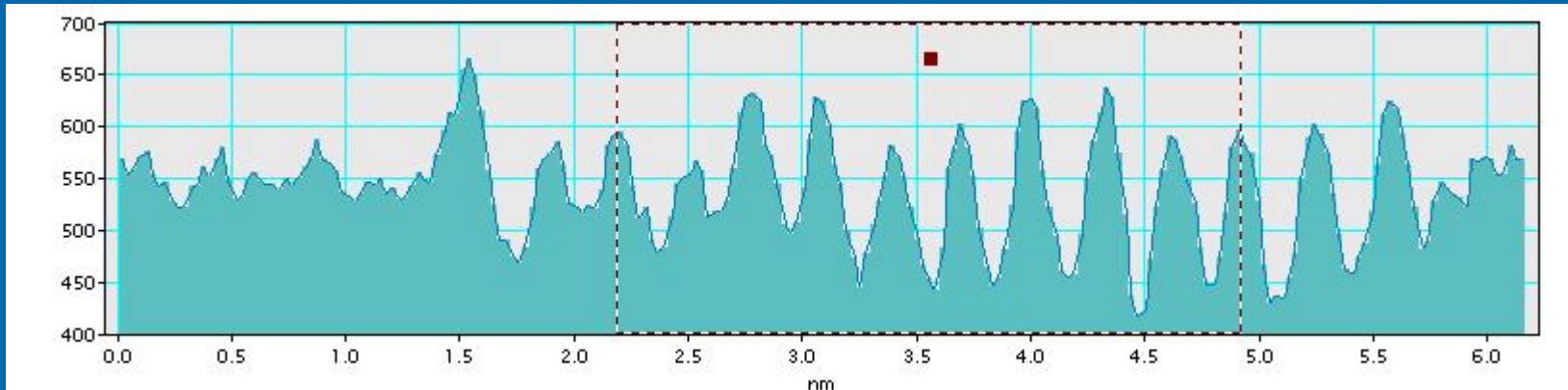
		WPPM	GSR-WPPM°
CELL PARAMETER			
cell parameter	(nm)	0.54153(3)	0.541134
SIZE DISTRIBUTION (spherical grains)			
lognormal μ		1.41(2)	1.42(1)
lognormal σ		0.355(7)	0.364(6)
average diameter	(nm)	4.37(1)	4.40(6)
DISLOCATIONS			
dislocation density	(m ⁻²)	1.4(10) 10 ¹⁶	1.08(4) 10 ¹⁶
edge dislocations content	(%)	50	50
cutoff radius R_e	(nm)	2(1)	3(1)
A (from elastic constants)		0.1187	0.1187
B (from elastic constants)		0.1618	0.1618
Wilkins parameter M		0.25(1)	0.31(3)
GRAIN SURFACE RELAXATION			
relaxation factor ξ	(nm)		0.008(3)
decay constant κ	(nm)		0.16(4)
STATISTICAL ESTIMATORS			
Rwp		5.51	5.58
Rexp		4.67	4.67
GOF		1.18	1.20

fixed!

(°) structural constraint

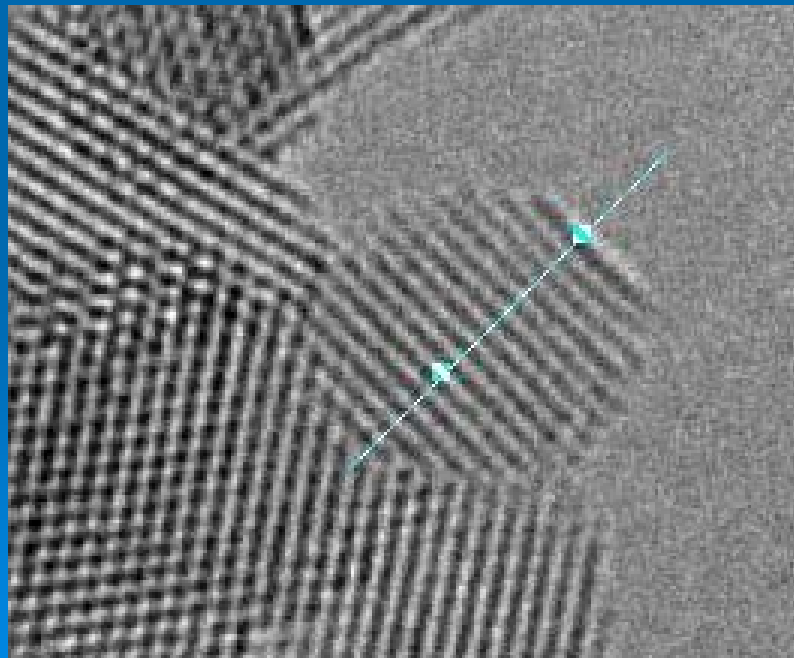
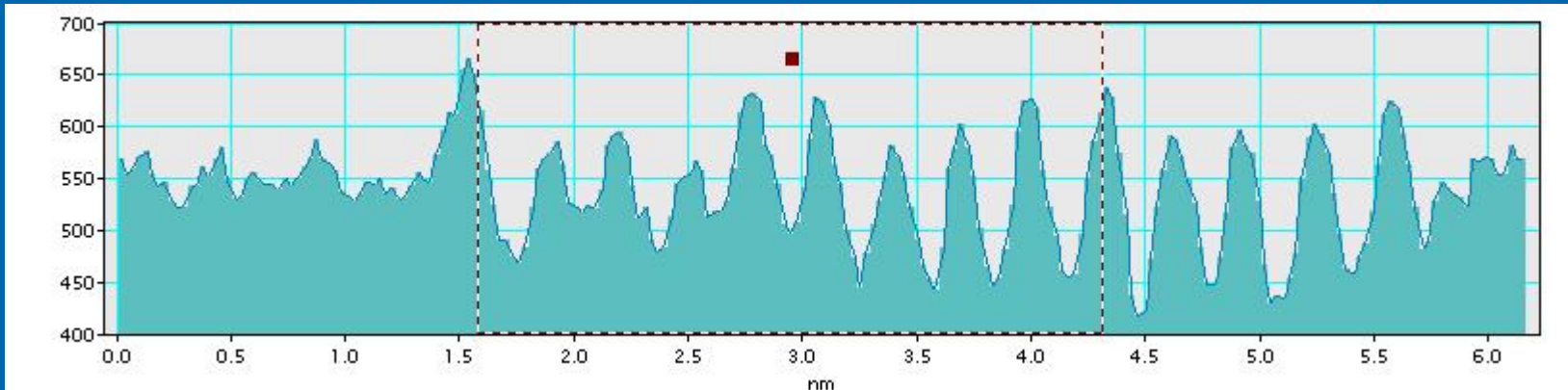


nanocrystalline CeO_2 , TEM evidence



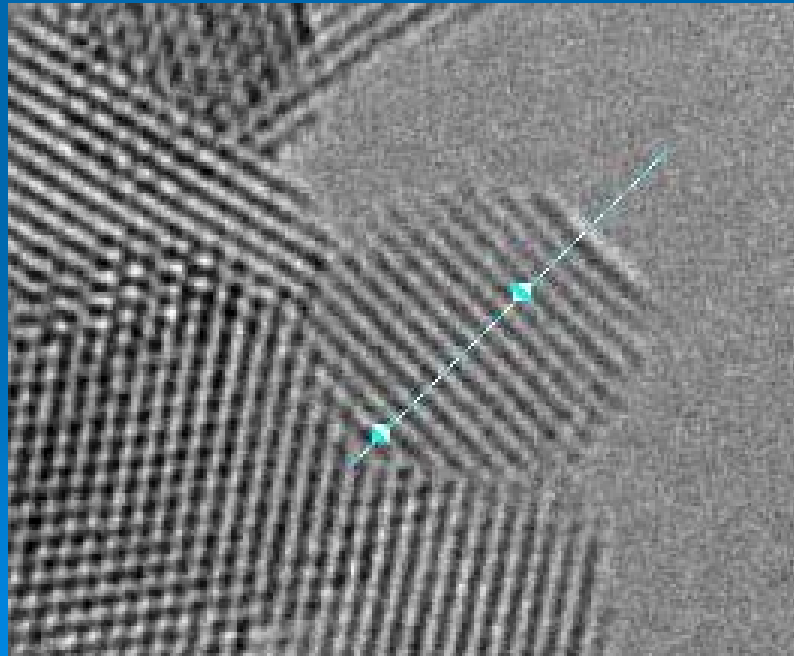
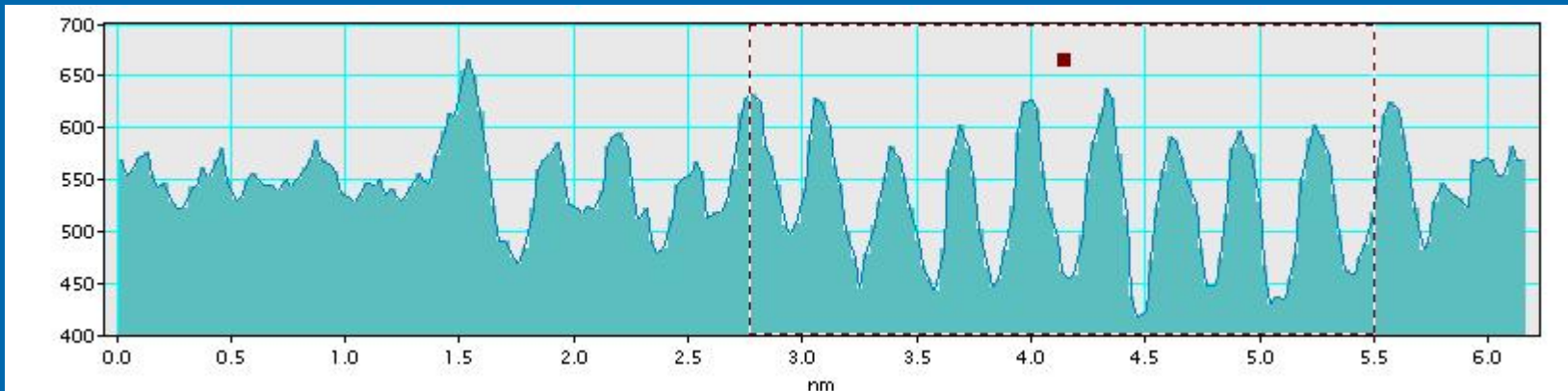


nanocrystalline CeO_2 , TEM evidence



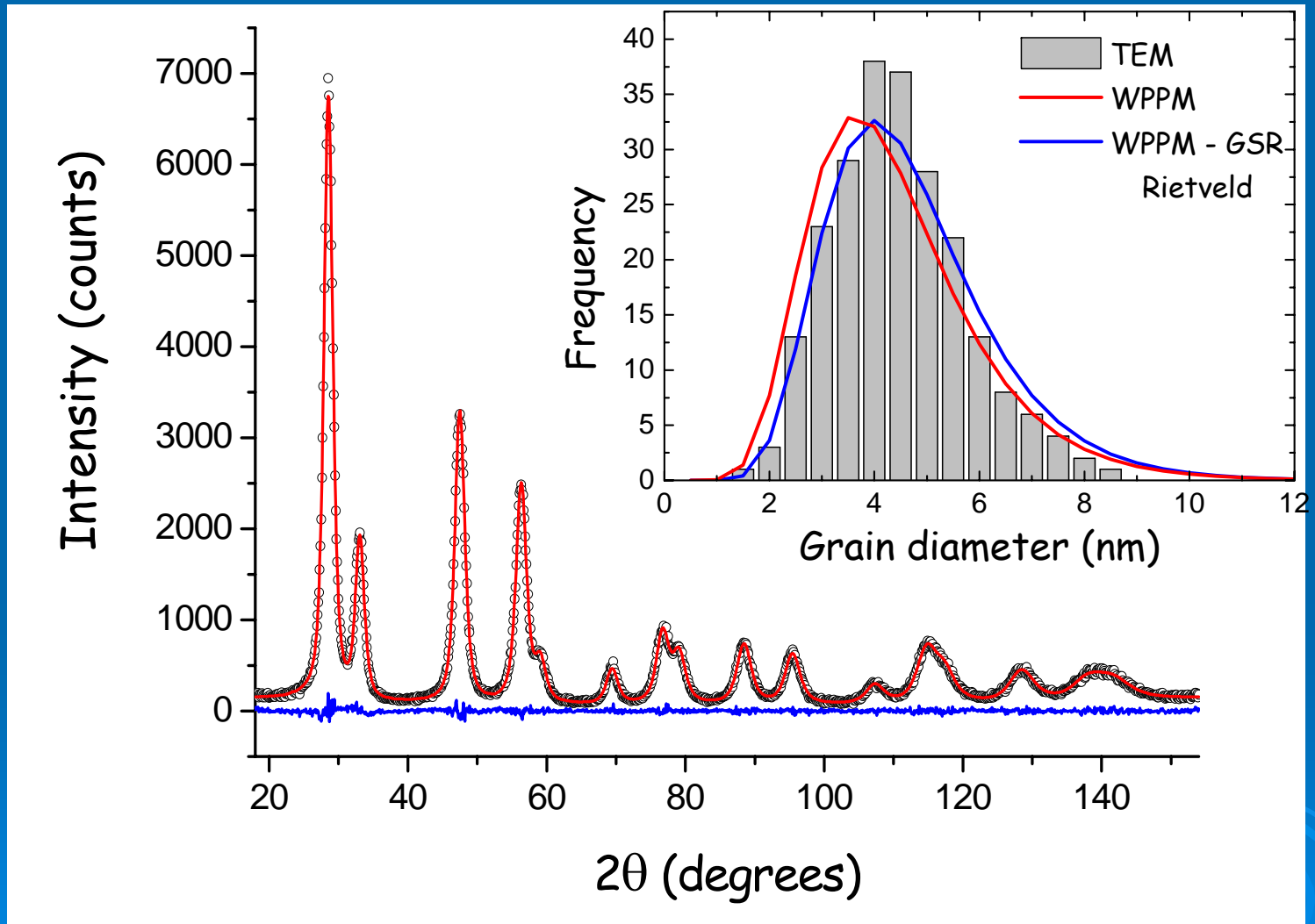


nanocrystalline CeO_2 , TEM evidence





nanocrystalline CeO_2 , WPPM vs. TEM

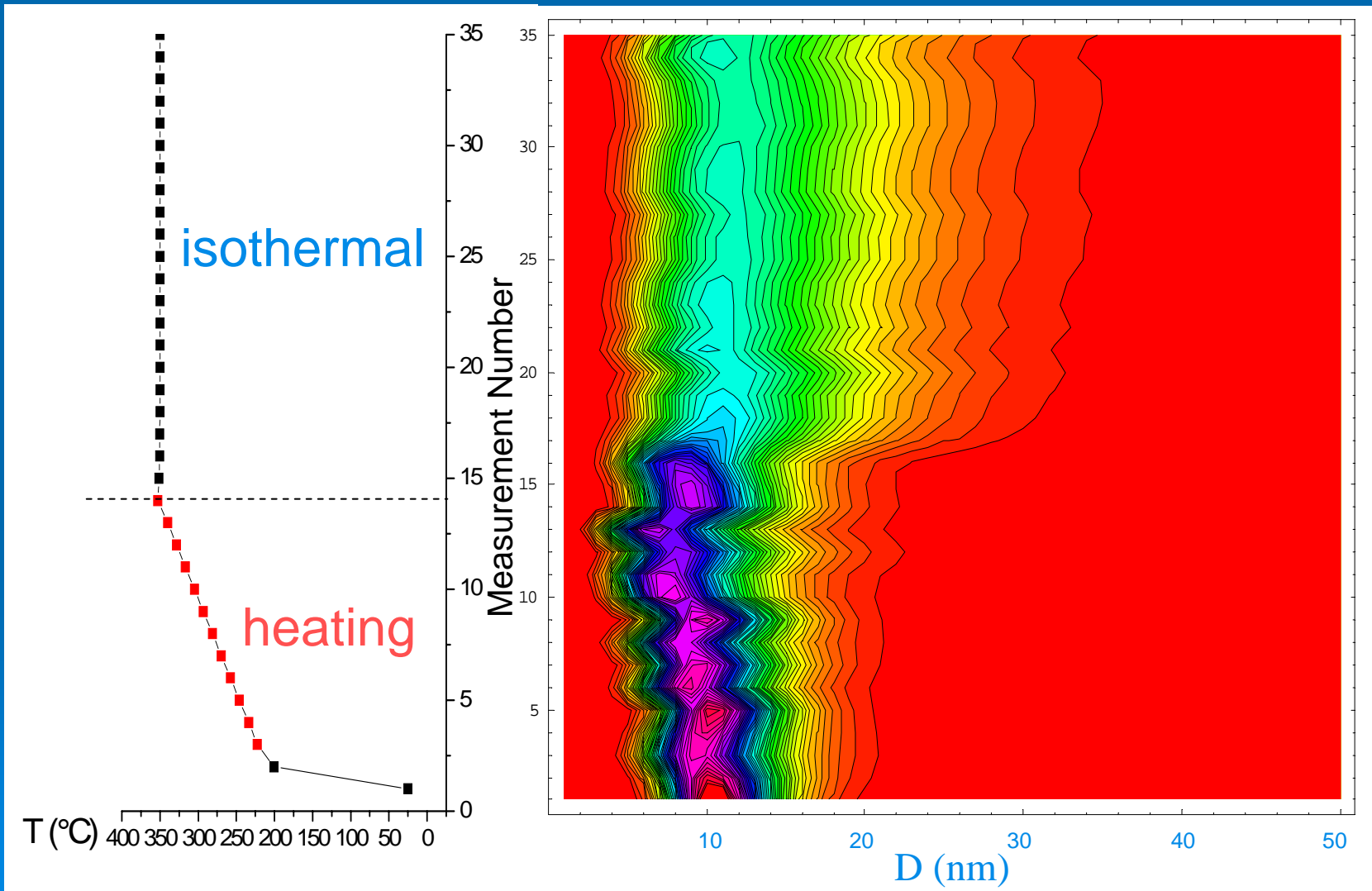


Structure + Microstructure refinement



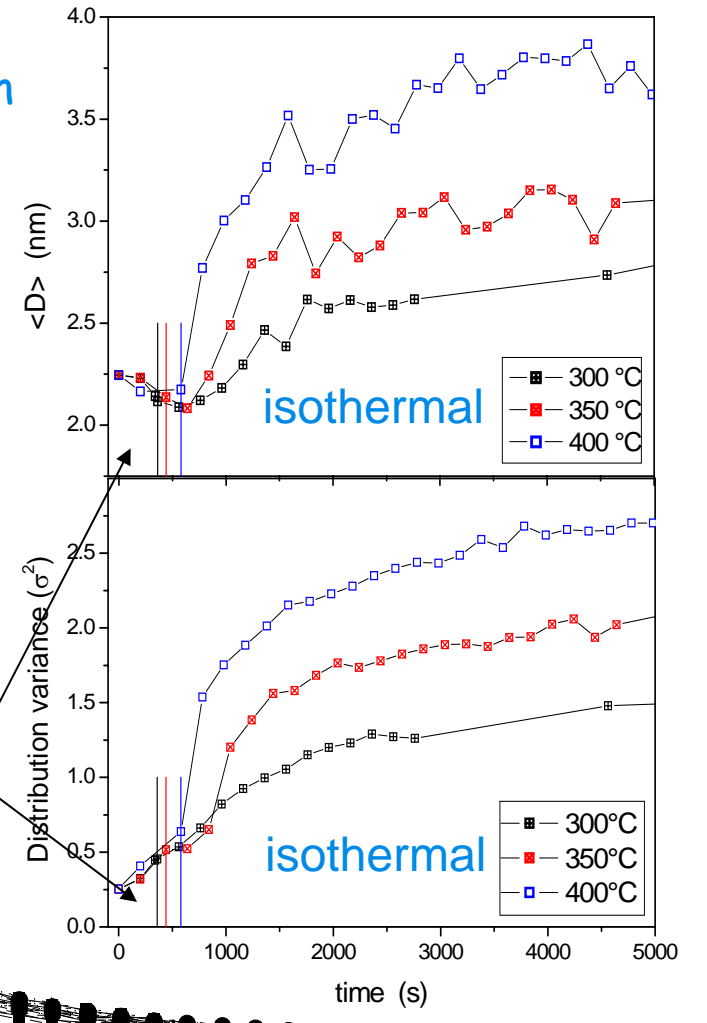
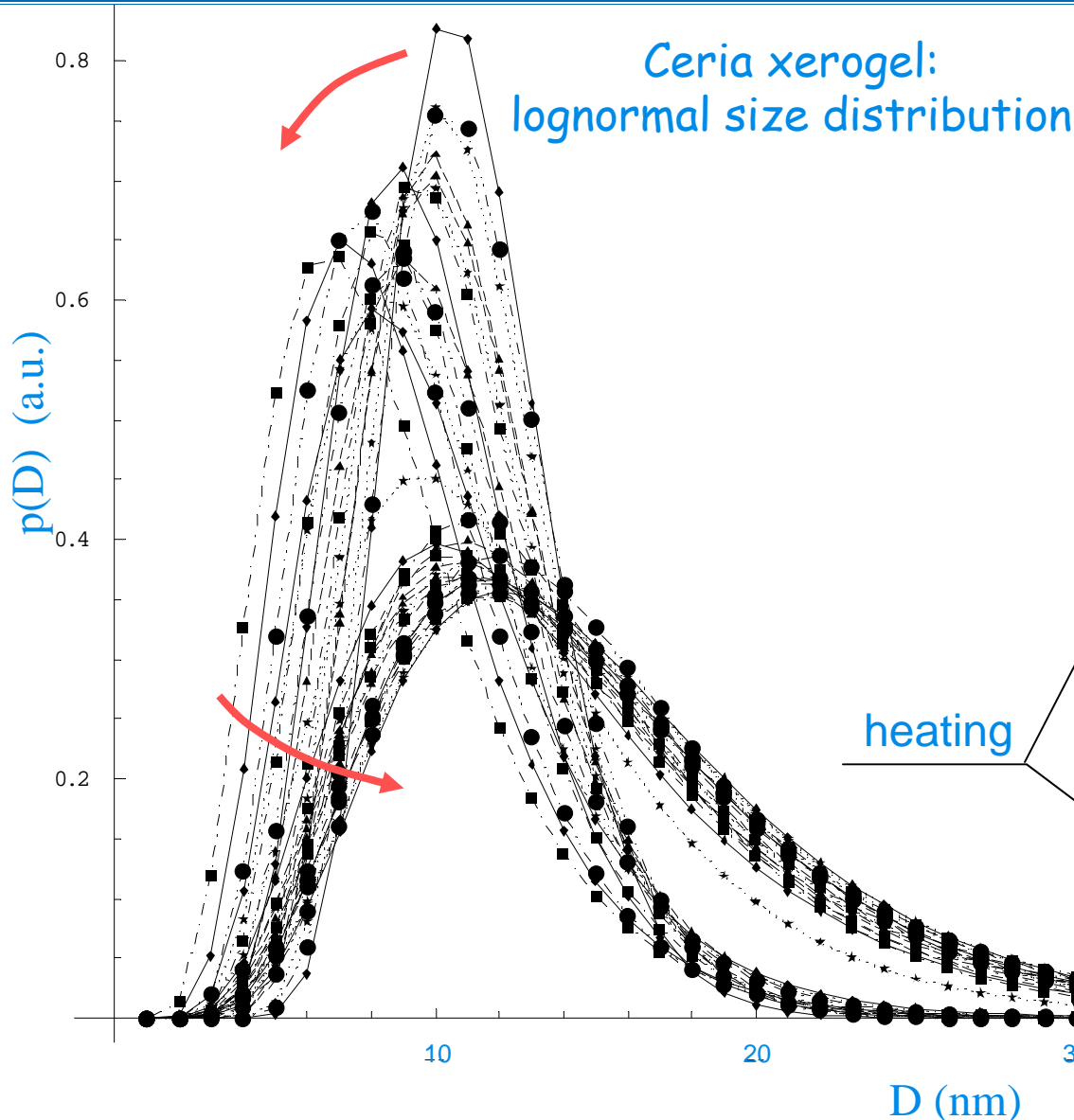
nanocrystalline CeO_2 , heating

Ceria xerogel heating and isothermal treatment: lognormal size distribution





nanocrystalline CeO_2 , heating





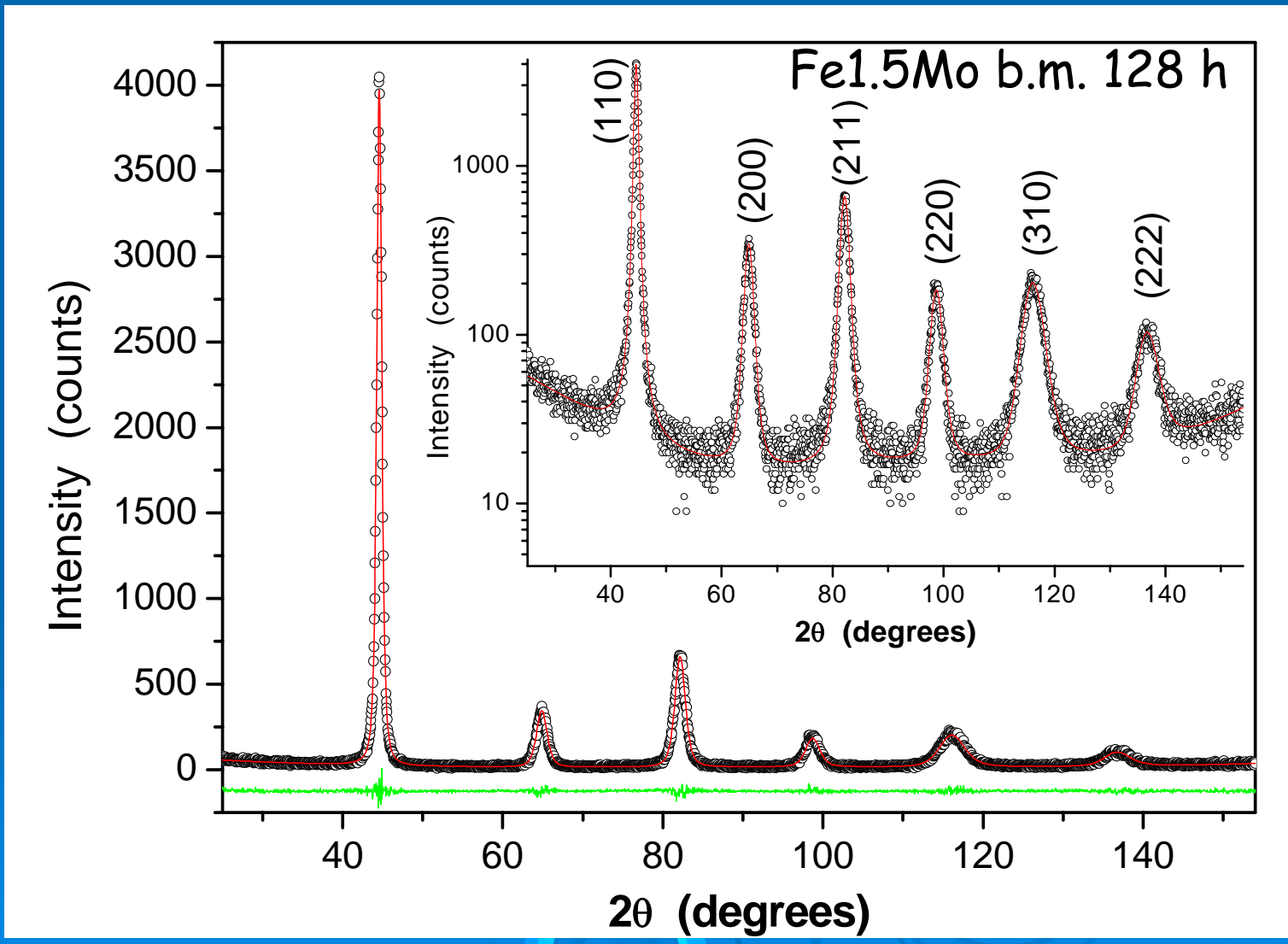
WPPM: applications

- Ball milled nickel powder
- Antiphase domains in Cu_3Au
- Nanocrystalline cerium oxide
- Ball milled Fe-1.5Mo
- Ball milled fluorite



Laboratory XRD result

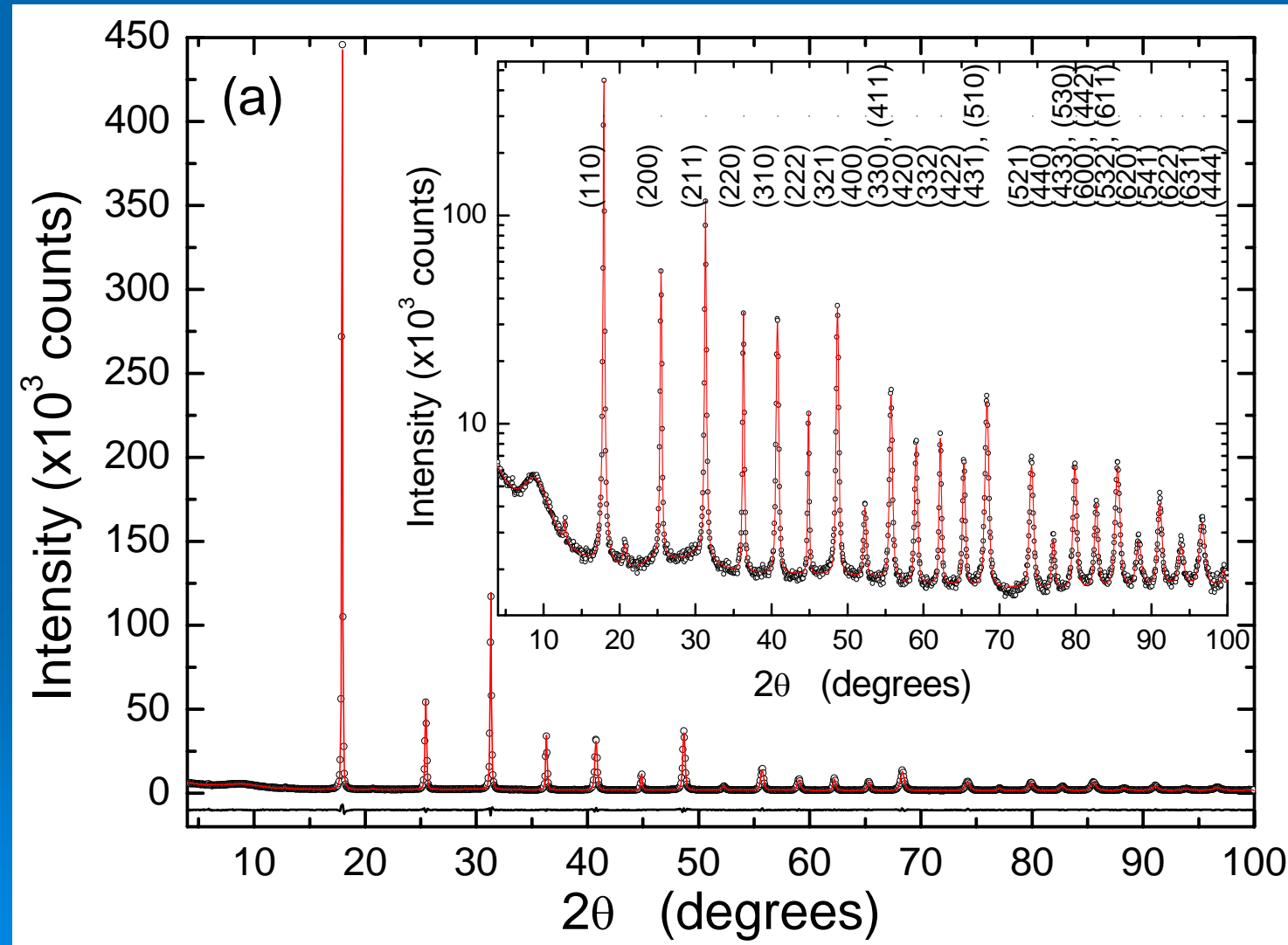
WPPM modelling result for a Fe1.5Mo powder milled 128h





SR XRD result (16h milling)

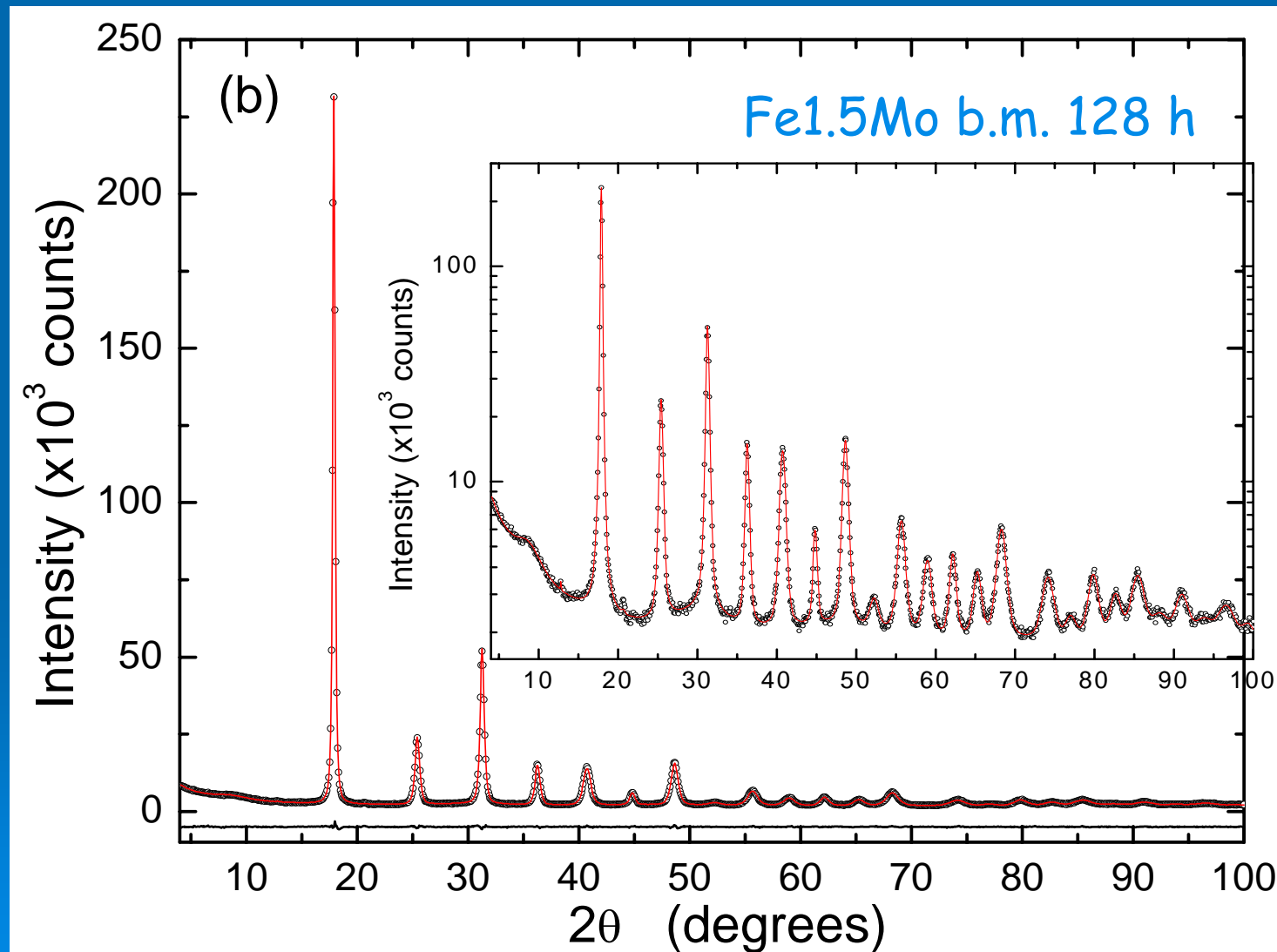
Fe1.5Mo powder ball-milled for **16 hours** in a Fritsch P4 planetary mill





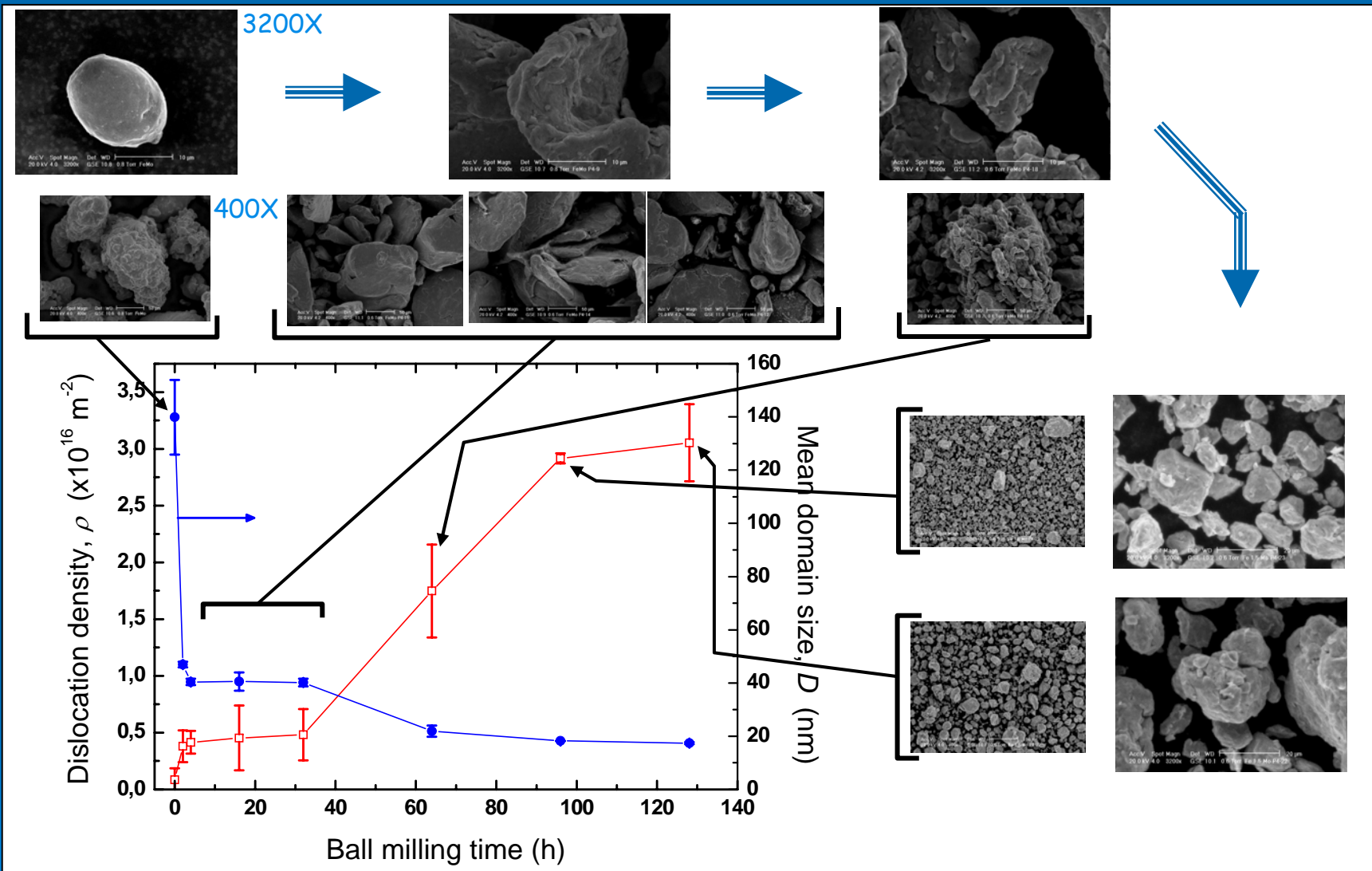
SR XRD result (96h milling)

Fe1.5Mo powder ball-milled for **96 hours** in a Fritsch P4 planetary mill





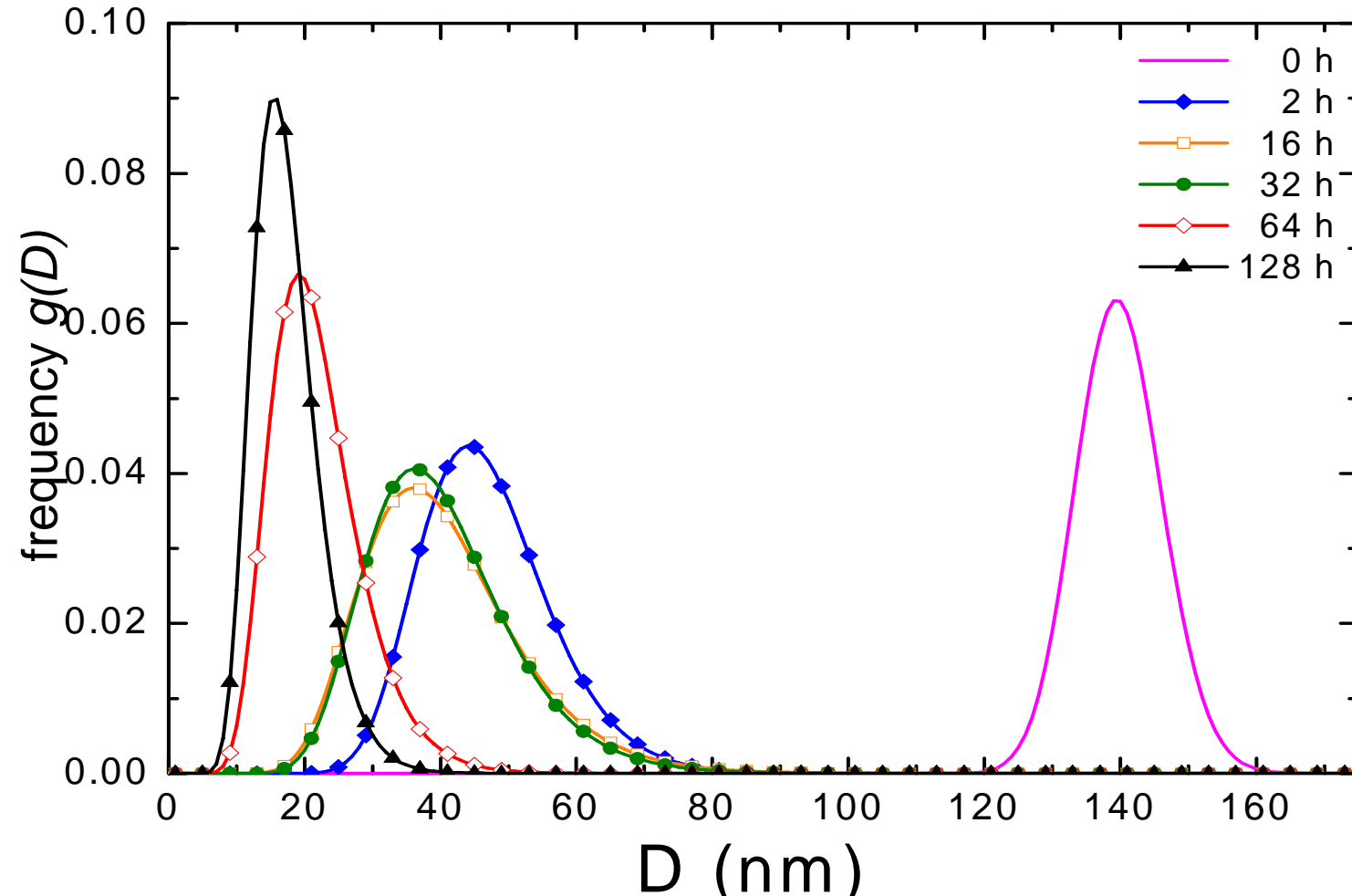
Size/dislocations versus morphology





Size distributions

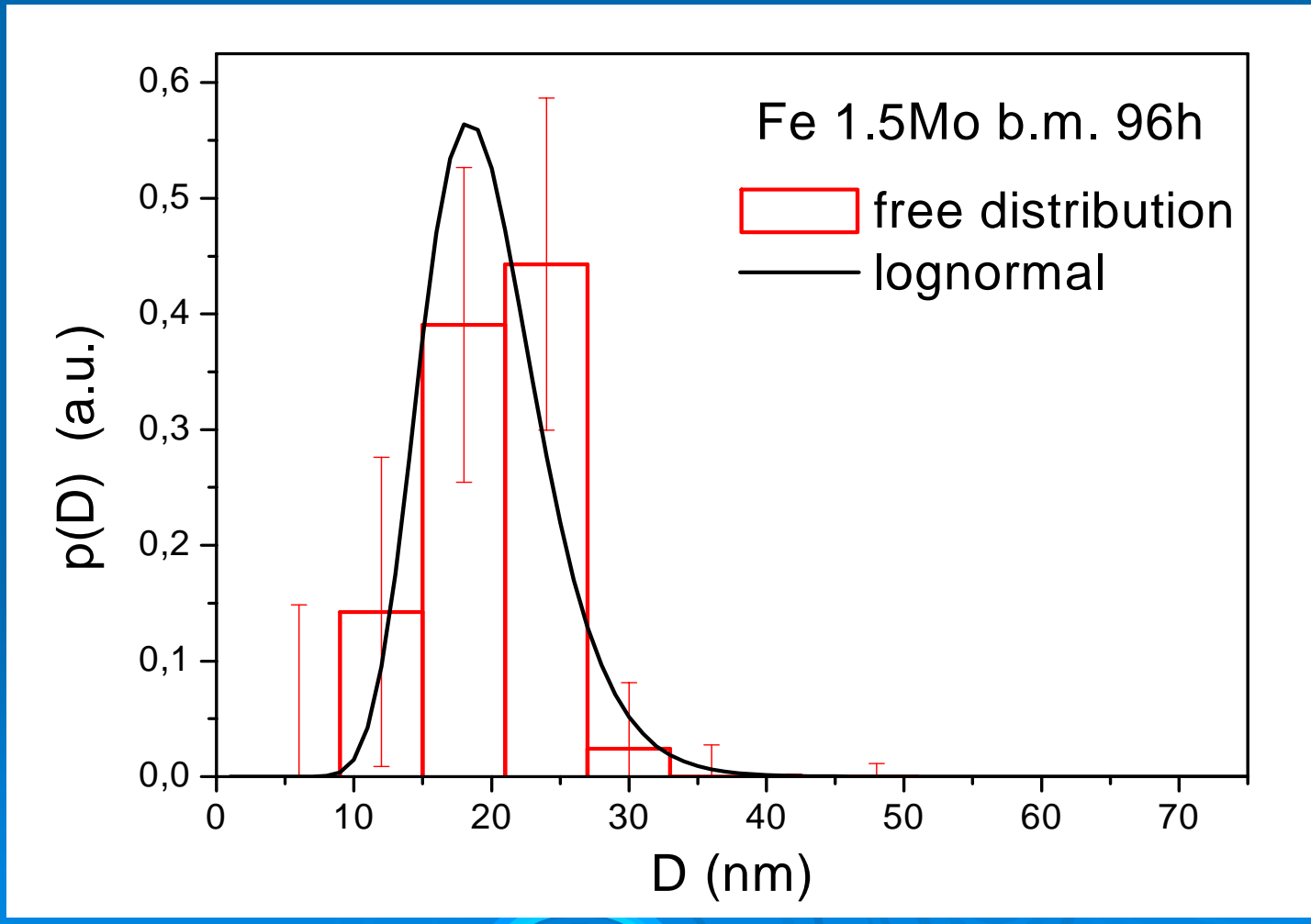
WPPM assuming a lognormal distribution





Size distributions (histogram)

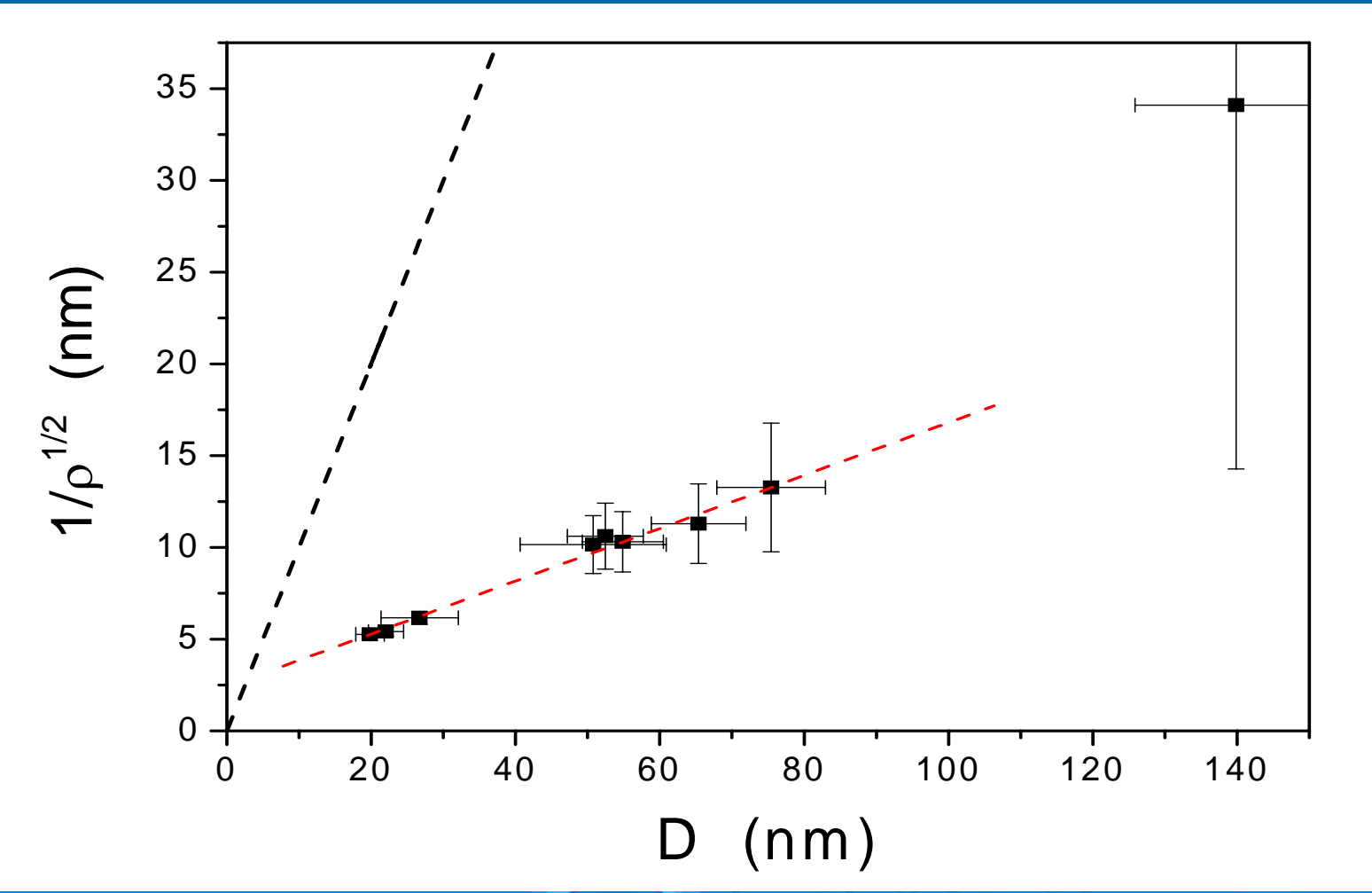
Reasonable agreement between a priori lognormal and 'free' histogram distribution: $\langle D \rangle = 19.8$ (2.0) and 20.1 (3.0) nm, respectively





Average number of dislocations

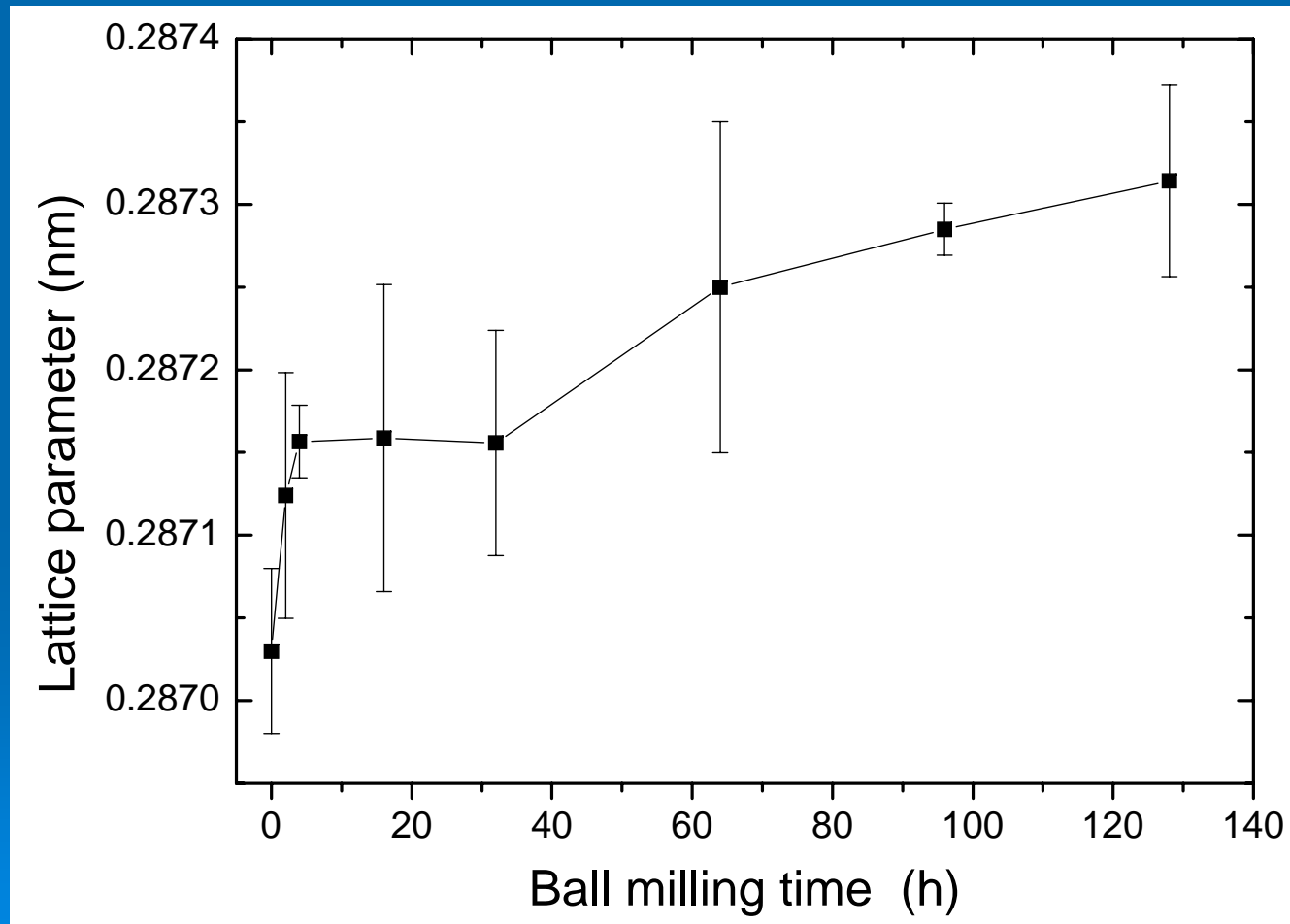
'Dislocation distance' versus domain size.
Average number of dislocations per grain: $4 \div 8$





Trend of cell parameter

Unit cell parameter: increasing with milling time. Effect of lattice defects and contamination (Cr, O_2)





Annealing kinetics (literature)

Problems with isothermal treatments:
materials may considerably change
during heating, before the isothermal
treatment starts.

'Grain' size after ball milling is ~35 nm,
increasing to ~70 nm during heating up
to treatment temperature.
Microstrain also changes (drastically
drops) during heating.

Some information is lost or mingled.

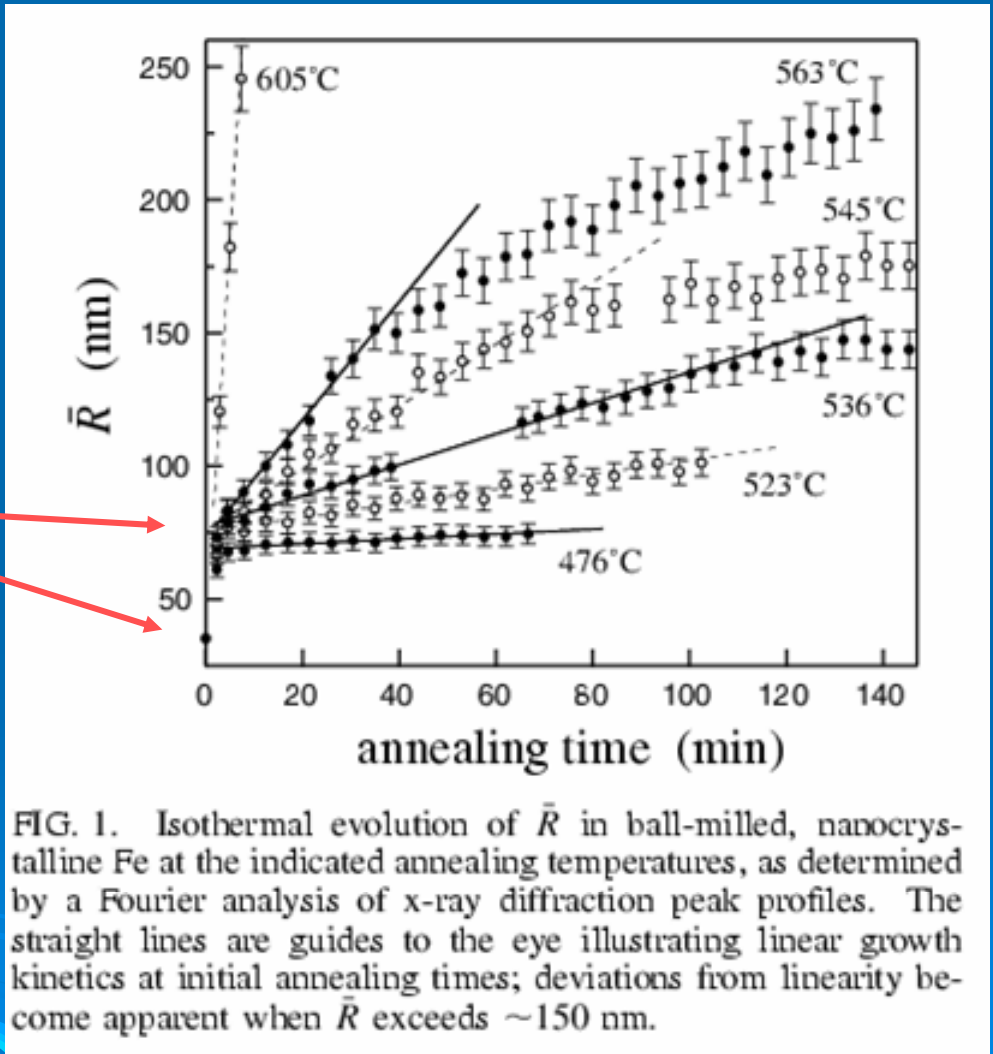
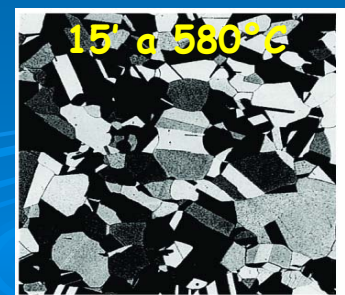
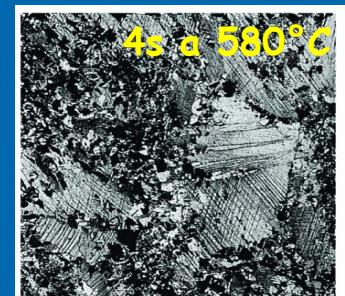
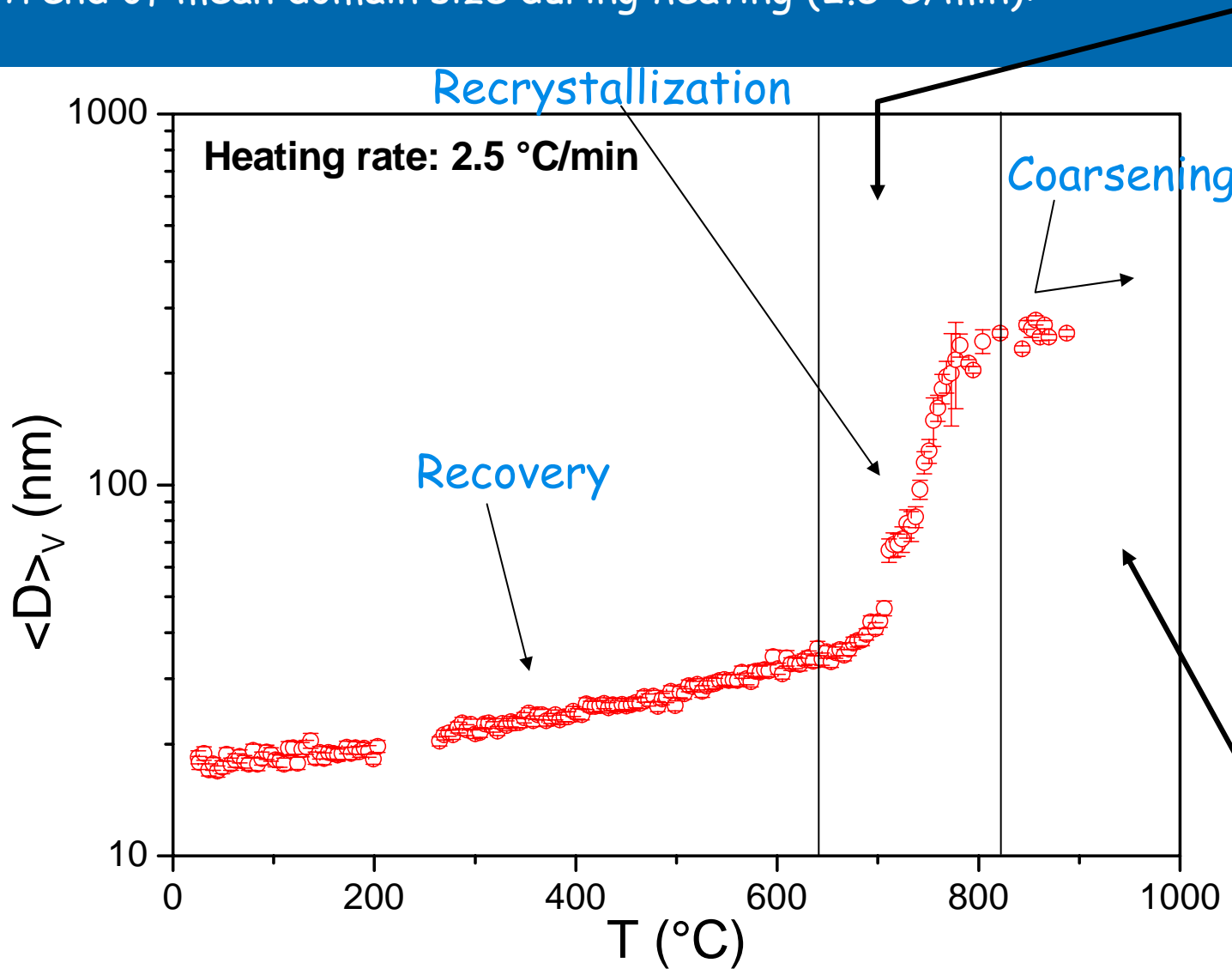


FIG. 1. Isothermal evolution of \bar{R} in ball-milled, nanocrystalline Fe at the indicated annealing temperatures, as determined by a Fourier analysis of x-ray diffraction peak profiles. The straight lines are guides to the eye illustrating linear growth kinetics at initial annealing times; deviations from linearity become apparent when \bar{R} exceeds ~ 150 nm.



Annealing kinetics (ramp+WPPM)

Trend of mean domain size during heating (2.5°C/min):

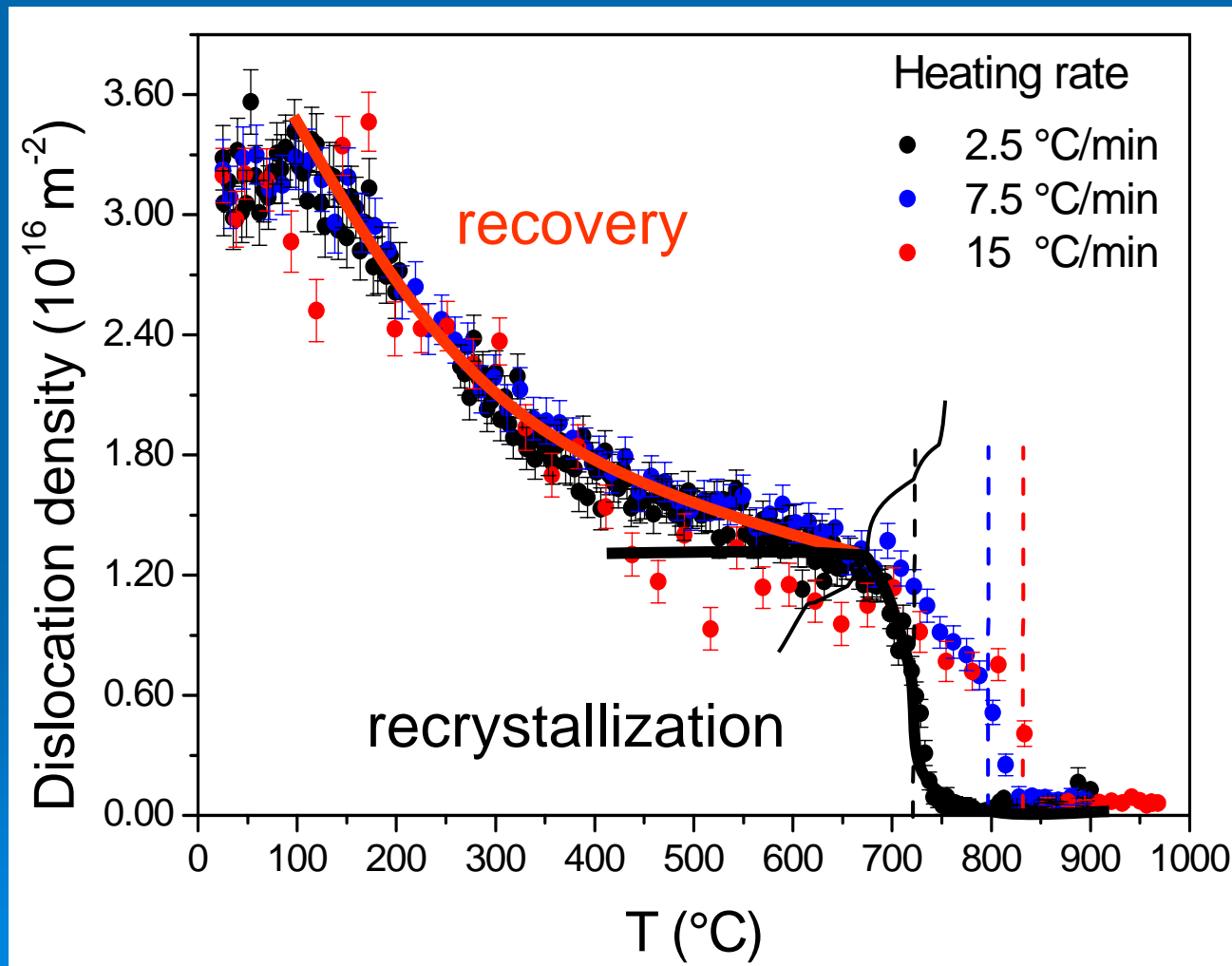


Callister
Scienza e Ingegneria dei materiali, una introduzione
EdiSES



Recovery/recrystallization

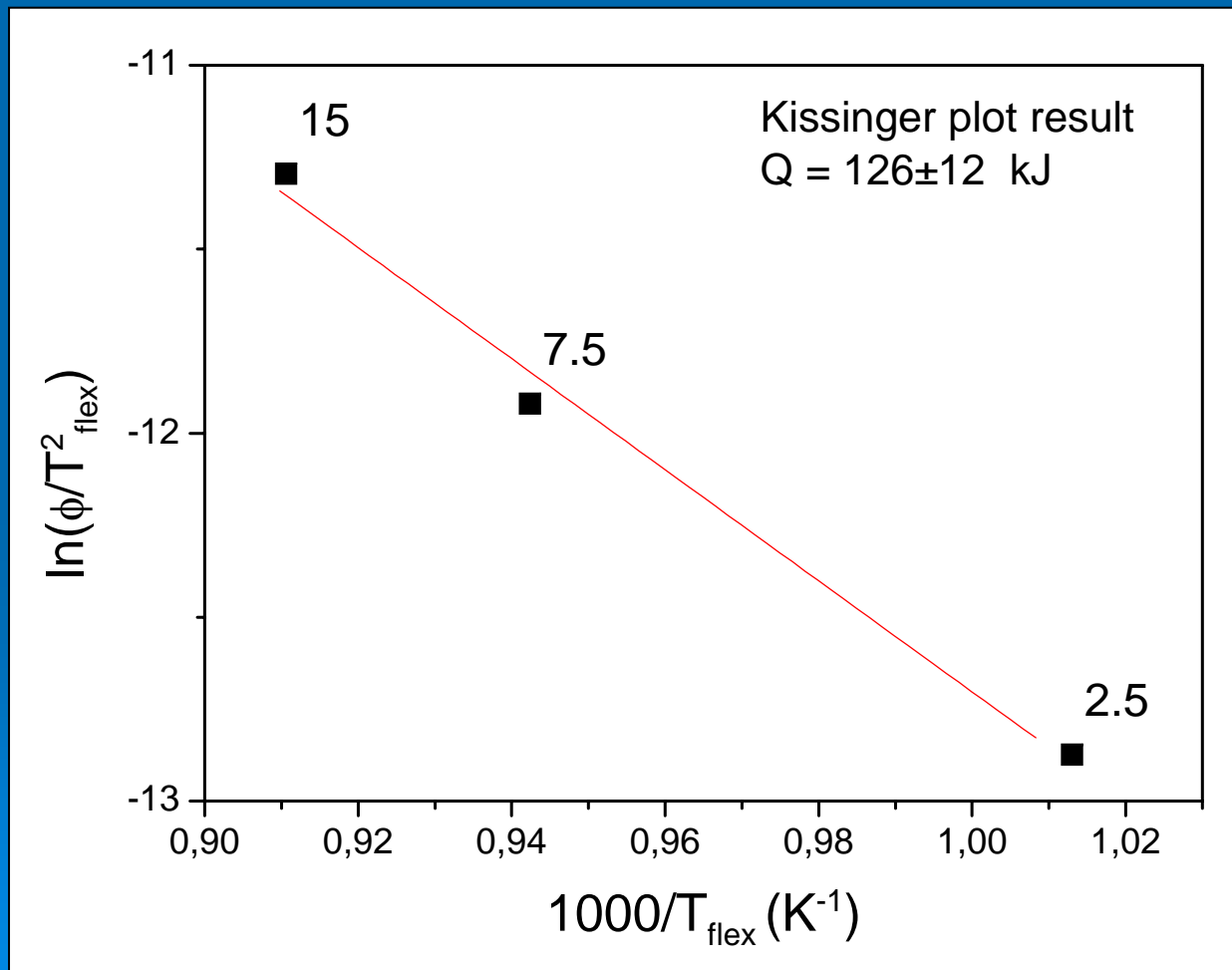
Advantage of using defect density: not affected by the recrystallization/grain coarsening transition. Ball milled Fe1.5Mo at different heating rates (2.5, 7.5, 15)





Recovery/recrystallization

Ball milled Fe1.5Mo at different heating rates ($\phi = 2.5, 7.5, 15 \text{ } ^\circ\text{C/min}$): activation energy of recrystallization by Kissinger method



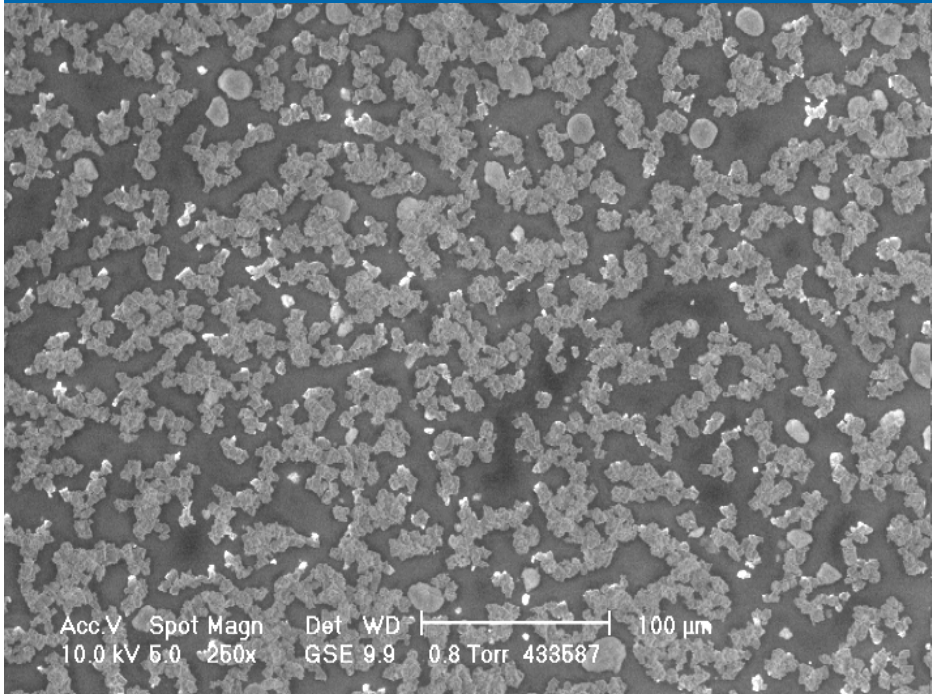


WPPM: applications

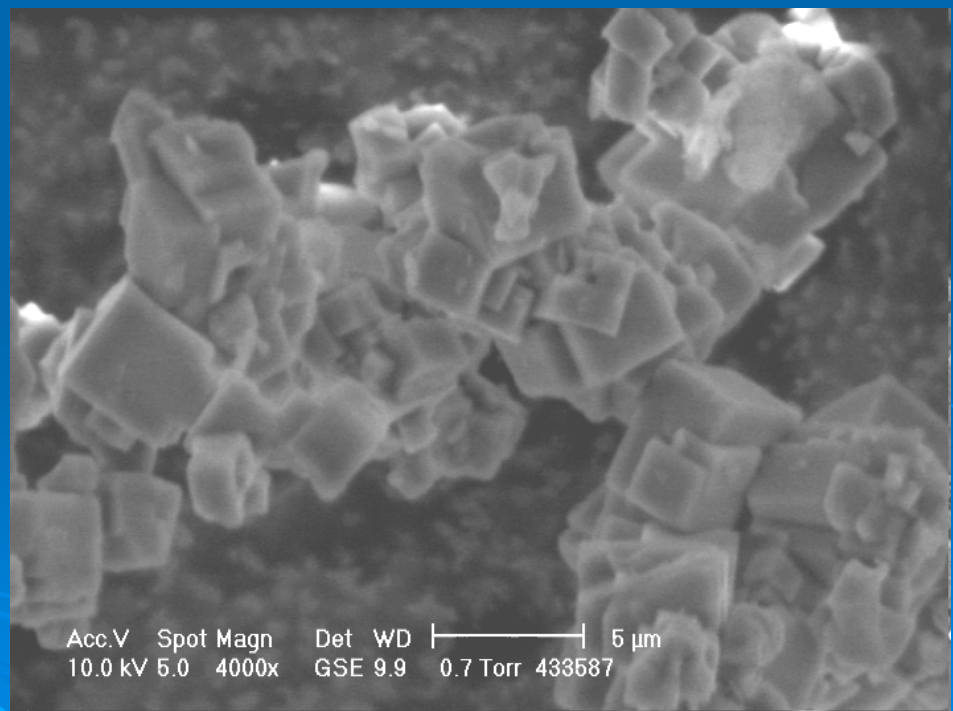
- Ball milled nickel powder
- Antiphase domains in Cu_3Au
- Nanocrystalline cerium oxide
- Ball milled Fe-1.5Mo
- Ball milled fluorite



ball milled CaF₂, ESEM



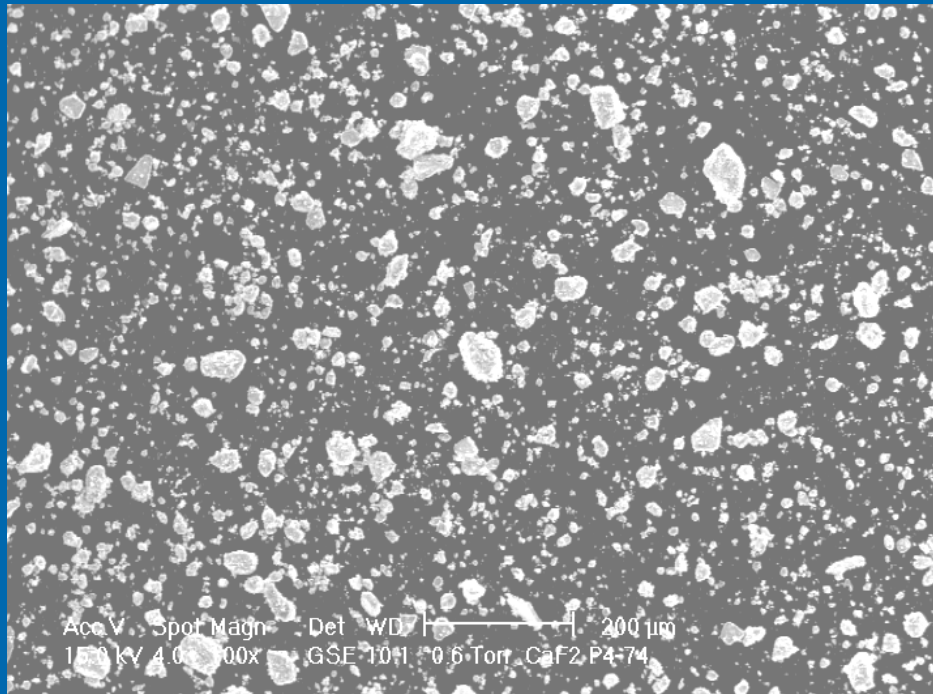
As-received powder



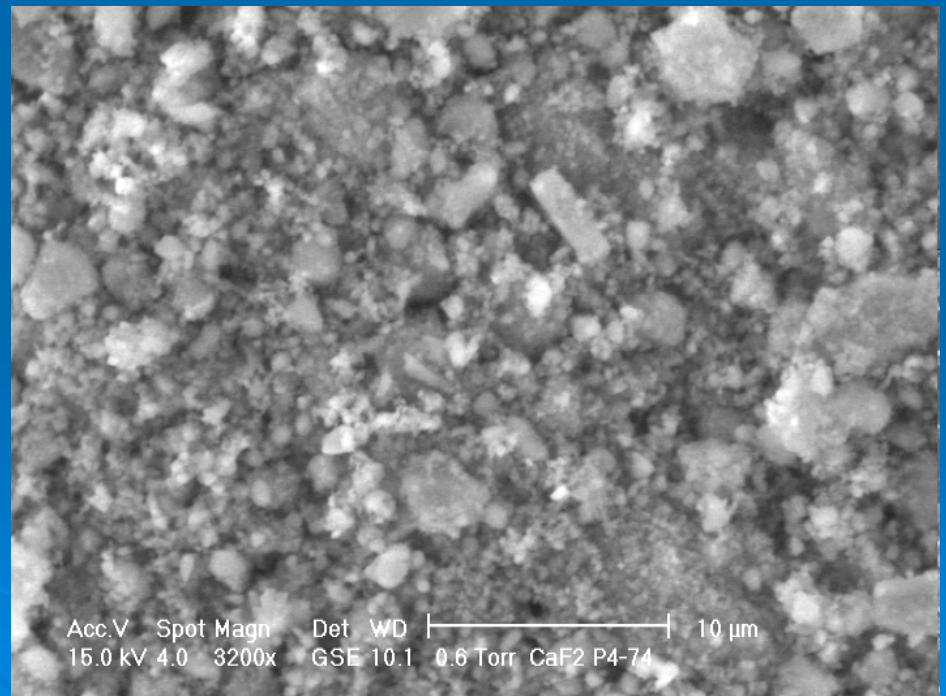
PARTICLES are cuboidal and micron-sized.
Aggregates are clearly present, but the powder is quite loose



ball milled CaF₂, ESEM



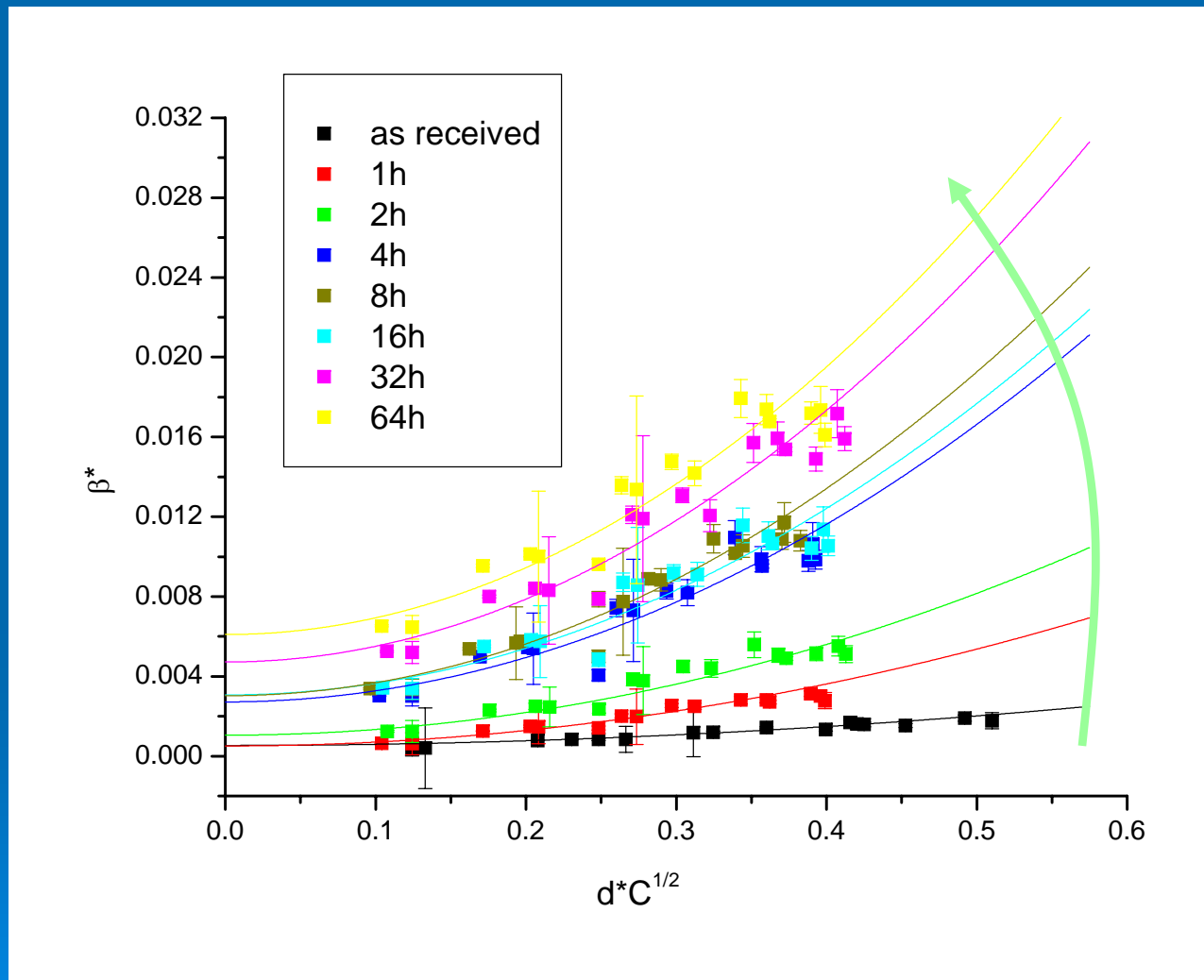
Powder milled 64h, $\Omega = 200$ rpm



Large aggregates are destroyed: smaller aggregates composed of small particles are present



ball milled CaF_2 , modified WH

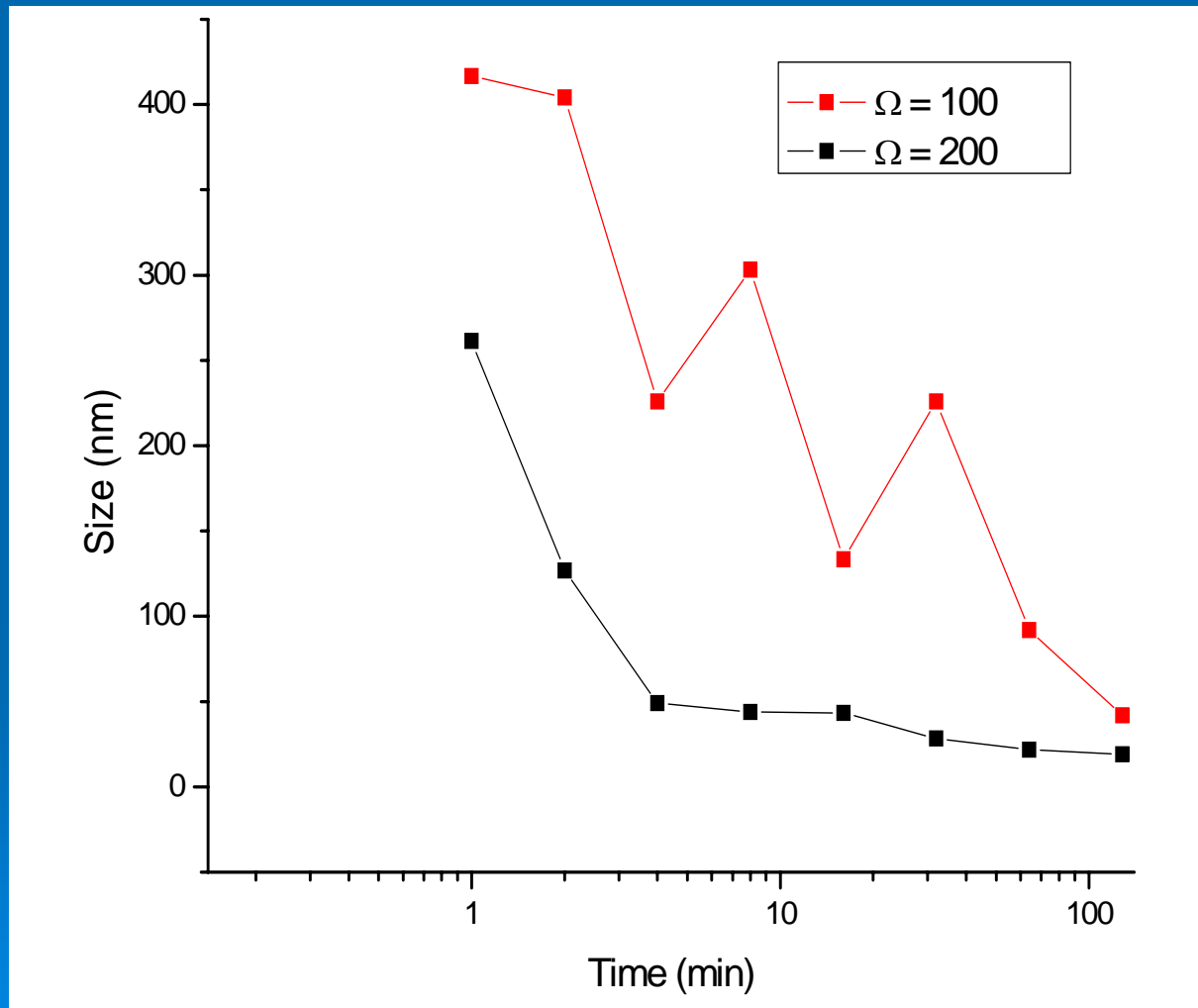


Trend of the modified Williamson-Hall plots by increasing the milling time.

An increase in the defect content (increase in the slope of the curves) is associated to a decrease in the domain size (increase in the intercept).



ball milled CaF_2 , modified WH

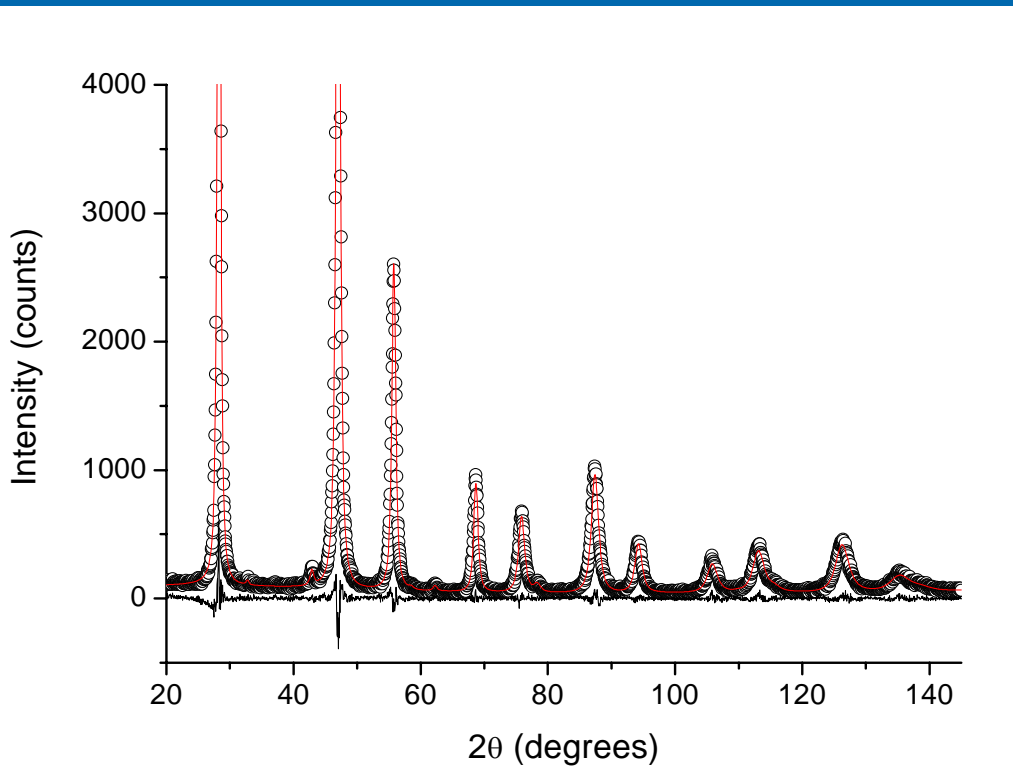


The modified Williamson-Hall analysis gives a **QUALITATIVE** trend of the average crystallite size trend with the milling time

$\Omega = 200$ is more severe than $\Omega = 100$

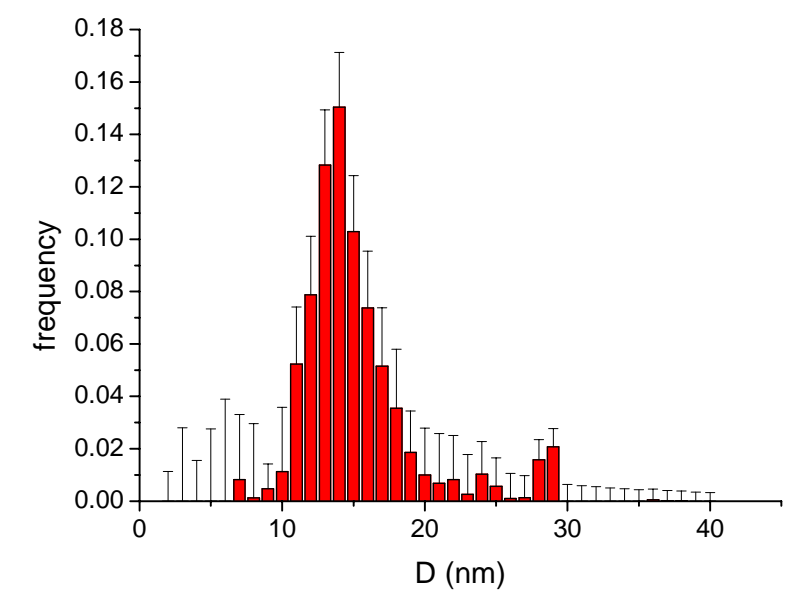


ball milled CaF_2 , WPPM result



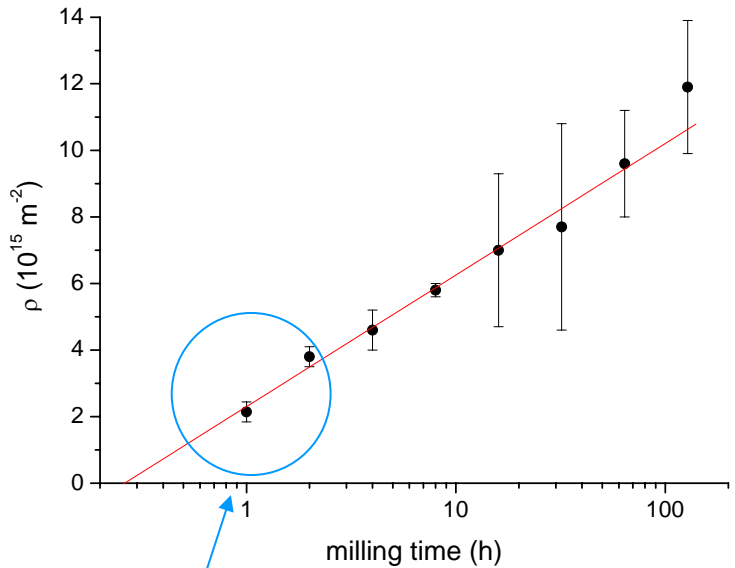
Modelled domain size distribution: large errors are associated to low frequencies. The average (12.9 nm) is almost the same as that obtained by assuming the distribution as being lognormal.

WPPM result for fluorite powder milled 128h: two phases are present (fluorite + iron, the latter coming from the vial and balls).

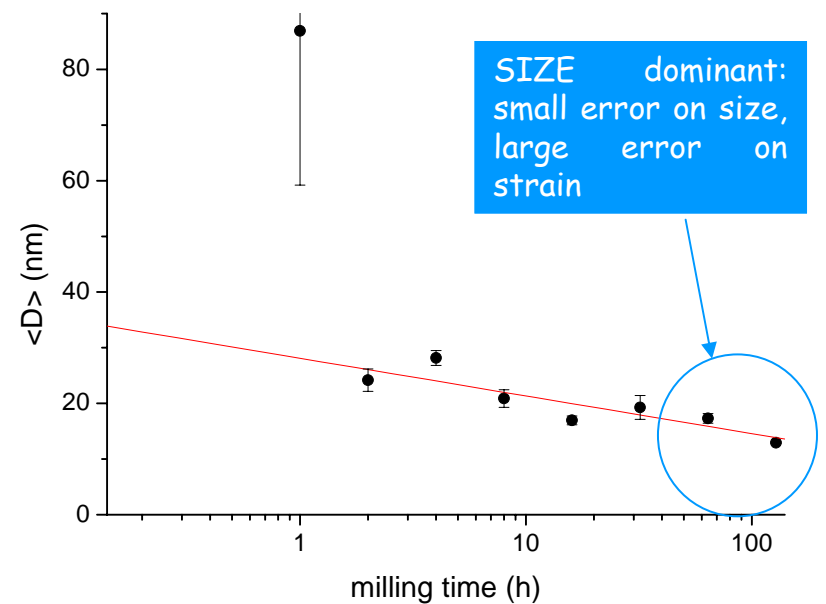




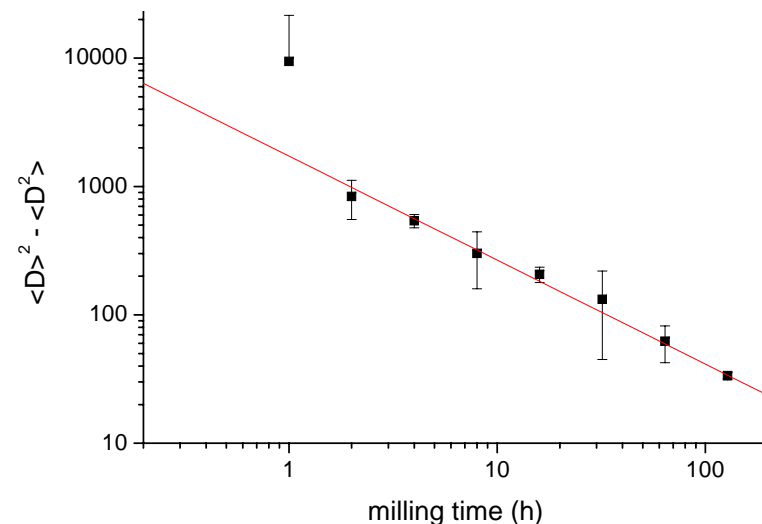
ball milled CaF_2 , WPPM result



STRAIN dominant:
small error on strain,
large error on size



SIZE dominant:
small error on size,
large error on strain



WPPM shows that
the process is
asymptotic as the
trends are linear
with the logarithm
of milling time



ball milled CaF_2 , WPPM result

A summary of the microstructural WPPM results is presented in table, together with the corresponding stored strain energy.

Milling time (h)	1	2	4	8	16	32	64	128
$\langle D \rangle$ (nm)	87(27)	24(2)	28(1)	20(1)	16.9(8)	19(2)	17.3(8)	12.9(1)
ρ_{disl} (10^{15} m^{-2})	2.1(3)	3.8(3)	4.6(6)	5.8(2)	7.0(20)	7.7(31)	9.6(16)	11.9(20)
R_e (nm)	3(1)	4.3(1)	7.5(1)	6.4(1)	4.6(1)	7.2(1)	6.6(1)	3.4(1)
f	0.47(3)	0.65(2)	0.9(1)	0.7(1)	0.96(6)	0.87(2)	0.67(9)	0.67(2)
U_{strain} (J/mol)	25	65	117	128	136	190	215	170

WPPM results confirm the qualitative finding of the modified Williamson Hall method, especially for very low and very high milling times where strain and size effects are dominant, respectively.

As expected, strain energy increases with increasing milling time and this can increase the reactivity of the powders.

Conclusions





WPPM: conclusions

Main advantages of the WPPM with respect to traditional methods

- correct counting statistics is used;
- problem of peak overlapping is intrinsically solved: peak profiles across the whole pattern are simultaneously refined;
- instrumental profile component can be easily included as well as appropriate background functions;
- different line profile models (e.g., dislocation, faulting, APBs, etc.) can be tested together (parameter correlations can be evaluated);
- structural constraints can be easily implemented: the WPPM algorithm can host a Rietveld routine (or vice-versa) for a simultaneous structure-microstructure refinement
- multiple phase samples can be studied (considering different microstructures) including quantitative phase analysis



WPPM: conclusions

For further information on:

WPPM

- seeing PM2K in action
- getting a personal copy of the software

*Structural/Microstructural analysis in more complex cases
(<3D materials such as layered silicates, heavily faulted
structures, etc.)*

- new DIFFaX+ release v. 2

please feel free to contact me at the conference or via e-mail
(I don't bite!)





WPPM: PM2K

PM2K interface

File Edit Min Help

New Open Save As... Copy Connect... Iter... Stop DATH INIT OUT Update Plot Get Init files Get Result

```
1 // Cerium oxide, test
2 // instrumental parameters (Caglioti)
3 par !W 1.790000E-02, !V 9.270000E-03, !U 3.060000E-03
4 par !a 1.287000E-01, !b 1.510000E-02, !c -4.900000E-05
5
6 loadData("a60433.raw", WPPM())
7 enableFileFit()
8
9 // Emission profile is made of 5 components (wavelength in nm and relative intensity)
10 // wavelengths from Berger et al.
11 addWavelength(!w11 0.1534753, !iRel11 0.0159)
12 addWavelength(!w12 0.1540596, !iRel12 0.57 )
13 addWavelength(!w13 0.1541058, !iRel13 0.0762)
14 addWavelength(!w14 0.1544441, !iRel14 0.2417)
15 addWavelength(!w15 0.1544721, !iRel15 0.0871)
16
```

Kernel address

Address: localhost Port: 5432

Remember kernel

OK Cancel

Input file Output file Plots Parameters



WPPM: PM2K

PM2K interface

File Edit Min Help

New Open Save As... Copy Connect... Iter... Stop PATH INIT OUT

Update Plot Get Init files Get Result

```
16
17 // add a phase (cubic ceria)
18 addPhase(aCeria 5.414830e-001, aCeria, aCeria, 90, 90, 90)
19
20 // Instrumental profile is pV and follows a Caglioti curve, both for HWHM
21 // and for eta:
22 // FWHM^2 = W + V tan(theta) + U tan(theta)^2
23 // eta = a + b theta + c theta^2
24 convolveFourier(CagliotiUVWabc(U, V, W, a, b, c))
25 //convolveFourier(Wilkens(rho 1E-2, Re 6.588880e-002, 0.0897934, 0.500537, 0.105762, 0.2
26 convolveFourier(SizeDistribution("sphere","lognormal",mu 1.311957e+000, sigma 4.246704e-
27 par !sigma0:=exp(sigma);
28 par !Dave:=exp(mu)*exp(sigma)^2/2;
29 par !sigma2:=exp(mu)^2*(sigma0)^2*(exp(log(sigma0)^2)-1);
30
31 // add the peaks
```

Input file Output file Plots Parameters



WPPM: PM2K

PM2K interface

File Edit Min Help

New Open Save As... Copy Connect... Iter... Stop PATH INIT OUT

Update Plot Get Init files Get Result

```
31 // add the peaks
32 addPeak( 1, 1, 1, 0 1.319137e+001)
33 addPeak( 2, 0, 0, 0 4.581557e+000)
34 addPeak( 2, 2, 0, 0 1.779966e+001)
35 addPeak( 3, 1, 1, 0 1.942435e+001)
36 addPeak( 2, 2, 2, 0 3.759934e+000)
37 addPeak( 4, 0, 0, 0 3.373513e+000)
38 addPeak( 3, 3, 1, 0 1.155818e+001)
39 addPeak( 4, 2, 0, 0 8.782537e+000)
40 addPeak( 4, 2, 2, 0 1.303231e+001)
41 addPeak( 3, 3, 3, Int333 3.287663e+000)
42 addPeak( 5, 1, 1, 0 :=Int333*2.8429;)
43 addPeak( 4, 4, 0, 0 4.808301e+000)
44 addPeak( 5, 3, 1, 0 2.425491e+001)
45 addPeak( 4, 4, 2, Int422 1.312990e+001)
46 addPeak( 6, 0, 0, 0 *=Tn+422/4-1)
```

Input file Output file Plots Parameters



WPPM: PM2K

PM2K interface

File Edit Min Help

New Open Save As... Copy Connect... Iter... Stop PATH INIT OUT

Update Plot Get Init files Get Result

```
42 addPeak( 5, 1, 1 , 0 :=Int333*2.8429;)
43 addPeak( 4, 4, 0 , 0 4.808301e+000)
44 addPeak( 5, 3, 1 , 0 2.425491e+001)
45 addPeak( 4, 4, 2 , Int422 1.312990e+001)
46 addPeak( 6, 0, 0 , 0 :=Int422/4;)
47 addPeak( 6, 2, 0 , 0 1.937525e+001)
48 addPeak( 5, 3, 3 , 0 1.908993e+001)
49 addPeak( 6, 2, 2 , 0 2.069929e+001)
50
51 // data collected on a traditional BB instrument with secondary graphite mono
52 // consider polarization as 0 and 2theta angle of the mono equal to 26.57°
53 mul(LPFactor(26.57))
54
55 // Chebyshev polynomial used to model the background
56 add(Chebyshev(0 2.643173e+002,0 -3.532247e+000,0 1.322374e-002,0 -1.370882e-005))
```

Kernel

Kernel address

Address: Port:

localhost 5432

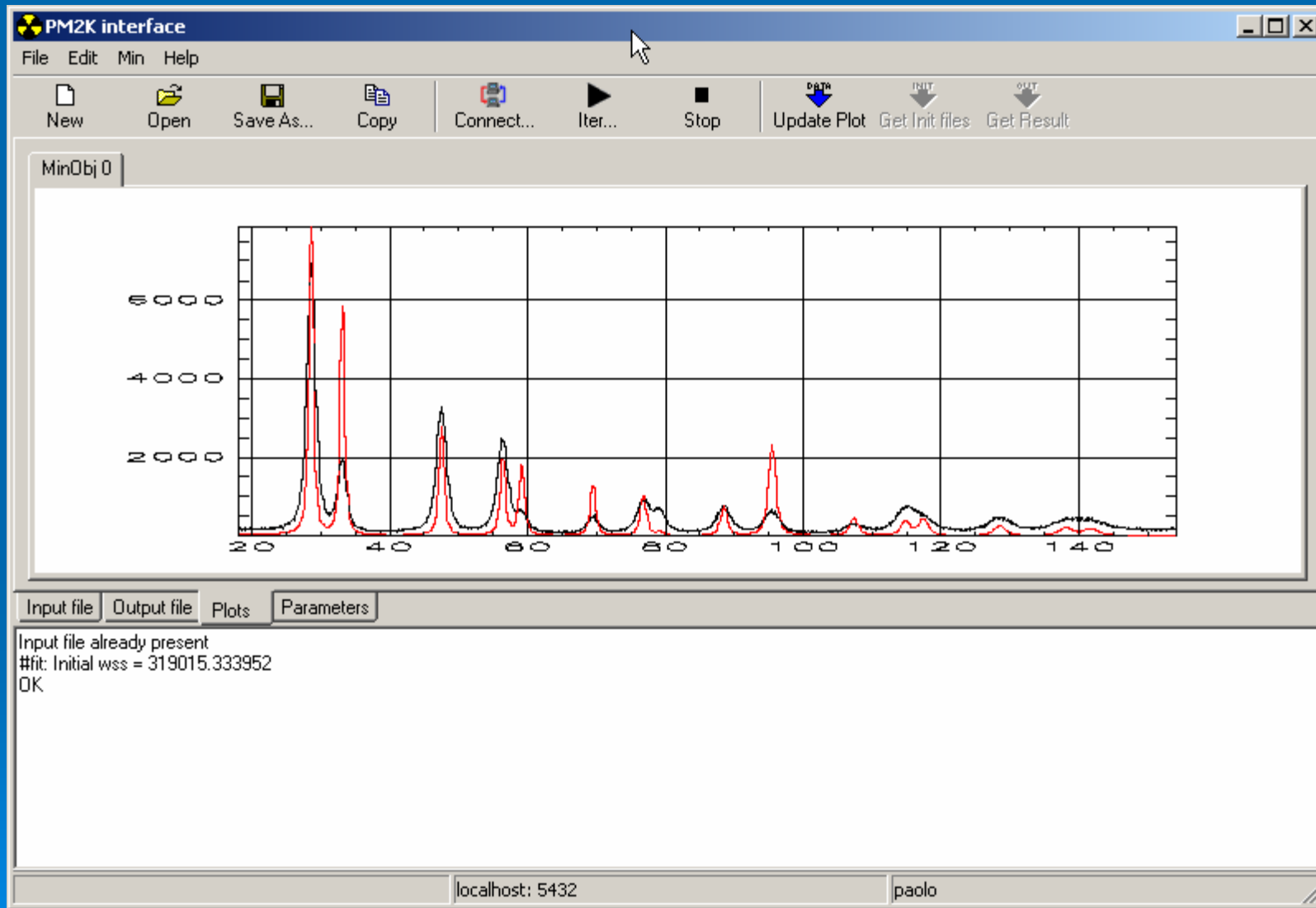
Remember kernel

OK Cancel

Input file Output file Plots Parameters

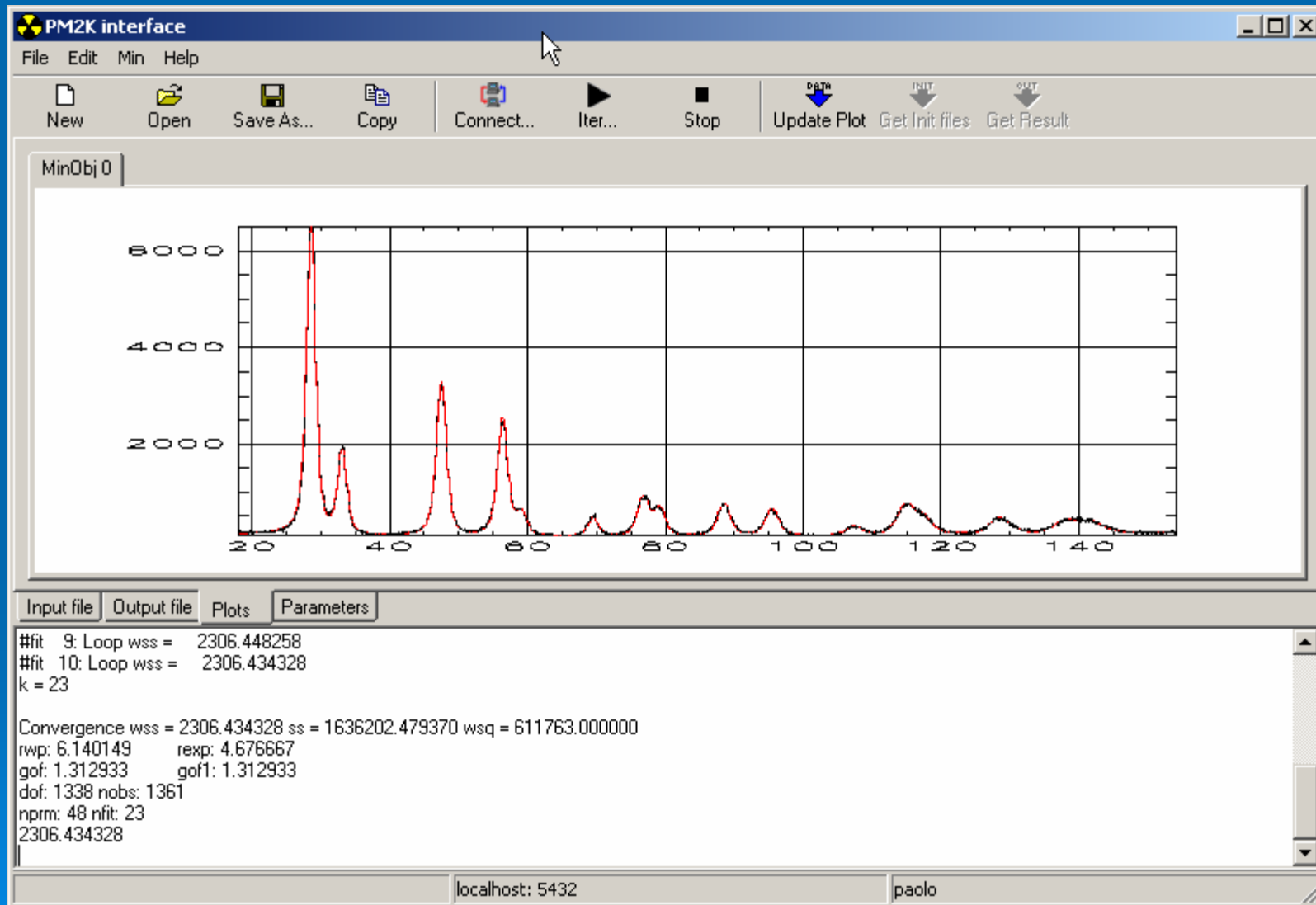


WPPM: PM2K





WPPM: PM2K





WPPM: PM2K

PM2K interface

File Edit Min Help

New Open Save As... Copy Connect... Iter... Stop PATH INIT OUT

Update Plot Get Init files Get Result

```
1 /*+
2 Convergence wss = 2306.43 ss = 1.6362e+006 wsq = 611763
3 rwp: 6.14015% rexp: 4.67667%
4 gof: 1.31293 gof1: 1.31293
5 dof: 1338 nobs: 1361
6 nprm: 48 nfit: 23
7 */
8
9 // Cerium oxide, test
10 // instrumental parameters (Caglioti)
11 par !W 1.790000E-02, !V 9.270000E-03, !U 3.060000E-03
12 par !a 1.287000E-01, !b 1.510000E-02, !c -4.900000E-05
13
14 loadData("a60433.raw", WPPM())
15 enableFileFit()
16
```

Input file Output file Plots Parameters

k = 23

Convergence wss = 2306.434328 ss = 1636202.479370 wsq = 611763.000000
rwp: 6.140149 rexp: 4.676667
gof: 1.312933 gof1: 1.312933
dof: 1338 nobs: 1361
nprm: 48 nfit: 23
2306.434328
Stop...###END 2306.434328
OK

localhost: 5432 paolo



WPPM: PM2K

PM2K interface

File Edit Min Help

New Open Save As... Copy Connect... Iter... Stop PATH INIT OUT

Update Plot Get Init files Get Result

```
25 // add a phase (cubic ceria)
26 addPhase(aCeria 5.412782e-001/+ esd: 3.997257e-003 +/, aCeria, aCeria, 90, 90, 90)
27
28 // Instrumental profile is pV and follows a Caglioti curve, both for HWHM
29 // and for eta:
30 // FWHM^2 = W + V tan(theta) + U tan(theta)^2
31 // eta = a + b theta + c theta^2
32 convolveFourier(CagliotiUVWabc(U, V, W, a, b, c))
33 //convolveFourier(Wilkens(rho 1E-2, Re 6.588880e-002, 0.0897934, 0.500537, 0.105762, 0.2
34 convolveFourier(SizeDistribution("sphere","lognormal",mu 1.386495e+000/+ esd: 1.641396e-
35 par !sigma0/+ 1.413994e+000, esd: 0.000000e+000 +/:=exp(sigma);
36 par !Dave/+ 3.999561e+000, esd: 0.000000e+000 +/:=exp(mu)*exp(sigma)^2/2;
37 par !sigma2/+ 4.080477e+000, esd: 0.000000e+000 +/:=exp(mu)^2*(sigma0)^2*(exp(log(sigma
38
39 // add the peaks
40 addPeak( 1 1 1 0 1 575602e+001/+ esd: 2 151369e-001 +/)
```

Input file Output file Plots Parameters

k = 23

Convergence wss = 2306.434328 ss = 1636202.479370 wsq = 611763.000000
rwp: 6.140149 rep: 4.676667
gof: 1.312933 gof1: 1.312933
dof: 1338 nobs: 1361
nprm: 48 nfit: 23
2306.434328
Stop...###END 2306.434328
OK

localhost: 5432 paolo